An Urban Weather Generator Coupling a Building Simulation Program with an Urban Canopy Model

By

Bruno Bueno Unzeta

Industrial Engineer
University of Malaga (2007)

Submitted to the Department of Architecture
in Partial Fulfillment of the Requirements for the Degree of
Master of Science in Building Technology

at the

Massachusetts Institute of Technology

June 2010

Signature of author: .....
Department of Architecture
March 31, 2010

Certified by: .....
Leslie K. Norford
Professor of Building Technology
Thesis Supervisor

Accepted by: .....
Julian Beinart
Professor of Architecture
Chair of the Department Committee on Graduate Students

Leslie K. Norford
Professor of Building Technology
Thesis Supervisor

Rex E. Britter
Visiting Scientist, Department of Urban Studies and Planning
Thesis Reader

An Urban Weather Generator Coupling a Building Simulation Program with an Urban Canopy Model

By

Bruno Bueno Unzeta

Submitted to the Department of Architecture on March 31, 2010 in Partial Fulfillment of the Requirements for the Degree of Master of Science in Building Technology

Abstract

The increase in air temperature observed in urban environments compared to the undeveloped rural surroundings, known as the Urban Heat Island (UHI) effect, is being intensely studied, due to its adverse environmental and economic impacts. Some of the causes of the UHI effect are related to the interactions between buildings and the urban environment.

This thesis presents a methodology intended to integrate building energy and urban climate studies for the first time. It is based on the premise that at the same time buildings are affected by their urban environment, the urban climate is affected by the energy performance of buildings. To predict this reciprocal interaction, the developed methodology couples a detailed building simulation program, EnergyPlus, with a physically based urban canopy model, the Town Energy Balance (TEB). Both modeling tools are leading their respective fields of study.

The Urban Weather Generator (UWG) methodology presented in this thesis is a transformation of meteorological information from a weather station located in an open area to a particular urban location. The UWG methodology fulfils two important needs. First, it is able to simulate the energy performance of buildings taking into account site-specific urban weather conditions. Second, it proposes a building parameterization for urban canopy models that takes advantage of the modelling experience of a state-of-the-art building simulation program.

This thesis also presents the application of the UWG methodology to a new urban area, Masdar (Abu Dhabi). The UHI effect produced in this hot and arid climate by an urban canyon configuration and its impact on the energy performance of buildings are analyzed.

Thesis Supervisor: Leslie K. Norford
Title: Professor of Building Technology, Department of Architecture

Acknowledgements

This project would not have been possible without the guidance and insights of Prof. Norford. During these two years of research, Prof. Norford has taught me with great pedagogy every step of the scientific method, which has an enormous value for my future career.

This project is also the result of the invaluable contribution of Prof. Britter, whose expertise in the meteorological field solved many of the questions arisen in the exploration of urban climate studies. Prof. Britter has also helped us shape the scope of this thesis and has very much enriched the human relations in our research group, facilitating the fluent and satisfactory exchange of ideas.

I would also like to thank the CNRM-GAME group for hosting me so friendly during the week I spent in Toulouse, and for their generosity in sharing with us their software and in answering all my questions. In particular, I want to acknowledge Dr. Pigeon, whose effort is also part of this project.

Essential funding and support of this research was provided by the MIT/Masdar Institute of Science and Technology Collaborative Research Program and by the Singapore National Research Foundation through the Singapore-MIT Alliance for Research and Technology Center for Environmental Sensing and Modeling.

To Kasia,
for sharing her life with mine.

Table of Contents

List of symbols

Symbol	Description	Unit
A	Surface area	m^2
Br	Brunt number	-
C_d	Drag coefficient	-
C_H	Stability factor	-
C_T	Surface soil/vegetation heat capacity	$Jm^{-2}K$
c_p	Specific heat of air	$Jkg^{-1}K^{-1}$
COP	Coefficient of performance of an HVAC system	-
$CTTC$	Cluster thermal time constant	s
E	Latent heat flux	Wm^{-2} - W
EIR	Energy input ratio	W
F	View factor; vertical flow rate of water in ISBA	-; ms^{-1}
FA	Building floor area	m^2
ff	Air flow rate ratio used in the characteristic curves of a cooling plant	-
G	Conduction heat flux	Wm^{-2}
g	Gravitational acceleration	ms^{-2}
H	Sensible heat flux	Wm^{-2} - W
h	Convection heat transfer coefficient; height of buildings	$Wm^{-2}K^{-1}$; m
h_u	Relative humidity at the ground surface	%
I	Solar radiation heat flux	Wm^{-2}
k	Thermal conductivity of the road	$Wm^{-1}K$
L	Longwave radiation	Wm^{-2}
l	Latent heat of air	Jkg^{-1}
l_v	Specific heat of evaporation	Jkg^{-1}
m	Solar absorptance of a surface	-
$\dot{m}$	Air mass flow rate	kgs^{-1}
N	Brünt- Väisälä frequency	s^{-1}
P	Perimeter; Precipitation rate	m ; $kg_w s^{-1}m^{-2}$
p	Thermodynamic pressure	Pa
PLF	Part load fraction	-
PSA	Partial shaded fraction of a surface	-
Q	Heat flux	W - Wm^{-2}
Q_X	Pollutant source strength per unit area	$kgs^{-1}m^{-2}$
q	Humidity content of air	$kgkg^{-1}$
q''	Heat flux per unit area	Wm^{-2}
R	Aerodynamic resistance; anisotropic shadowing factor	sm^{-1}; -
R_r	Drainage of the interception reservoir	-
Re	Reynolds number	-
Ri	Richardson number	-

S	Shortwave radiation	Wm^{-2}
S_l	External source/sink of water	$kgm^{-3}s^{-1}$
SVF	Sky view factor	-
T	Temperature; air temperature	$^{\circ}C, K$
t	Time	s
TR	Mass transfer due to transpiration	$kg_w s^{-1} m^{-2}$
U	Wind speed magnitude	ms^{-1}
u,v,w	Wind speed components	ms^{-1}
u_*	Friction velocity	ms^{-1}
UHI	Urban heat island intensity	$^{\circ}C$
V	Air volume; Mass transfer due to evaporation	m^3; $kgs^{-1}m^{-2}$
veg	Fractional vegetation cover	-
w	Width of buildings; volumetric soil water content; characteristic wind velocity	m; m^3m^{-3}; ms^{-1}
w_*	Free-convection velocity	ms^{-1}
W_r	Reservoir of water content	kgm^{-2}
WA	Building wall area	m^2
$X,Y,Z,$	Conduction transfer function (CTF) coefficient	-
X	Air pollution concentration	kgm^{-3}
x,y,z	Spatial coordinates	m
z_i	Urban boundary layer thickness	m
z_o	Roughness length	m

Greek symbols

α	Thermal diffusivity; solar absorptance of a surface	m^2s^{-1}; -
β	Thermal expansion coefficient of the air	K^{-1}
δ	Time step	s
ε	Emissivity of a surface	-
θ	Ground temperature in the CTTC model; solar angle; potential temperature	$^{\circ}C$; -; $^{\circ}C$
κ	Von Kármán constant	-
ν	Viscous diffusivity of the air	m^2s^{-1}
Π	Pi group of the Buckingham theorem	-
ρ	Density of air	kgm^{-3}
ρ_w	Density of water	kgm^{-3}
σ	Stefan–Boltzmann constant	$Wm^{-2}K^{-4}$
τ_o	Surface shear stress	Nm^{-2}
Φ_j	conduction flux transfer function CTF coefficient	-
Ψ	View factor	-
ϕ,ψ	Generic functions	

Subscripts

A	Advection heat
a	Above the urban canopy layer
air	Air
B	Building
c	Condenser of an HVAC system
can	Inside the canyon
circumsolar	Region circumsolar to the sun
conv	Convection
dif	Diffuse component of the solar radiation
dir	Direct component of the solar radiation
dome	Sky dome
E	Latent heat
eff	Effective
elect	Electric consumption
equip	Equipment
F	Anthropogenic heat
f	Forced convection
gnd	Ground
H	Sensible heat
hor	Horizontal
horizon	Horizon line
i	Inside
in	Incoming
inf	Infiltration
int.gains	Internal gains
k	Conduction
load	Building loads
lw	Longwave
M	Momentum
met	Meteorological
n	Natural convection
o	Outdoor, outside
out	Outgoing
r	Radiant; road; rural; radial
ref	Reference
reflec	Reflected solar radiation
S	Heat storage
s	Soil
sky	Sky
sol	Solar
sp	Thermal control set point
sun	Sunlit; azimuth
sup	System supply
surf	Surface
sw	Shortwave
sys	System
top	Interactions between the canyon and the atmosphere above the canyon

u, urb	Urban
veg	Vegetation
ver	Vertical
w	Wall; water
waste	Waste heat released
wb	Web bulb
z	Zone; zenith
2	Deep soil
*	Net-radiation
$\Downarrow$	Incoming direct radiation
$\downarrow$	Incoming diffuse radiation

CHAPTER 1

Introduction

1.1. Introduction

The increase in air temperature observed in urban environments compared to the undeveloped rural surroundings, known as the Urban Heat Island (UHI) effect, is being intensively studied, due to its adverse environmental and economic impacts. However, there is still a lack of tools dedicated to the design and analysis of buildings in urban areas that take into account this effect.

Traditionally, the built environment has been divided into indoor and outdoor domains. The indoor domain has been mainly studied by building engineers to be used in the design and analysis of building systems. The outdoor domain, however, has been a research field of physics, studied by meteorologists to account for the effects of cities on the atmosphere. Both domains have been developed independently with little interaction with each other.

This thesis presents a methodology, called the Urban Weather Generator (UWG) scheme, intended to integrate building energy and urban climate studies. It is based on the premise that at the same time buildings are affected by their urban environment, the urban climate is affected by the energy performance of buildings. To predict this reciprocal interaction, the developed methodology couples a building energy model with an urban climate model. The UWG scheme was initially thought to generate urban weather files that could be used in the simulation of buildings, but it has been proven to have applications beyond its initial definition.

This document is composed of nine chapters that cover the motivation (chapter 1), the background (chapter 2), the operation (chapter 3), and the models (chapters 4-7) of the UWG scheme. The thesis includes an application of the scheme to an urban area in Abu Dhabi (chapter 8) and closes with final remarks (chapter 9).

1.2. Problem statement

Climate information in building simulation programs

Building simulation programs use weather data files as boundary conditions for annual energy calculations. These weather files contain hourly values of meteorological information that is obtained from measurements at a weather station. As a requirement, a meteorological weather station has to be located in an open field without nearby obstructions. This condition can make meteorological weather files inappropriate for energy simulations of buildings in cities, where the local climate is affected by the presence of urban structures.

The weather information used in building simulation programs is critical for the design and analysis of building systems. Energy consumption in buildings with poor insulation or low internal heat gains can be dominated by outdoor conditions. Moreover, the energy efficiency and capacity of heating, ventilating and air-conditioning (HVAC) systems depend also on outdoor conditions. In building systems with an inherent close interaction with the

environment, such as natural ventilation systems or economizers, small changes in outdoor conditions produce significant changes in their energy performance.

Building simulation programs, such as EnergyPlus™, do not account for the differences in climate between a weather station and a particular urban location. The meteorological transformations carried out by EnergyPlus are limited to the decrease in air temperature with altitude (approx. 1 °C/100 m) and the logarithmic profile of wind speed with altitude. Therefore, phenomena such as the Urban Heat Island (UHI) effect are not considered in current building simulation practices. Depending on the building and the building system configuration under study, the error of not considering the site-specific urban climate can lead to unacceptable building simulation results.

Building representation in urban climate studies

Urban canopy models are used in meteorology to predict the effect of urban areas on the atmosphere (e.g. Masson, 2000). These models implement a geometric representation of a street or urban canyon (see section 1.5.1) and are able to calculate the urban climate conditions by solving an energy balance of the heat fluxes coming from buildings and the road.

Urban canopy models are implemented with a simple representation of buildings, often as transient conduction heat transfer equation through a multi-layered wall and roof. To better represent building effects within urban canopy models, some authors have developed simplified building models that are able to estimate building thermal loads (e.g. Salamanca et al., 2009).

However, from the point of view of building energy performance evaluations, these simplified building models present important limitations. For example, the interaction between building systems and the environment is poorly represented. This fact, together with a very simplified calculation of building loads, limits the calculation of waste heat from HVAC equipment, which can have a great impact on urban climate, as will be shown in this thesis.

Furthermore, these building parameterizations do not include specific models for passive systems, which can influence significantly the energy performance of buildings; and they are unable to perform daylight analysis, which is an important factor in the design and analysis of buildings in urban areas.

1.3. The Urban Weather Generator (UWG) concept

The Urban Weather Generator (UWG) concept is the meteorological transformation of available weather data files measured at a weather station into site-specific urban weather files. This transformation is carried out in three steps, which are described in detail in chapter 3, and involves an iterative procedure between the building simulation program EnergyPlus (DOE, 2009) and an adapted version of the urban canopy model TEB (Masson, 2000). Both programs have been extensively validated and are leading their respective fields of study.

The UWG scheme fulfills the two important needs stated in the previous section: first, it calculates site-specific urban weather files that can be directly used in a building simulation program; and second, it proposes a building parameterization for urban canopy models that

takes advantage of the modelling experience of a state-of-the-art building simulation program.

1.4. Research objectives

This thesis pursues the following research objectives:

(1) The development of an Urban Weather Generator (UWG) scheme that has the following missions: (a) Calculate site-specific urban weather files that can be used in the simulation of buildings. (b) Simulate buildings in urban environments taking into account the microclimate around them.

(2) The application of the UWG scheme to the case study of a new urban area in Masdar (Abu Dhabi). This application investigates the impact of the Urban Heat Island (UHI) effect on the energy consumption of buildings, as well as the impact of building performance on the urban climate.

1.5. Important concepts in urban climate modelling

1.5.1. Urban canyon

In urban climate studies, an urban canyon is often referred as the basic urban unit. An urban canyon is basically a street surrounded along its sides by building walls (Fig.1.1). In urban climate modelling, the urban canyon concept is often represented as a two-dimensional configuration, where the third dimension is infinitely long and homogeneous. Then, a city is assumed to be formed by a set of idealized urban canyons oriented in different directions. This approximation has made possible the development of urban canopy models based on two-dimensional energy balances.

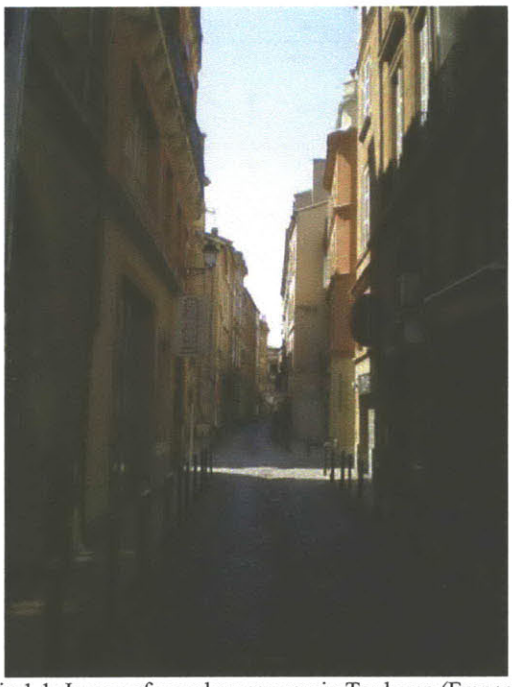

Fig.1.1: Image of an urban canyon in Toulouse (France).

In this thesis, we will distinguish between an average urban canyon and a specific urban canyon. In the first case, all the input data and the calculations carried out by the UWG scheme are averaged over a certain neighborhood or urban area. In the second case, the UWG calculations are specific for the geometry, orientation, and building configuration of a certain urban canyon.

1.5.2. Atmospheric boundary layers

The *planetary boundary layer* (PBL) is the region of the atmosphere strongly affected by diurnal variations in surface conditions such as ground temperature. The lower part of the PBL is the *surface boundary layer*, characterized by an air velocity gradient due to the no-slip condition at the surface. Some authors (i.e. Hanna and Britter, 2002) divide this layer into an inertial sublayer and a roughness sublayer. In the *roughness sublayer*, the flow is directly affected by the presence of obstacles (Fig.1.2). Hanna and Britter (2002) estimate the height of the roughness sublayer as twice the average obstacle height. The *canopy layer* extends vertically from the ground up to an upper level where all structures of the surface contributing to the energy balance of the canopy layer lie below. The top of the *urban canopy layer* is consequently situated above roof level, while the top of the *rural canopy layer* is just above the crops, or the grass, or the trees. Some authors (e.g. Kuttler, 2008) refer to the *urban boundary layer* as the region of the atmosphere that has a higher temperature than the surroundings due to the presence of a city (Fig.1.3).

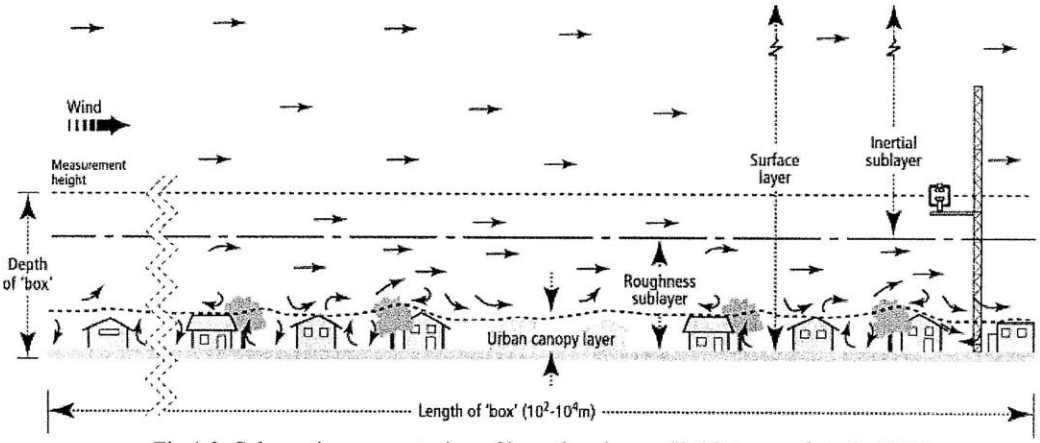

Fig.1.2: Schematic representation of boundary layers (I) (*Grimmond et al., 2002*).

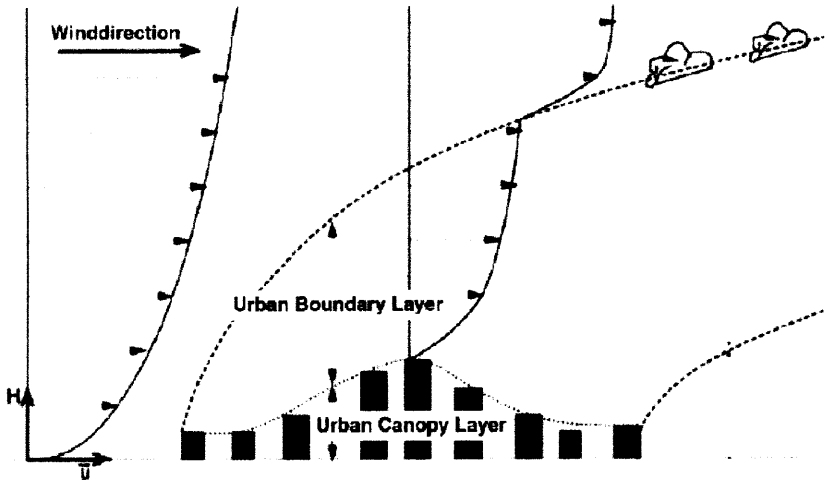

Fig.1.3: Schematic representation of boundary layers (II) (*Kuttler, 2008*).

1.5.3. The Urban Heat Island (UHI) effect

Many studies have reported observations of the UHI effect in cities (e.g. Pon et al., 2000; Priyadarsini et al., 2008; Chow and Roth, 2006). One of the most discussed topics related to the UHI effect is its own definition. The UHI effect is generally defined as the increase in air temperature observed in urban environments compared to the undeveloped rural surroundings. This definition assumes that, in absence of urban structures, the area where the city is located would have the same air temperatures as the undeveloped surroundings. One of the problems of this definition is to determine which "undeveloped surrounding" is the most representative, or alternatively, which surface cover would substitute the area where the city is located in absence of urban structures.

This question leads to two different definitions of the UHI effect:

- Geographical definition: the substituting surface cover would be the same as the current surface cover of the surroundings (e.g. crops).
- Historical definition: the substituting surface cover would be the one that existed before the city was built (e.g. tropical forest).

Both definitions still face the difficulty of assessing the UHI effect without introducing uncertainty in the measurements. This uncertainty can be related to the micro-scale climate at the measurement location, to differences in mesoscale conditions between the rural site and the urban site (e.g. influenced by bodies of water or mountains), or to large time-scale changes in climate.

To be able to make progress, this thesis defines the UHI intensity as the difference in air temperature between a weather station and an urban site. Two different scales of UHI effect will be considered: the UHI effect at the urban boundary layer scale, which will be studied in chapter 7; and the UHI effect at the urban canopy layer scale. The following list, adapted from Kuttler (2008), summarizes the causes of UHI effect associated with each layer:

Urban boundary layer

- Anthropogenic heat from roofs and industry.
- Entrainment of heat from the urban canopy layer.
- Other meteorological effects.

Urban canopy layer

- Anthropogenic heat from building façades.
- Heat storage due to reduced albedo and massive urban structures.
- Longwave trapping at night due to reduced sky view factors.
- Lower evaporation due to the reduction of vegetated areas.
- Lower evaporation due to reduced absorption by the ground, as a result of increased run-off.
- Less removal of sensible heat due to lower wind speed in the canopy.

1.5.4. Atmospheric stability

Like most large-scale engineering flows, the atmosphere is nearly always turbulent. The atmospheric turbulence can be of two types, depending on the generating mechanism: mechanical turbulence and buoyant turbulence. Hanna and Britter (2002) define the term *stability* as the ratio of the suppression of turbulence by thermal effects to the generation of turbulence by mechanical effects such as wind shear. The stability of an airmass defines its ability to resist vertical motion. A stable atmosphere makes vertical movement difficult. In an unstable atmosphere, vertical air movements tend to become larger, resulting in turbulent airflow and convective activity.

1.5.5. Atmospheric inversion

Inversion refers to a situation when the actual temperature gradient is positive (i.e., the temperature increases with height). An inversion typically occurs near the ground surface during a clear night, due to longwave radiation exchange with the sky. An inversion is associated with stable conditions with little vertical turbulence and mixing. In the morning, the nocturnal inversion layer is eliminated and replaced by a neutral or unstable layer due to solar heating. Another type of inversion occurs at an elevation of about 1000 m and determines the top of the layer of air subjected to strong vertical mixing during the day. This latter inversion is called the *capping inversion.*

1.5.6. Potential temperature

The potential temperature is used in meteorology to account for the decrease in air temperature with height. As a parcel of air rises, it experiences an adiabatic expansion and a consequent lost of internal energy (i.e., temperature). As a result, in a neutral atmosphere, the temperature decreases with height at a rate of about 1 °C/100 m. The vertical gradient of *potential temperature*, $d\theta/dz$, is defined such that it equals the vertical gradient of actual temperature, dT/dz, plus 1 °C/100 m. Therefore, in a neutral atmosphere the vertical gradient of potential temperature is 0.0 °C/100 m.

1.5.7. Monin-Obukhov similarity theory

The *Monin–Obukhov similarity theory* (e.g. Hanna and Britter, 2002) is used in many transport and dispersion models to estimate winds, temperatures, and turbulence in the atmospheric boundary layer. This theory states that the mean wind, temperature profiles, and turbulent velocities in the boundary layer are determined by the friction velocity (u^*) and three scaling lengths: the roughness length (z_o), the displacement length (d), and the Monin-Obukhov length (L).

The *friction velocity* is defined as $u^* = \sqrt{\tau_o / \rho}$, where τ_o is the surface shear stress (Nm^{-2}) and ρ is the density of the air (kgm^{-3}). A rough rule of thumb is that the ratio u^*/u is about 0.05 to 0.1 (Hanna and Britter, 2002), where u is the local wind speed. The friction velocity u^* can be considered constant near the ground. Turbulent velocities are proportional to u^* in the urban canopy layer.

The *surface roughness length* is a measure of the amount of mechanical mixing introduced by the surface roughness elements and can be calculated as 0.1 the average height of obstacles (Hanna and Britter, 2002). The *displacement length* describes the vertical displacement (from the ground surface) of the effective ground level and is approximately equal to 0.5 the average height of buildings (Hanna and Britter, 2002). The *Monin–Obukhov length* accounts for the effects of stability and it is defined by the following expression:

$$L = -\frac{u^{*3} / \kappa}{g H_{surf} / (\rho c_p T)}, \tag{1.1}$$

where κ is the Von Kármán constant, H_{surf} is the turbulent heat flux from the surface (Wm^{-2}), g is the gravity acceleration (ms^{-2}), c_p is the specific heat of the air ($Jkg^{-1}K^{-1}$), and T is the air temperature (K).

Although the Monin-Obukhov similarity theory has been substituted by more sophisticated urban models to represent the effect of cities on the atmosphere, the parameters defined in this formulation are still used in current urban climate studies.

CHAPTER 2

State-of-the-art in urban modelling applied to buildings

2.1. Introduction

This chapter provides a theoretical background in urban climate studies applied to buildings. The objective is to explain some important concepts that will be used later in this thesis, as well as to present the modelling approaches that have inspired this work. This chapter will be useful for those readers with a building-oriented education who are seeking to understand the basics of current urban climate studies, as well as for starting urban climatologists looking for a summary of current urban climate studies from the building perspective.

The first section of this chapter is dedicated to the Cluster Thermal Time Constant (CTTC) model (Swaid and Hoffman, 1990). This model calculates urban air temperatures from air temperatures recorded at a meteorological station, applying very simple analytical expressions that take into account the storage and release of heat in the built area. The CTTC model has currently been replaced with more sophisticated models, but the idea of generating urban temperatures from meteorological information has been an important contribution.

The new generation of urban canopy models is based on the Surface Energy Balance (SEB) (Oke, 1988). This energy balance accounts for the area-averaged fluxes through the surface of an imaginary box which represents an urban canyon. Based on SEB, there are different urban canopy models reported in the literature, which can be based on physical or empirical approaches. The most important empirical urban canopy model is the Local-scale Urban Meteorological Parameterization Scheme (LUMPS) (Grimmond and Oke, 2002). The LUMPS calculates the energy terms of the SEB equation taking into account fundamental physical relations and applying empirical coefficients.

Physically based urban canopy models are significantly more complex than the empirical ones, but they do not require calibration of empirical parameters. These models compute the heat transfer involved in a two-dimensional representation of an urban canyon through the application of heat balances. Radiative exchanges are calculated based on view factors between urban surfaces, and heat storage is modelled by the heat conduction equation.

One of the most relevant urban canopy models is the Town Energy Balance (TEB) model (Masson, 2000), which has been improved and validated for almost one decade (Masson et al., 2002; Lemonsu et al., 2003; Pigeon et al., 2008). Still, the TEB model implements a simple representation of buildings, basically a transient conduction through a multi-layered wall and roof. Such other phenomena as transmission through windows, internal heat gains, and infiltration, as well as the calculation of cooling loads are not yet included. In order to better represent the building effect within urban climate studies, other authors have developed building parameterizations (e.g. Salamanca et al., 2009), which are simplified building models integrated in urban canopy models that are able to estimate building thermal loads. However, the computational restrictions of this integration require that these models remain fairly simple, which limit their application to building performance evaluations.

A more effective coupling method uses the urban model to modify the weather information that the building simulation uses as input. This method was suggested by the CTTC model

and was finally implemented by the Canyon Air Temperature (CAT) model (Erell and Williamson, 2006). The CAT model, based on the LUMPS, is able to generate site-specific temperature data series from meteorological weather files. Then, this information can be used as input for building simulations. One of the main limitations of the CAT model is its empirical nature, since it requires the calibration of some parameters at the location of analysis. It also lacks an energy definition of the buildings in the urban site, which limits the evaluation of the interactions between buildings and their urban environment.

2.2. The Cluster Thermal Time Constant (CTTC) model

The analytical Cluster Thermal Time Constant (CTTC) model was initially proposed by Swaid and Hoffman (1990) and has been subsequently developed and expanded in a series of papers. The Green CTTC model (Shashua-Bar and Hoffman, 2002) was released later to account for the effect of urban vegetation, but it incorporated an empirical approach that proved to be too dependent on local experiments.

A modified version of the CTTC model was proposed by a different research group to extend its applicability to a wider range of weather conditions and urban landscapes (Elnahas and Williamson, 1997). The main modification consisted of using hourly air temperature data measured at a reference weather station to establish boundary conditions for the model. In contrast, the previous CTTC model used a fixed reference temperature representing the regional mesoscale conditions. Later publications from both research groups showed a lively discussion about the suitability of the two alternative approaches (Erell and Williamson, 2006b).

The improved CTTC model of Elnahas and Williamson has already been overtaken by a more sophisticated urban canopy model that abandoned the CTTC methodology of describing the heat flux and storage characteristics of the canyon surfaces in favour of empirical parameterizations based on the LUMPS (Grimmond and Oke, 2002). This is the Canyon Air Temperature (CAT) model (Erell and Williamson, 2006) described in section 2.4.

Still, the CTTC model has made the important contribution of providing the basis of an analytical methodology that can be used for the calculation of urban temperatures from measured data in a meteorological station.

2.2.1. The original CTTC model

The CTTC model was developed for predicting air temperature variations in the urban canopy layer, compared with a reference or rural constant temperature. The developed theory is based on the concept of the Surface Thermal Time Constant (STTC) previously published by the same authors (Swaid and Hoffman, 1989). The model considers the urban area as a single body characterized by a CTTC parameter, which represents the thermal inertia of urban soil and constructions.

Assumptions

Swaid and Hoffman described the assumptions and constraints of the CTTC model as:

- There is a predominance of fair-weather conditions, i.e. clear skies and light to moderate winds.
- Buildings and surface characteristics are spatially homogeneous.

- The solar radiation absorption of roof surfaces and their thermal mass do not affect diurnal variations of air temperature inside the urban canopy.
- The urban canopy air volume is well mixed.
- Green space fraction and anthropogenic heat addition are not included.

It is interesting to note that modern urban canopy models maintain many of these assumptions.

Formulation

The original formulation of the CTTC model calculates the difference in urban air temperature due to the solar radiation and the longwave radiation (Eq. 2.1). These two terms are added to a constant base temperature taken as the mean daily rural air temperature. The general expression can be written as:

$$T_{urb}(t) = T_{ref} + \Delta T_{sol}(t) - \Delta T_{lw}(t) \quad , \tag{2.1}$$

where T_{urb} is the urban air temperature, T_{ref} is the base temperature, $\Delta T_{sol}(t)$ is the time dependent contribution of solar radiation, and $\Delta T_{lw}(t)$ is the time dependent contribution of net-longwave radiation. These two contribution terms are given by the following equations:

$$\Delta T_{sol}(t) = \sum_{\lambda=0}^{t} \frac{m\Delta I_{pen}(\lambda)}{h}\left[1 - \exp\left(-\frac{t-\lambda}{CTTC}\right)\right], \tag{2.2}$$

$$\Delta T_{lw}(t) = \frac{\left(\sigma T^4 - \sigma Br T^4\right) SVF}{h}, \tag{2.3}$$

where m is the solar absorptivity of the surface, $\Delta I_{pen}(t)$ is the step-change in the mean magnitude of solar radiation received at ground surface (Wm^{-2}), h is the surface convective heat transfer coefficient ($Wm^{-2}K^{-1}$), σ is the Stefan–Boltzmann constant ($Wm^{-2}K^{-4}$), T is the air temperature, Br is the Brunt number or effective emissivity of the atmosphere, SVF is the sky view factor of the street canyon, and CTTC is the cluster thermal time constant (s) defined as the heat energy stored in the participating built layer per unit change in the heat flux through it.

Note that in equations (2.2) and (2.3), the solar term and the longwave term are inversely proportional to the convective heat transfer coefficient (h). As a result, the CTTC model is highly sensitive to this parameter, which can vary significantly depending on the thermal and dynamical conditions of the urban canopy. Available correlations to predict convective heat transfer coefficients are far from covering the large variability of conditions existing in urban contexts. This represents a limitation to the practical implementation of the CTTC model.

Coming back to Eq. (2.1), the base temperature (T_{ref}) appears as another undetermined parameter. Swaid and Hoffman suggested two methods for estimating this base temperature: (1) equating it to the mean daily air temperature measured at a representative rural meteorological station; or (2) calculating it by solving Eq. (2.1), using the measured minimum air temperature at the site and the predicted values of the parametric factors

$\Delta T_{sol}(t)$ and $\Delta T_{lw}(t)$ at that time. In either case, the base temperature is constant during the whole period simulated, typically 24 h.

Theoretical background

The CTTC model is an analytical transformation of a heat balance at the surface of the ground when, at time $t = 0$, a step change of magnitude in incident solar radiation ΔI occurs. After that, the ground surface temperature and air temperature rise until a new thermal equilibrium is reached. This surface heat balance can be expressed as:

$$-k\left.\frac{\partial\theta(x,t)}{\partial x}\right|_{x=0} = m\Delta I + h[T(t)-\theta_s(t)] - I_{lw}(t)\ , \tag{2.4}$$

where θ is the temperature of the ground at a depth x, and θ_s is the surface temperature of the ground. The left-hand side of Eq. (2.4) represents the conduction from the surface to the ground (storage), while the right-hand side represents the ground absorption of solar radiation, the convective heat flux, and the net-longwave radiation flux exchange between the surface and the atmosphere.

The air temperature (T) is then expressed as the sum of a base temperature (T_1) and a temperature rise ($\Delta T''(t)$) in response to the step change in solar radiation, as follows:

$$T(t) = T_1 + \Delta T''(t)\,. \tag{2.5}$$

The authors proved that the temperature difference ($\Delta T''(t)$) can be expressed by an exponential response function, namely:

$$\Delta T''(t) = \frac{m\Delta I}{h}\left[1-\exp\left(-\frac{t}{CTTC}\right)\right]. \tag{2.6}$$

Likewise, the air temperature rise in a built-up environment in response to a series of changes in solar radiation intensity can be obtained applying superposition in a summation form, as given in Eq. (2.2).

The CTTC parameter, representing the inertia of the active thermal mass to air temperature variations, is constant for a given construction. The authors stated that it was always possible to find a homogeneous equivalent construction (road or walls) subject to the same depth of penetration as a multilayered construction, so layered constructions have one characteristic CTTC. An experimental procedure was proposed to determine the CTTC parameter of existing clusters in Tel-Aviv. As a result, they proposed a CTTC value of 8h for massive external walls, while less massive ones received a value of about 6h.

The characteristic CTTC value of a built-up environment can be evaluated averaging the characteristic CTTC values of walls and ground, according to their relative external area, as follows:

$$CTTC = (1-FA/S)CTTC_{ground} + (WA/S)CTTC_{walls}\,, \tag{2.7}$$

where (1 - FA/S) is the partial open-space area (streets and courtyards) and (WA/S) the external wall area relative to the plot area.

In order to visualize the effect of the CTTC parameter, Fig.2.1 represents the solar radiation term, $\Delta T_{sol}(t)$, in Eq. (2.2), for a typical day in summer, applying different values of the CTTC parameter.

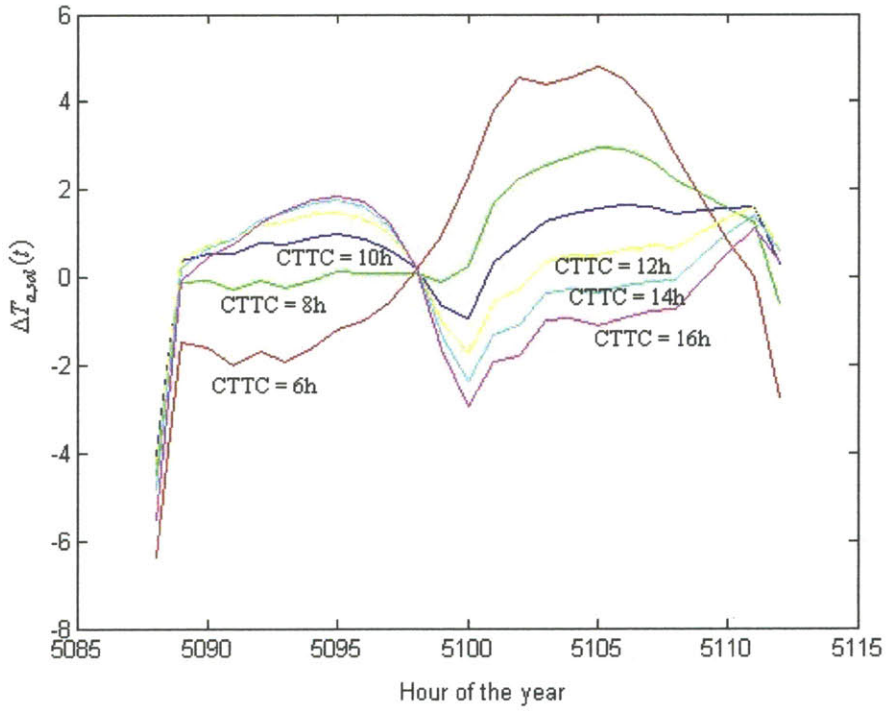

Fig.2.1: Solar radiation term, $\Delta T_{sol}(t)$, for a day in summer, given different values for the CTTC parameter: 6 h, 8 h, 10h, 12h, 14h, 16h.

It can be seen that for low values of the CTTC parameter, the increase in air temperature is in phase with the solar heat wave (the graph starts at midnight); while for higher values of the CTTC parameter, there is a shift in the response compared to the excitation. It can also be observed that for low values of the CTTC parameter, the influence on the solar term is important; while for higher values, the model is less sensitive to this parameter.

The longwave radiation term $\Delta T_{lw}(t)$ in Eq. (2.3) is obtained assuming a balance between the longwave heat flux and the convective heat flux. The mean outgoing longwave radiation flux in the urban canopy, I_{lw} (Wm^{-2}) is calculated from the Stephan-Boltzmann law, as follows:

$$I_{lw}(t) = \left(\sigma T^4 - \sigma Br T^4\right) SVF, \qquad (2.8)$$

where σ is the Stefan–Boltzmann constant, T_a is the air temperature, Br is the Brunt number, and SVF is the sky view factor of the street canyon.

2.2.2. The improved CTTC model

The original formulation of the CTTC model is based on predicting the contribution to the mean diurnal rural air temperature of the solar radiation and the longwave exchange. Elnahas and Williamson (1997) proposed a modified version of this model that uses hourly values of air temperatures recorded at a weather station instead of a constant reference temperature. The restriction imposed by the original formulation of fair weather conditions is also relaxed to account for other weather conditions.

The modified CTTC model established that the original CTTC model could be applied in both an urban site and a meteorological station. Then, assuming the same base temperature representing the mesoscale conditions in both locations, the air temperature at the urban site could be calculated as:

$$T_{urb}(t) = T_{met}(t) + (\Delta T_{urb,sol}(t) - \Delta T_{met,sol}(t)) \\ -(\Delta T_{urb,lw}(t) - \Delta T_{met,lw}(t)) \quad , \tag{2.9}$$

where the subscripts *urb* and *met* represent the conditions at the urban site and at the meteorological station, respectively.

Another modification to the original CTTC formulation is the calculation of the longwave radiation term. In the improved model, the effect of clouds on the longwave radiation term ($\Delta T_{lw}{}^{*}(t)$) is taken into account by the following expression:

$$\Delta T_{lw}{}^{*}(t) = \Delta T_{lw}(t)(1 - bc^2), \tag{2.10}$$

where c is the cloud cover on a scale from zero to unity, and b is a coefficient used to allow for decreasing cloud temperature with height.

2.3. Urban canopy models

2.3.1. The surface energy balance (SEB)

The surface energy balance (SEB) computes the area-averaged fluxes through the surface of an imaginary box that represents an urban canyon (Oke, 1988). The top of the box is a horizontal plane at a reference height above the urban canyon, and the sides and the base of the box lies at a depth in the urban surfaces such that there is no net flux over the period of reference (Fig.2.2). Then the balance is written as:

$$Q^{*} + Q_F = Q_H + Q_E + \Delta Q_S + \Delta Q_A, \tag{2.11}$$

, where

Q^{*} - Net all-wave radiation flux (W)

Q_F - Anthropogenic heat flux (W)

Q_H - Turbulent sensible heat flux (W)

Q_E - Turbulent latent heat flux (W)

ΔQ_S - Flux due to the net heat storage change (W)

ΔQ_A - Advection heat flux (W)

Terms are positive when they are an energy source for the surface. The available energy (Q^* + Q_F - ΔQ_S) goes to the atmosphere, either through vertical turbulent exchanges of sensible heat (Q_H) or latent heat (Q_E). The advection term (ΔQ_A) represents the heat transport due to the mean flow from the external environment. This heat transport can be accomplished by a longitudinal flow through the ends of the canyon air volume or by a transversal flow at the top of the canyon (Fig.2.2). The advection term is often neglected in urban models (e.g. Grimmond and Oke, 2002).

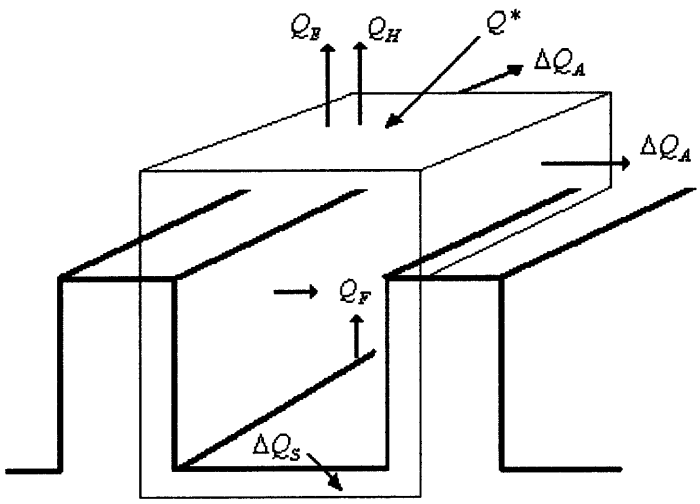

Fig.2.2: Representation of the surface energy balance of an urban canyon.

2.3.2. Empirical urban canopy models. The Local-scale Urban Meteorological Parameterization Scheme (LUMPS)

Empirical models correlate the different energy terms in the SEB equation (Eq. 2.11) by identifying the physical variables relevant to each phenomenon, and applying coefficients of proportionality based on observed data. The resulting equations are often easy to compute, and once calibrated are able to make a good estimation of urban meteorological conditions. However, their application is limited to the range of conditions (land cover, climate, season, etc.) encountered in their original studies, although some studies recommend values of the empirical parameter for a wider range of situations.

One of the most evaluated and comprehensive empirical scheme is the LUMPS (Grimmond and Oke, 2002). This model can be summarized as:

- The net radiation term (Q^*) is calculated from the incoming solar radiation, the air temperature, the relative humidity, and surface radiative properties.
- The heat storage term (ΔQ_S) is estimated with the Objective Hysteresis Model (Grimmond et al., 1991) as a function of Q^*, and needs three coefficients empirically calibrated.

- The turbulent fluxes (Q_H, Q_E) are calculated in terms of Q^* and ΔQ_S, and require two more empirical parameters.

Formulation

The surface sensible and latent heat fluxes (Q_H, Q_E) are parameterized as a function of the net radiant balance (Q^*) and the storage flux (ΔQ_S). The specific relations used in LUMPS are

$$Q_H = \frac{(1-\alpha)+(\gamma/s)}{1+(\gamma/s)}(Q^*-\Delta Q_S)-\beta, \tag{2.12}$$

and

$$Q_E = \frac{\alpha}{1+(\gamma/s)}(Q^*-\Delta Q_S)+\beta, \tag{2.13}$$

where s is the slope of the saturation vapour pressure-versus-temperature curve, γ is a constant, and α and β are empirical parameters. The heat storage term ΔQ_S is also parameterized in terms of the net all-wave radiation (Q^*), as follows:

$$\Delta Q_S = \sum_{i=1}^{n}(f_i a_{1i})Q^* + \sum_{i=1}^{n}(f_i a_{2i})\left(\frac{\partial Q^*}{\partial t}\right) + \sum_{i=1}^{n}(f_i a_{3i}), \tag{2.14}$$

where n is the number of surface types within the area of interest, and f is the fraction of each surface type. a_1, a_2 and a_3 are empirical coefficients.

Theoretical background

The expressions for the surface heat fluxes (Eqs. 2.12 and 2.13) come from the SEB equation (Eq. 2.11). Neglecting advection and anthropogenic heat, the sum of the sensible and latent heat fluxes is given by:

$$Q_H + Q_E = Q^* - \Delta Q_S, \tag{2.15}$$

Assuming that the net-radiation term can be evaluated from cloud cover, air temperature and global radiation using semi-empirical relations, the problem is reduced to the determination of the split of the available energy into sensible and latent components. Priestly and Taylor (1972) proposed the following expressions for this partitioning:

$$Q_H = \frac{(1-\alpha)s+\gamma}{s+\gamma}(Q^*-\Delta Q_S), \tag{2.16}$$

and

$$Q_E = \alpha\frac{s}{s+\gamma}(Q^*-\Delta Q_S), \tag{2.17}$$

where α is the Priestly-Taylor parameter. Bruin and Keijman (1982) demonstrated that Priestly-Taylor's concept caused a relatively large error in Q_H, and they proposed a two-parameter approach, which is the one incorporated by LUMPS in equations (2.12) and (2.13).

The expression for the heat storage term (Eq. 2.14) is taken from the Objective Hysteresis Model (OHM) of Grimmond et al. (1991). The background of this model comes from the assumption used in old mesoscale models that the surface heat storage is proportional to the net-radiation ($\Delta Q_S = aQ^*$). Later on, further studies proved that there was a non-linear relation between ΔQ_S and Q^* that gave a hysteresis loop if ΔQ_S was plotted as a dependent variable of Q^* (Fig.2.3). This behavior can be explained considering the charge and discharge of a thermal mass exposed to variable surface radiation heat flux.

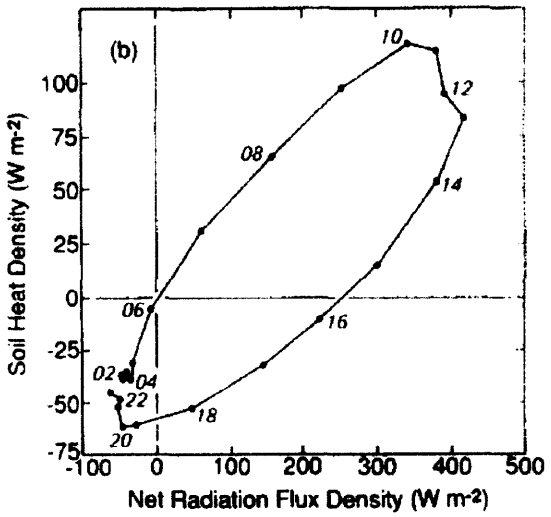

Fig 2.3: Hysteresis loop between the heat storage term and the net-radiation term (*Grimmond et al., 1991*).

The hysteresis effect can be represented by the following equation:

$$\Delta Q_S = a_1 Q^* + a_2 \frac{\partial Q^*}{\partial t} + a_3, \tag{2.18}$$

where $a_1, a_2(s)$, and $a_3(W)$ are empirical parameters. This equation was then expanded by LUMPS in Eq. (2.14).

Limitations

According to the authors, in the situations in which the effects of wind and large sources of anthropogenic heat are important, LUMPS does not give adequate results. Moreover, due to the assumption of a one-dimensional energy balance, LUMPS does not perform well in areas of significant spatial variability of land cover and building morphology. In addition, a comparative study (Robert et al., 2006) has proven that, in general, LUMPS shows worse performance than physically based urban canopy models.

2.3.3. Physically based urban canopy models

Physically based urban canopy models are also based on the SEB equation, but they apply heat balances to a realistic quasi-three-dimensional urban canopy (considering the solar radiation evolution as three-dimensional). All these models share the following features:

- Two-dimensional geometric representation of an urban canyon.
- Separate energy balances for roofs, roads, and walls.
- Explicitly solved radiative interactions between road, walls and sky.

These models use a relatively simple methodology to compute the complex radiative exchanges that occur in the urban canopy, based on view factors between the different urban surfaces. Heat storage in urban structures is modelled by the heat conduction equation for a multilayered construction.

Urban canopy models can be classified into single-layer and multi-layer schemes. In a multi-layer approach, the boundary conditions of the urban model are provided at different vertical levels inside the urban canyon, generally by a mesoscale model. This approach allows a higher resolution of atmospheric processes, but it requires a fine discretization of the mesoscale model near the surface, which significantly increases the computational cost of simulations. In contrast, in a single-layer approach, the boundary conditions are defined at a reference height above the urban canyon. This reference level is supposed to be above the urban canopy layer, typically about twice the average building height. This approach has the advantage of simplicity and transferability, but implies that the air conditions inside the urban canyon have to be specified. Generally, logarithmic and exponential laws are used for the wind, and air temperature and humidity are assumed to be uniform in the canyon. Advanced single-layer schemes are now implementing the fine description of air profiles near the ground of the multi-layer schemes (Fig. 2.4).

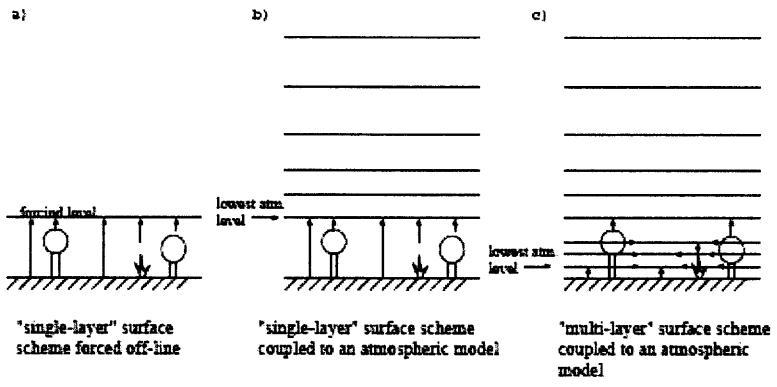

Fig. 2.4: Schematic view of surface scheme coupling: a) single-layer scheme forced offline; b) single-layer scheme forced by a mesoscale model; c) multi-layer scheme forced by a mesoscale model (*Le Moigne., 2009*).

The Town Energy Balance (TEB) scheme of Masson (2000) is the most developed single-layer urban canopy model. The difference with other single-layer models is that it uses only one generic roof, one generic wall and one generic road. Averaging is performed over all directions in order to keep only these generic surfaces. Kusaka et al. (2001) proposed an urban canopy model similar to TEB, but it incorporated solar calculations for specific orientations of the urban canyon. The most developed multi-layer urban canopy model was proposed by Martilli et al. (2002).

2.3.4. Building parameterizations

Urban canopy models are generally implemented with a simple representation of the building energy performance. In the case of the TEB model, a transient conduction equation through a multi-layered wall and roof is solved, and the force-restore method is applied to calculate indoor conditions from the contributions of the different building surfaces. Further developments of the TEB model include a minimum threshold of 19°C to calculate the heating loads of the building associated with transmission through building surfaces (Pigeon et al., 2008). However, such other phenomena as transmission through windows, internal heat gains, and infiltration, as well as the calculation of cooling loads are not yet included.

A further step in representing the effects of buildings on urban climate was carried out by Kikegawa et al. (2003), who implemented a simplified building energy model in an urban canopy parameterization for mesoscale models. In addition to solving the diffusion equation in walls and glazing, this model took into account the internal sources of heat, the transmitted solar radiation through windows, the longwave radiation exchange among interior surfaces, and the thermal load due to ventilation.

Applying sensible and latent energy balances (Eqs. 2.19 and 2.20), the model was able to estimate the energy demand required to maintain certain indoor conditions. In order to evaluate the energy consumption of the HVAC system and, eventually, the heat released from outside equipment, the model applied a constant coefficient of performance (COP).

The time evolution of zone air temperature (T_z) and zone air humidity (q_z ($kg_w kg_{air}^{-1}$)) is calculated in this model through the following sensible and latent heat balances:

$$\rho c_p V_B \frac{dT_z}{dt} = H_{in} - H_{out}, \tag{2.19}$$

and

$$\rho l V_B \frac{dq_z}{dt} = E_{in} - E_{out}, \tag{2.20}$$

where V_B is the total air volume of the building (m^3), ρc_p is the volumetric heat capacity of the air ($Jm^{-3}K^{-1}$), and ρl is the volumetric latent heat of the air($Jm^{-3}kg_{air}kg_w^{-1}$). The terms H_{out} and E_{out} represent the sensible and latent heat fluxes supplied by the HVAC system (W). The terms H_{in} and E_{in} take into account the contribution of convection heat transfer from surfaces (*conv*), the thermal loads from ventilation (*vent*), and the internal gains (*int.gains*). This can be expressed by the following heat and mass balances:

$$H_{in} = \sum_j H_{conv} + H_{vent} + H_{\text{int}.gains}, \tag{2.21}$$

and

$$E_{in} = E_{vent} + E_{\text{int}.gains}. \tag{2.22}$$

Recently, Salamanca et al. (2009) developed a new building energy model, similar to that of Kikegawa et al. (2003), coupled with a multi-layer urban canopy model (Martilli et al., 2002). This model allows the definition of multiple-story buildings and incorporates a more detailed

algorithm to calculate the solar radiation through windows and its distribution among indoor surfaces. Furthermore, the model allows free evolution of indoor air temperature, and the definition of a range of comfort.

Although important improvements are being implemented to current building parameterizations, they are still not comparable to detailed building simulation programs. Building parameterizations are computationally restricted, since they are intended to be integrated with mesoscale models. Therefore, they tend to reduce complexity and make generalizations, which limit their accuracy in predicting both the effect of climate on building energy performance, and the effect of buildings on climate. This thesis proposes an alternative method, where an urban canopy model is externally coupled with a widely used building simulation program. This approach takes advantage of many years of experience in building modelling, and it is able to include much more detail in the energy definition of a building than current building parameterizations, while keeping the computational cost relatively low.

2.4. The Canyon Air Temperature (CAT) model

The Canyon Air Temperature (CAT) model was proposed in a PhD thesis (Erell, 2005), and published in a subsequent paper (Erell and Williamson, 2006). The relevance of this model to the present work is that it shares the same objective of obtaining urban weather files from meteorological recorded data applicable to building energy simulations. However, the method used here is different.

The CAT model uses the SEB concept (section 2.3.1) to calculate the sensible heat exchange between an urban canyon and the atmosphere, and then estimates urban air temperatures applying the CTTC approach of comparing a rural site with an urban site. The sensible heat flux is calculated from LUMPS (see section 2.3.2), and it needs the net-radiation and heat storage terms. It also allows adding an anthropogenic heat term to the sensible heat balance, but it does not specify how to calculate it. Special attention was paid to the calculation of convective heat transfer coefficients and urban wind speeds, as is described in this section.

The CAT model has been validated in a few cities, including an important experimental campaign in Adelaide, and, more recently, in Gothenburg, where the model improved the parameterization of turbulent heat fluxes to account for humid conditions. However, its application still entails important limitations, mostly due to the empirical nature of the model, but also because it does not take into account the heat transfer processes inside buildings. As a result, this model is very limited for evaluating the climate effect on building performance, and it cannot calculate the effects of building configurations on urban climate.

2.4.1. Radiative heat fluxes

The net-radiation term (Q^*) of the SEB equation is calculated in CAT by splitting it into a solar term, an incoming longwave radiation term, and an outgoing longwave radiation term.

The solar radiation incident on a surface is calculated from the measured solar radiation, applying a sky view factor, and adding the first reflection of solar radiation on the other surfaces of the urban canyon. This can be expressed as:

$$I(t) = I_{dir}(t)(1 - PSA(t)) + I_{dif}(t)\psi_{sky} + \sum_j I_{dir+dif-j}(t)(1 - m_j)(\psi_{i-j}), \quad (2.23)$$

where

$I(t)$ - Mean hourly total solar radiation incident on the surface (Wm^{-2})

$PSA(t)$ - Partial shaded fraction of the surface

$I_{dir}(t)$ - Hourly mean unobstructed direct component of the solar radiation (Wm^{-2})

$I_{dif}(t)$ - Hourly mean unobstructed diffuse component of the solar radiation (Wm^{-2})

ψ_{sky} - Mean sky view factor of the surface.

$I_{dir+dif-j}$ - Combined direct and diffuse components of the solar radiation from surface j (Wm^{-2})

ψ_{i-j} - View factor between two surfaces

m_j - Solar absorptivity of surface j

The incoming longwave radiation (L_i (Wm^{-2})) is calculated from the dry bulb temperature of the air and from the atmospheric humidity, applying the following correlation:

$$L_i = \sigma \varepsilon_{sky} T^4, \quad (2.24)$$

where σ is the Stefan-Boltzmann constant; ε_{sky} is the sky emissivity, calculated from the partial water vapor pressure of air; and T is the air temperature.

The outgoing longwave radiation (L_o) is calculated by an implicit procedure, involving the concept of "sol–air temperature." The sol-air temperature is defined as the equivalent outdoor temperature that would cause the same surface heat flux as that caused by the actual outdoor air temperature and the net-radiation exchange with the environment. This can be expressed as:

$$T_{sol} = T + \frac{S_i m + \varepsilon_{surf} L^*}{h}, \quad (2.25)$$

where T_{sol} is the sol-air temperature, T is the air temperature, S_i is the incoming shortwave radiation (Wm^{-2}), m is the shortwave absorptivity of the surface, ε_{surf} is the longwave emissivity of the surface, L^* is the net-longwave radiation at the surface ($L_i - L_o$) (Wm^{-2}), and h is the surface convective heat transfer coefficient.

Surface temperature is approximated by this definition of the sol-air temperature, and the outgoing longwave radiation is obtained by iterative calculation of the expression above. The contributions of the ground surface and vertical surfaces of the canyon are calculated separately taking into account their respective view factors to the sky.

2.4.2. Heat storage and surface heat fluxes

The CAT model applies the LUMPS (see section 2.3.2) to calculate the heat storage term (Eq. 2.14). Then, this term is used together with the net-radiation to obtain the surface heat flux terms (Eqs. 2.12 and 2.13).

2.4.3. Urban air temperature

The urban air temperature is calculated from the sensible heat exchange between the canopy and the mixed layer above it. This relation is expressed in terms of a bulk aerodynamic formulation, of general form:

$$Q_H = \Delta T / R, \tag{2.26}$$

where Q_H is the sensible heat flux per unit area (Wm^{-2}), obtained from the sum of the contributions of the individual surfaces comprising the envelope of the site, weighted by their respective areas; ΔT is the temperature difference between the urban air temperature and the air temperature at the reference level; and R is an aerodynamic resistance ($W^{-1}m^2K$) expressed as the inverse of a convective heat transfer coefficient.

The change in air temperature is calculated for both the urban site and the reference site, taking into account their local characteristics. Then, the air temperature in the urban canyon is calculated applying the same concept as in the improved CTTC model (see section 2.2.2). Eq. (2.9) is therefore transformed into:

$$T_{urb}(t) = T_{met}(t) + (\Delta T_{urb}(t) - \Delta T_{met}(t)), \tag{2.27}$$

where the subscript *urb* refers to the urban site, and the subscript *met* refers to the reference site or meteorological station.

2.4.4. Convective heat transfer coefficients

The convective heat transfer coefficients used to obtain the aerodynamic resistances (Eq. 2.26) are calculated as:

$$h_{hor} = 3.96U + 6.42, \tag{2.28}$$

and

$$h_{ver} = 10.2U + 4.47, \tag{2.29}$$

where U is the modulus of the wind vector (ms^{-1}). These expressions were obtained experimentally by Hagishima et al. (2003) on vertical and horizontal building surfaces in an urban site. The linear relation between the convection coefficients and the wind speed agrees with the expressions used in other urban canopy models (i.e. Masson, 2000; Martilli et al., 2002). In contrast, EnergyPlus™ proposes a relation proportional to the square root of the wind speed, which gives quite different convective heat transfer coefficients for the same problem. These differences will be discussed in more detail in section 4.3.5.

2.4.5. Urban wind speeds

The CAT calculates the wind speed inside the urban canyon based on a formulation by Yamartino et al. (1986). This formulation assumes that the transverse and longitudinal components of the wind speed are decoupled. The longitudinal component (v_{can}) is calculated using the following logarithmic profile:

$$v_{can}(z) = v_a \log\left[\frac{z + z_o}{z_o}\right] / \log\left[\frac{z_{ref} + z_o}{z_o}\right], \tag{2.30}$$

where v_a is the component of the wind speed along the urban canyon at a reference height above it, z is the vertical position inside the canyon, z_{ref} is the reference height, and z_o is the roughness length. The transverse component (u_{can}) is divided into a horizontal direction and a vertical direction (Fig.2.5), assuming a vortex is formed inside the canyon. The resulting expressions have a sinusoidal form, and depend on the geometry of the urban canyon. These are

$$u_{can}(x,z) = u_a \gamma(w,h;z)\sin(kx), \tag{2.31}$$

and

$$w_{can}(x,z) = -u_a \beta(w,h;z)\cos(kx), \tag{2.32}$$

where γ and β depend on the height (h) and width (w) of the urban canyon, x is the transverse direction, and u_a is the transverse component of wind speed at the reference height above the canyon.

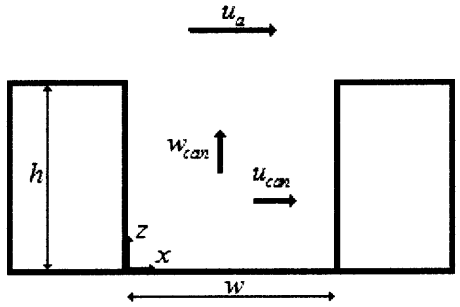

Fig.2.5: Schematic representation of air velocities inside the canyon.

CHAPTER 3

The Urban Weather Generator (UWG) scheme

3.1. Introduction

This chapter analyzes the structure and operation of the UWG scheme. The process of transforming recorded meteorological information into urban weather information is carried out in three stages, and four modules or subprograms must interact with each other. The chapter starts presenting the meteorological information used in the scheme and the conversion of data formats required to establish a communication among modules. Then, the three steps of the UWG scheme are described, and an outline of each module is presented. The next section defines the information flow among modules. Then, the two iterative procedures required in the first and the third stages of the scheme are explained. Finally, some guidelines about how to prepare a case study for UWG simulations are presented.

3.2. Weather data files and formats

The UWG scheme starts reading an EnergyPlus™ weather (*epw*) file. There are *epw* files available for many cities in the world, and they can be downloaded from the web-site of EnergyPlus (http://apps1.eere.energy.gov/buildings/energyplus/). These weather data files have a text-based format and contain hourly values of meteorological variables for a Typical Meteorological Year (TMY). In TMY2 and TMY3 formats, weather files are built from representative days and months assembled from recorded data over a number of years.

The meteorological variables contained in an *epw* file are listed in Table 3.1 (DOE, 2009b):

Table 3.1: Meteorological variables in a *epw* file

Field	Variable	Unit
N6	**Dry Bulb Temperature**	*°C*
N7	**Dew Point Temperature**	*°C*
N8	**Relative Humidity**	*%*
N9	**Atmospheric Station Pressure**	*Pa*
N10	Extraterrestrial Horizontal Radiation	
N11	Extraterrestrial Direct Normal Radiation	
N12	**Horizontal Infrared Radiation Intensity**	Wh/m^2
N13	Global Horizontal Radiation	
N14	**Direct Normal Radiation**	Wh/m^2
N15	**Diffuse Horizontal Radiation**	Wh/m^2
N16	Global Horizontal Illuminance	
N17	Direct Normal Illuminance	
N18	Diffuse Horizontal Illuminance	
N19	Zenith Luminance	
N20	**Wind Direction**	°
N21	**Wind Speed**	*m/s*
N22	**Total Sky Cover** (used if Horizontal IR Intensity missing)	
N23	**Opaque Sky Cover** (used if Horizontal IR Intensity missing)	
N24	Visibility	
N25	Ceiling Height	
N26	**Present Weather Observation**	-
N27	**Present Weather Codes**	-
N28	Precipitable Water	
N29	Aerosol Optical Depth	
N30	Snow Depth	
N31	Days Since Last Snowfall	
N33	**Liquid Precipitation Depth**	*mm/h*

The variables highlighted in bold indicate that they are currently used by EnergyPlus and by the UWG scheme. It is important to note that precipitation data is often missing in *epw* files. This fact has a significant effect on the latent heat calculations carried out by the surface climate models used in the UWG scheme. Updated *epw* files have started to include this information, which is currently available for US cities. The effect of snow is not considered in the current version of the UWG scheme.

As we will see in the following sections, the UWG scheme includes two surface climate schemes, a vegetation model and an urban canopy model, which are part of an integrated program called SURFEX, developed by the *Centre National de Recherches Météorlogiques* (CNRM, France) to compute energy and mass exchanges between the planetary surface and the atmosphere. SURFEX schemes can also be initialized by hourly values of meteorological information in text-format files, but each variable has to have a separate file. Most SURFEX meteorological variables are the same as the *epw* variables listed above, so they can be directly converted. One exception is the air humidity, which in SURFEX is represented by specific humidity (*kg/kg*) instead of by relative humidity (%). Therefore, the format conversion procedure has to include psychrometric transformations. Another difference is that the output of wind speed from SURFEX calculations is expressed in terms of its two components (u,v), instead of by a module and a direction. The format conversion routines used in the UWG scheme are detailed in appendices A and B. Although all the above mentioned meteorological variables are used in the UWG scheme, only the air temperature,

air humidity, wind speed, and atmospheric pressure are transformed by the different modules of the scheme from the meteorological station to the urban site.

3.3. Meteorological transformation from a weather station to an urban site

The transformation of meteorological information from a weather station to an urban site is represented in Fig.3.1.

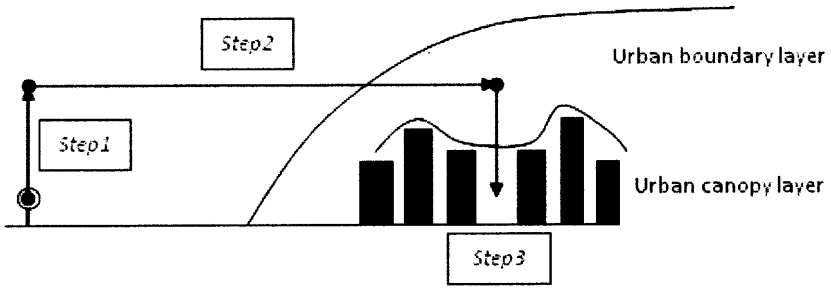

Fig.3.1: Meteorological transformation from a weather station to an urban site.

Step1 applies a vegetation module to transform the measured meteorological variables of an *epw* file into meteorological conditions at a certain height above the weather station. This reference height is imposed by the characteristics of the urban site. Typically, a reference height of twice the average building height is used, but it is recommended to analyze the sensitivity of the simulations to this parameter in each new case study (see, for example, section 8.4.6).

Step2 is a horizontal transformation that accounts for the UHI effect inside the urban boundary layer (see section 1.5.2). Given the meteorological conditions at a certain height above the weather station, it calculates the conditions above the urban canopy layer.

Once we have the conditions above the urban canopy layer at the location of the analysis, we can apply a physically based urban canopy model (see section 2.3.3) to calculate the conditions inside the urban canyon. Then, this information can be used by a building simulation program to analyze the energy performance of the buildings in that location. The premise of the UWG scheme is that, at the same time a building is affected by its surrounding weather conditions, the urban climate around a building is also affected by its energy performance.

Step3 is, therefore, an iterative procedure between an urban canopy model and a building simulation program. The interaction between these two models is the core idea of the UWG scheme. This step constitutes a building parameterization like the ones presented in section 2.3.4, but with the advantage of incorporating all the modeling possibilities of an advanced building simulation program. This new building parameterization could be also coupled with a mesoscale model, increasing the accuracy of low-atmosphere calculations in cities. This approach departs from the scope of this thesis but leaves the door open for further applications of the UWG concept.

3.4. UWG modules

The UWG scheme is composed of the four modules presented here, which are described in detail in the following chapters.

3.4.1. Vegetation scheme at the weather station

Step1 of the UWG procedure is carried out by the Interaction Soil Biosphere Atmosphere (ISBA) model (Noilhan and Planton, 1989). The ISBA module computes the exchanges of heat and water between the low-level atmosphere, the vegetation, and the soil at the weather station (see chapter 6).

3.4.2. Mesoscale correlations

Step2 of the UWG procedure accounts for the UHI effect at the urban boundary layer level. In the situations where this effect is important, simplified mesoscale correlations are applied. The model distinguishes between a natural convection and a forced convection dominated problem. For the first situation, the work of Lu et al. (1997) and Hidalgo et al. (2009) are adapted to this particular problem. For the second situation, a new correlation is proposed (chapter 7). All these correlations still require validation with field data in order to be definitively implemented in the UWG scheme. This validation is left for further developments of the scheme.

3.4.3. Urban canopy model

Step3 of the UWG procedure is performed through an iterative process between an urban canopy model and a building energy model. The urban canopy model used here is a modified version of the Town Energy Balance (TEB) model (Masson, 2000). The TEB model considers a two-dimensional approximation of an urban canyon and calculates air temperature, air humidity and wind speed inside the canyon, given the meteorological conditions above the urban canopy (see chapter 5). The modified version of TEB, instead of solving the energy problem inside buildings, uses the information provided by the building energy model as boundary conditions for its calculations.

3.4.4. Building energy model

The second module that plays a role in step3 is a building simulation program. The UWG scheme uses EnergyPlus™ (EP) to solve the heat and mass transfer processes that occur inside buildings (see chapter 4), as well as to predict the energy performance of HVAC systems, if defined. EP has been developed and validated for more than a decade, and it is considered the state-of-the-art in building energy modeling. Applied to the UWG scheme, EP supplies the urban canopy model with the heat fluxes from the buildings, from which it needs the urban climate conditions calculated by the urban canopy model.

3.5. Information flow

The information flow among the four modules is represented in Fig.3.2.

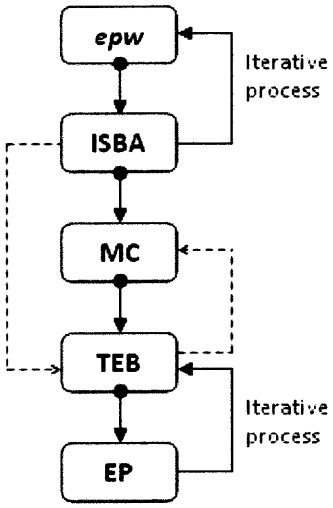

Fig.3.2: Information flow among the modules of the UWG scheme.

First, the ISBA module iterates to calculate the weather conditions at a reference height above the meteorological station. The information required for this step is the type of terrain and vegetation around the station, and an *epw* file, which have been previously converted into SURFEX format (see section 3.2). Then, a mesoscale correlation can be applied to calculate the conditions above the urban canopy layer. The mesoscale correlations need hourly values of sensible heat flux from the weather station and from the urban site. Sensible heat flux is directly obtained from *step1*, but a preliminary TEB simulation forced with the results from *step1* is needed to obtain a first estimation of sensible heat fluxes from the urban site. Finally, TEB and EP iterate to calculate the climate conditions inside the urban canyon and the energy performance of the reference buildings.

3.6. Iterative procedures

3.6.1. ISBA iterative procedure

In practice, the ISBA scheme calculates meteorological information near the ground, given the meteorological conditions at a reference height. This is the opposite of what is needed in *step1*, and therefore, an iterative procedure is required in order to calculate forcing conditions from measured data. The iterative procedure starts forcing the module with measured data, so new conditions are calculated at measurement height (2 m- temperature; 10 m- wind speed). These conditions are compared with the actual measured data, and if there is a significant error, a new simulation is carried out forcing the model with the last measurement height data. Whenever a convergence criterion is satisfied, the last forcing conditions obtained represent the conditions at the reference height above the meteorological station.

The convergence error is calculated as the minimum negative difference and the maximum positive difference between iterations for each meteorological variable. This iterative procedure was developed by Masson (2009, personal communication).

3.6.2. TEB-EP iterative procedure

The UWG scheme uses an iterative procedure to calculate the interactions between EP and TEB accurately. The process starts from a preliminary EP simulation using the original *epw* file. As a result, a first estimation of wall temperatures, surface convection coefficients, and heat released from HVAC equipment is obtained. The next step is to run TEB using the information provided by EP as boundary conditions. As a result, we get a new estimation of urban air temperatures, air humidity, and wind speeds. The *epw* file used in the first building simulation is modified with the information calculated by TEB, and a new EP simulation is carried out. This process (Fig.3.3) is repeated until a convergence criterion is satisfied.

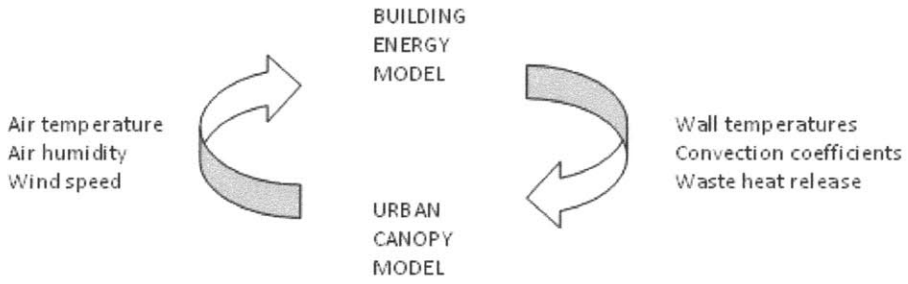

Fig.3.3: EP-TEB iterative coupling process.

3.7. Definition of a reference urban canyon for UWG simulations

The mission of the UWG scheme can be the analysis of either a particular urban canyon or an average urban canyon (see section 1.5.1). In the first case, the user knows specific information about the geometry, orientation, and building characteristics of the site being studied; in the second case, only general information about the average geometry and building characteristics is required. In any case, the first step to run a UWG simulation is to define a reference urban canyon in EP.

3.7.1. Specific urban canyon

If the mission of the UWG simulation is to analyze a specific urban canyon, various buildings facing each other can be modeled in EP with certain detail in the plane perpendicular to the urban canyon direction. The heterogeneity in the longitudinal direction is taken into account in the building simulation, but it will not have an effect on urban climate, since the urban canyon is a two-dimensional representation. The level of detail of the building model depends on the purpose of the simulation and on the experience of identifying the most relevant building features in each particular case. A general recommendation is to keep general building features, while paying attention to those that have a greater interaction with the environment.

Fig.3.4. shows an example of a reference set of buildings for a particular urban canyon. Here, the buildings are modeled in EnergyPlus as four separated zones with external facades facing an east-west oriented urban canyon. Even though for EnergyPlus this configuration is treated as a single building; the two pairs of zones are able to shadow and reflect onto each other.

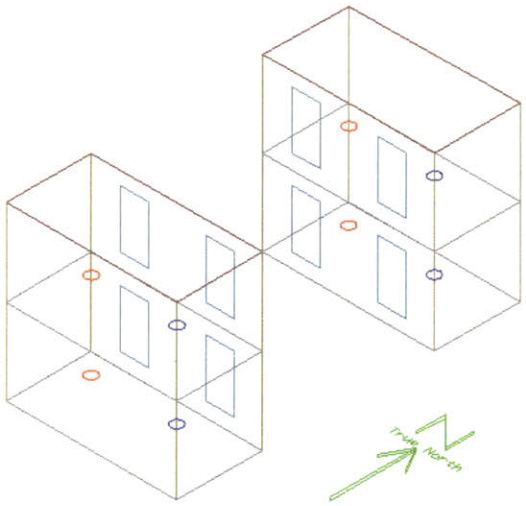

Fig.3.4: Example of a specific urban canyon of reference.

It is important to note that the current version of the TEB model implemented in the UWG scheme does not allow specifying a particular orientation of the urban canyon. As we will see in section 5.6.2, solar calculations in TEB are averaged for all orientations, which limit the accuracy of the specific-orientation approach considered here. Other urban canopy models (e.g. Kusaka et al., 2001) are able to calculate the solar radiation for a certain geometry of an urban canyon (see section 5.6.3), and the next version of the TEB model is expected to include this option as well.

3.7.2. Average urban canyon

If the object of the UWG simulation is to calculate average values of a larger scale urban unit (neighborhood or town), the definition of the building in EP can be simplified. One practical solution is to define a single-zone building with two external facades facing opposite directions. All the other surfaces of the zone would be set to adiabatic, representing the effect of neighboring zones with the same conditions. In this way, each external façade would be looking at a different urban canyon, and the energy calculations of the building would have to be split into two. The other side of each urban canyon can be represented by shadowing polygons (Fig.3.5). The reference zone can be defined at a certain height with respect to the ground to represent a zone situated at an intermediate vertical level within the building. The shadowing polygons have to be as high as the average building height and enough wide to neglect lateral effects.

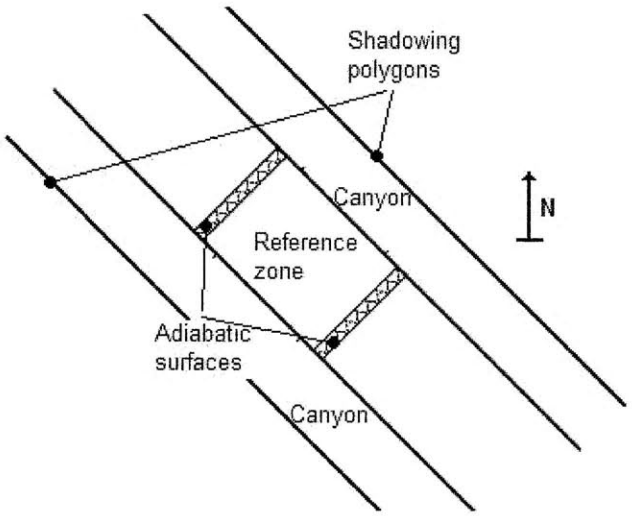

Fig.3.5: Example of an average urban canyon of reference (floor plan).

This configuration overpredicts the solar radiation reflected from the shadowing surfaces onto the building, since they have a larger sky view factor than in an enclosed urban canyon. This can be avoided by defining other shadowing surfaces in the same plane as the external facades of the building. Still, if the glazing ratio is small, the shadowing effect would dominate over the solar reflections.

In order to calculate the average values of urban climate and building performance over an urban space, more than one canyon orientation would have to be simulated per iteration. One useful approximation is to consider an orientation of ±45° angle from the north-south coordinate. To analyze the suitability of this solution, Fig.3.6 compares wall surface temperatures calculated by EP for a reference urban canyon in Abu Dhabi. The x-axis represents the average wall temperatures for all orientations of an urban canyon, and the y-axis represents the wall temperatures for a specific orientation of an urban canyon.

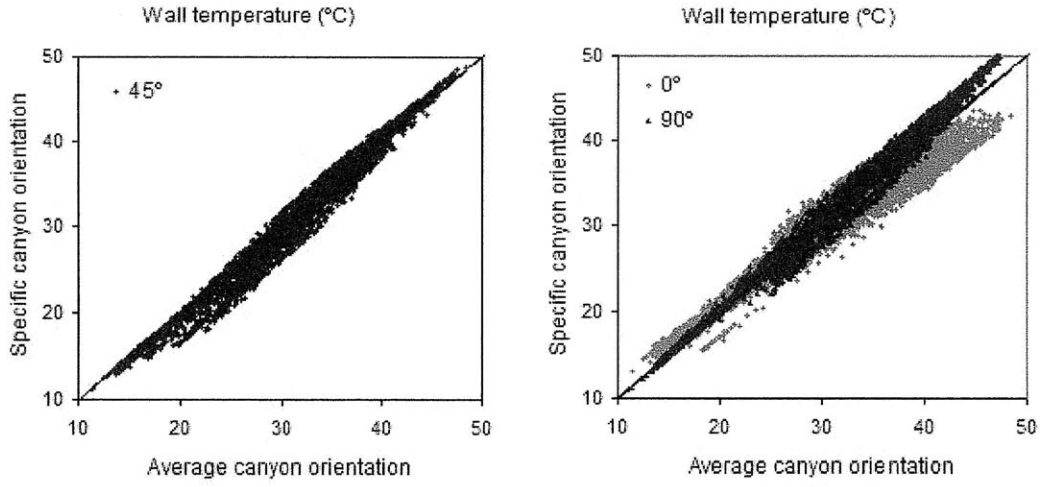

Fig.3.6: Wall surface temperatures for a specific orientation vs. an average orientation. (Left) Specific orientation of 45° from the north-south axis. (Right) Specific orientation of 0° and 90° from the north-south axis.

As can be seen, the results of a 45° oriented canyon match reasonably well with the results of an averaged oriented canyon. Other orientations of the canyon present larger deviations from the average oriented canyon. This approximation allows a single building simulation per iteration, which reduces significantly the computational cost of UWG calculations.

CHAPTER 4

The building energy model

4.1. Introduction

In the previous chapter, we saw that the building energy model of choice in the UWG scheme is EnergyPlus™ (EP). This building simulation program is coupled with an urban canopy model in *step3* of the scheme (Fig.3.1). This chapter provides the theoretical background of those EP calculations relevant to the scheme, and it shows the advantages of using a detailed building simulation program for this application.

EP is an energy analysis and thermal load simulation program. It calculates the heating and cooling loads necessary to maintain thermal control set points, as well as the energy required for heating and cooling a building using a specific Heating Ventilating Air-Conditioning (HVAC) system. It does this by simulating the building and associated HVAC systems when they are exposed to different environmental and operating conditions. The core of the simulation is a model of a building based on fundamental heat balance principles.

The advantage of using EP to represent the effect of buildings on urban climate, instead of a building parameterization (see section 2.3.4), is that it allows a much more detailed analysis of buildings and HVAC systems. EP is based on more than a decade of experience (much longer if considering its predecessors DOE-2 and BLAST), and it is considered the state-of-the-art in energy building modelling. Apart from incorporating detailed algorithms for building heat transfer processes, EP implements models for advanced building technologies, such as natural ventilation, advanced façade configurations, low energy HVAC systems, and daylight devices, which determine the energy performance of buildings and affect their local microclimate. Furthermore, EP routines are optimized to keep the computational cost of the simulations low.

In the next section, the specific features that distinguish EP from other building simulation programs are described. Then, the most relevant EP calculations to represent the interactions between buildings and environment are presented. This chapter also includes an introduction to daylighting modelling and its importance; and the last section is dedicated to the interactions between passive and active building systems and their environment, including the calculation of waste heat from HVAC systems. The capacity of modelling both daylighting and building systems makes EP especially interesting for urban climate studies within the UWG framework. This chapter, together with chapter 5, will help the reader to understand the basic modelling behind the EP-TEB coupling process (see section 3.5.2).

4.2. General features and program structure

4.2.1. Integrated solution manager

One of the most important features of EP is the integrated solution manager where building and systems are solved simultaneously. In building simulation programs with sequential simulation, such as BLAST or DOE-2, building zones and HVAC systems are simulated sequentially with no feedback from one to the other. This simulation technique works well when the system response is a well-defined function of the air temperature of the conditioned

space. However, in most situations, the system capacity is dependent on outside and inside conditions, which in sequential simulations would lead to non-physical results. For the purposes of the UWG scheme, we are interested in evaluating the effects of outdoor conditions on the energy performance of HVAC systems and on the thermal comfort of occupants; and these effects can only be represented by an integrated simulation.

4.2.2. Modularity and management simulation structure

Another important feature of EP is that it implements a "manager philosophy." The program consists of many modules organized in branches. When a sub-branch is called, the main branch exercises the control over it. This modularity and hierarchy of the program is very useful for adding new capabilities to the program and for coupling it with other simulation tools. In this way, different people can work on different EP modules without interfering with each other and with only a limited knowledge of the entire program structure. This makes EP especially suitable for prospective expansions of the UWG idea.

Fig.4.1 shows the basic structure of EP. Here, we can see the main EP simulation manager routine, which is connected with the three main sub-routines: the surface heat balance manager, the air heat balance manager, and the HVAC system manager. Interacting with the main routines of the program, there are auxiliary modules; for example, the sky model module, the shading module, or the daylighting module.

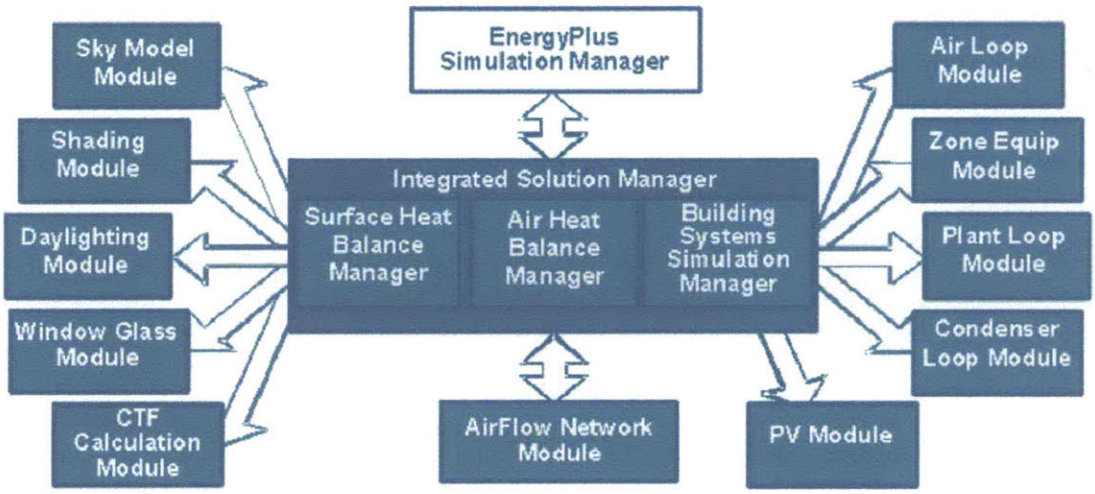

Fig.4.1: EnergyPlus simulation manager diagram (*DOE, 2009*).

4.2.3. Other modelling features

Other features, relevant from the UWG perspective, include the possibility of defining time steps of less than an hour for the interaction between buildings and environment, which can take advantage of sub-hourly weather data measurements. In addition, all input and output files used in EP have a text-based format, so it is relatively easy to develop applications for processing them. Also, the code has been programmed in Fortran90 and is open source for public inspection; and finally, EP has an available Linux version, which was the operative system used by SURFEX (see section 3.2).

4.3. Interactions between buildings and environment

4.3.1. Indoor air heat balance

In order to understand how a building interacts with its environment; we will start with an overview of the indoor air heat balance, which connects all the heat transfer processes that occur inside a building. Consider a building controlled by an air system; in each time step, the integrated simulator (see section 4.2.1) uses information from previous time steps to predict the HVAC system response and update the zone temperature. The predictor-corrector scheme can be summarized as follows:
1) Using an air heat balance where the air capacitance is neglected (Eq.4.1), an estimate is made of the system energy required to balance the heating or cooling loads of the zone. In this equation, the zone temperature equals the set point temperature.

$$-Q_{sys} = Q_{\text{int.gains}} + Q_{conv} + Q_{zones} + Q_{\text{inf}}, \tag{4.1}$$

where $Q_{\text{int.gains}}$ is the convective internal loads (W), Q_{conv} is the convective heat flux from internal surfaces, Q_{inf} is the heat flux due to infiltration of outside air, Q_{zones} is the heat flux due to interzone air mixing, and Q_{sys} is the system heat supply.

2) With the calculated Q_{sys} as a demand, the system is simulated to determine its actual supply capability at the time of the simulation. This will include a plant simulation if necessary.

3) The actual system capability is used in the air heat balance to calculate the resulting zone temperature (T_z). The differential equation solved to calculate T_z is given by:

$$\begin{aligned} \rho c_p V_z \frac{dT_z}{dt} = Q_{\text{int.gains}} + \sum_{i=1}^{N_{surfaces}} h_i A_i (T_{si} - T_z) + \sum_{i=1}^{N_{zones}} \dot{m}_i c_p (T_{zi} - T_z) \\ + \dot{m}_{\text{inf}} c_p (T_o - T_z) + \dot{m}_{sys} c_p (T_{\text{sup}} - T_z) \end{aligned}, \tag{4.2}$$

where ρc_p is the volumetric heat capacity of the air ($Jm^{-3}K^{-1}$), V_z is the total air volume of the zone (m^3), h_i, A_i and T_{si} are the convection heat transfer coefficient ($Wm^{-2}K^{-1}$), the area (m^2), and the temperature (K) of each surface i. $\dot{m}_i$ is the air flow rate from other zones (kgs^{-1}), T_{zi} is the air temperature of other zones, $\dot{m}_{\text{inf}}$ is the infiltration flow rate, and T_o is the outdoor air temperature.

4.3.2. Indoor surface heat balance

The temperature of the interior surfaces (T_{si}) is calculated from a surface heat balance. This heat balance is generally modelled with four coupled heat transfer components: 1) conduction through the building element, 2) convection to the air, 3) short wave radiation, and 4) longwave radiant exchange. Then, the indoor surface heat balance is written as follows:

$$q''_{lw} + q''_{sw} + q''_{lw,equip} + q''_{ki} + q''_{sol} + q''_{conv} = 0, \tag{4.3}$$

where

q''_{lw} = Net longwave radiant exchange flux between zone surfaces (Wm^{-2})

q''_{sw} = Net shortwave radiation flux to surface from lights (Wm^{-2})

$q''_{lw,equip}$ = Longwave radiation flux from equipments (Wm^{-2})

q''_{ki} = Conduction flux through the wall (Wm^{-2})

q''_{sol} = Transmitted solar radiation flux absorbed by the surface (Wm^{-2})

q''_{conv} = Convective heat flux to the zone air (Wm^{-2})

These fluxes are graphically represented in the Fig.4.2:

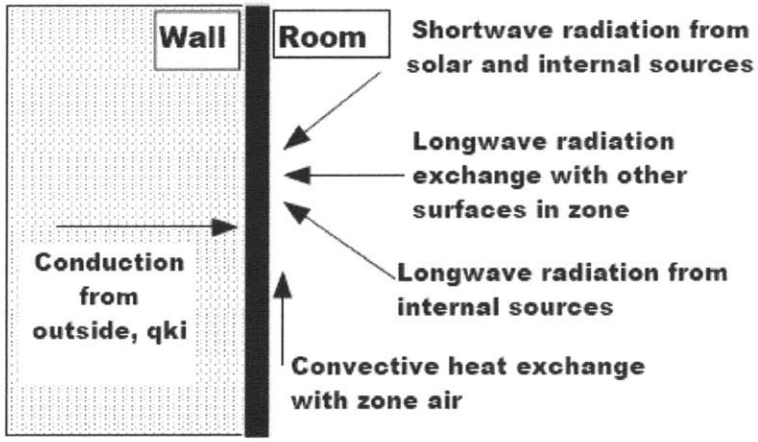

Fig.4.2: Inside heat balance control volume diagram (*DOE, 2009*).

4.3.3. Outdoor surface heat balance

The calculation of the conduction heat flux through walls used in Eq.(4.3) needs external surface temperatures as boundary conditions. Therefore, an outdoor surface heat balance is also solved, and it is expressed as:

$$q''_{\alpha sol} + q''_{lw} + q''_{conv} - q''_{ko} = 0, \tag{4.4}$$

where

$q''_{\alpha sol}$ = Absorbed direct and diffuse solar radiation (Wm^{-2})

q''_{lw} = Net longwave radiation flux (Wm^{-2})

q''_{conv} = Convective heat flux with outside air (Wm^{-2})

q''_{ko} = Conduction heat flux into the wall (Wm^{-2})

These fluxes are graphically represented in Fig.4.3.

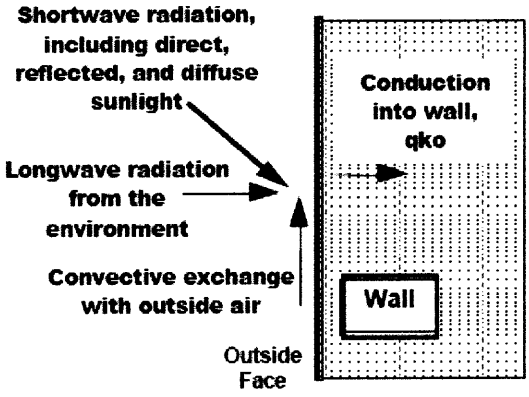

Fig.4.3: Outside heat balance control volume diagram (*DOE, 2009*).

4.3.4. Conduction through walls

EP calculates the heat conduction through enclosures using a transfer function method. The basic form of a conduction transfer function for the interior and the exterior faces is shown in the following equations:

$$q''_{ki}(t) = -Z_o T_{i,t} - \sum_{j=1}^{nz} Z_j T_{i,t-j\delta} + Y_o T_{o,t} + \sum_{j=1}^{nz} Y_j T_{o,t-j\delta} + \sum_{j=1}^{nq} \Phi_j q''_{ki,t-j\delta}, \quad (4.5)$$

and

$$q''_{ko}(t) = -Y_o T_{i,t} - \sum_{j=1}^{nz} Y_j T_{i,t-j\delta} + X_o T_{o,t} + \sum_{j=1}^{nz} X_j T_{o,t-j\delta} + \sum_{j=1}^{nq} \Phi_j q''_{ko,t-j\delta}, \quad (4.6)$$

where

X_j = Outside conduction transfer function (CTF) coefficient ($Wm^{-2}K^{-1}$)

Y_j = Cross CTF coefficient ($Wm^{-2}K^{-1}$)

Z_j = Inside CTF coefficient ($Wm^{-2}K^{-1}$)

Φ_j = Flux CTF coefficient

T_i = Inside face temperature (K)

T_o = Outside face temperature (K)

q''_{ko} = Conduction heat flux on outside face (Wm^{-2})

q''_{ki} = Conduction heat flux on inside face (Wm^{-2})

The subscript following the comma indicates the time period for the quantity in terms of the time step δ. These equations state that the heat flux at the surface of a wall is linearly related to the current and some of the previous temperatures at both the interior and exterior surfaces, as well as to some of the previous values of heat flux at the surface.

This formulation is computationally more efficient than the alternative finite difference method. Here, with a simple linear equation with constant coefficients, the conduction heat transfer through an element can be calculated. The coefficients (CTF) are constants that need only to be determined once for each construction type. The only storage of data required is the CTF coefficients themselves and a limited number of temperature and flux terms. This

formulation is valid for any surface type and does not require the calculation of inter layer temperatures.

4.3.5. Convection

EP calculates the convective heat exchange between an exterior surface and the outside air based on convective heat transfer coefficients (CHTC). This classical formulation is given by:

$$q''_{conv} = h(T_{surf} - T_{air}), \tag{4.7}$$

where q''_{conv} is the convective heat flux (Wm^{-2}), h is the convective heat transfer coefficient, T_{surf} is the surface temperature, and T_{air} is the outdoor air temperature.

The external CHTC can be calculated in EP by a simple or a detailed convection algorithm. The Simple Algorithm calculates a combined convection and radiation heat transfer coefficient through a quadratic expression that depends on the surface roughness and the local wind speed (DOE, 2009). The quadratic coefficient is usually small, and it is identically zero for medium rough surfaces. The resulting correlation for a medium roughness is given by:

$$h = 10.79 + 4.192U_a. \tag{4.8}$$

Note that this heat transfer coefficient is directly proportional to the local wind speed, which agrees with the correlations used in current urban canopy models. However, these correlations account only for the convective heat flux, since the longwave radiation is calculated separately. Therefore, they should not be compared with the simple algorithm used in EP, which includes a radiation component.

On the other hand, the Detailed Algorithm of EP is the one intended to calculate the actual CHTC (only convection). This algorithm divides the CHTC into a forced convection component (h_f) and a natural convection component (h_n). Then, the forced convection component is calculated as:

$$h_f = 2.537 W_f R_f \left(\frac{P}{A} U_a\right)^{1/2}, \tag{4.9}$$

where W_f = 1.0 for windward surfaces, and W_f =0.5 for leeward surfaces, and where the multiplier R_f depends on the roughness of the surface (R_f = 1.52 for a medium rough surface - concrete). The natural convection component is calculated from the following correlation for a vertical surface:

$$h_n = 1.31 \left|T_{surf} - T_{air}\right|^{1/3}. \tag{4.10}$$

The Detailed Algorithm of EP proposes a relation of the CHTC with the square root of the local wind speed, which differs from the linear relationship proposed by urban canopy

models. Fig.4.4 compares the CHTC correlations used by urban canopy models with EP algorithms. Here, the first week of May corresponding to the *epw* file for Abu Dhabi is represented.

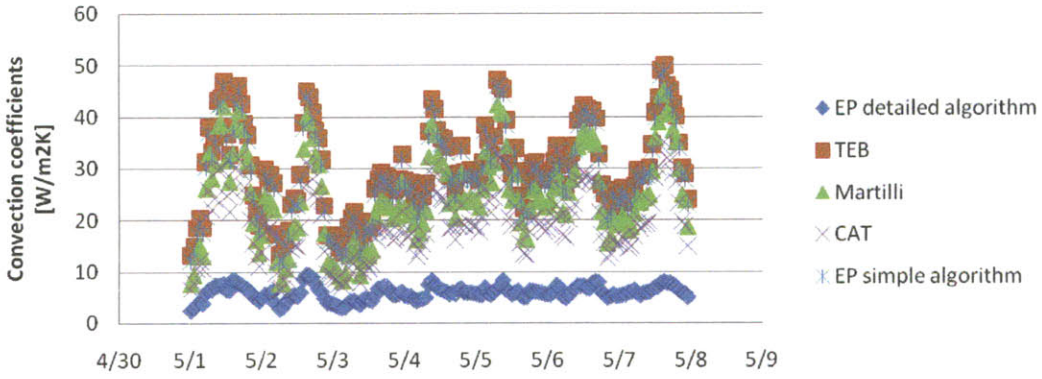

Fig.4.4: Comparison of CHTC from urban canopy model correlations and EP algorithms.

The graph shows a significant inconsistency between the correlations used by urban canopy models and the EP detailed algorithm. Surprisingly, these correlations match well with the EP simple algorithm, which includes a radiation component. In the UWG scheme, the CHTC are calculated by the EP detailed algorithm and then used in the urban canopy model (see section 3.5.2). This election is based on the fact that the EP algorithm refers to ASHRAE published calculations, while urban canopy models do not justify their correlations. Even so, further investigation would be required to evaluate the suitability of current CHTC correlations applied to buildings.

4.3.6. Longwave radiation

EP calculates the longwave radiation exchange between an exterior surface and its environment using the formulation proposed by Walton (1983). In this model, the following general assumptions are applied:

- Each surface emits or reflects diffusely and is grey and opaque ($\alpha = \varepsilon, \tau = 0, \rho = 1 - \varepsilon$).
- Each surface is at a uniform temperature.
- Energy flux leaving a surface is evenly distributed across the surface.
- The medium (air) is non-participating.

In addition, the following is also assumed:

- Surface emissivities are high enough to neglect interreflections.
- The ground and external obstructions are assumed to be at the air temperature and have an emissivity of 0.9.
- The sky radiation is split into a radiation exchange with the air and a radiation exchange with the sky. This split was not justified in Walton's book (1983), where this formulation was presented, although this formulation has been extensively used in many building models since then.

In this model, the total longwave radiative heat flux (Wm^{-2}) is the sum of the radiation exchange with the ground, sky, and air:

$$q''_{lw} = q''_{gnd} + q''_{sky} + q''_{air}. \tag{4.11}$$

The longwave shadowing effect from obstructions, such as other building surfaces, is applied to the sky component through a tri-dimensional isotropic shading factor, *Rdome*, described in section 4.3.7. The longwave radiation from these obstructions is added to the longwave radiation from the ground.

Each component of Eq.(4.11) is calculated applying the Stefan-Boltzmann Law and linearized radiative heat transfer coefficients, as follows:

$$q''_{lw} = h_{r,gnd}(T_{surf} - T_{air}) + h_{r,sky}(T_{surf} - T_{sky}) + h_{r,air}(T_{surf} - T_{air}), \tag{4.12}$$

where the radiative heat transfer coefficients are calculated as:

$$h_{r,i} = \frac{\varepsilon\sigma\Psi_i(T_{surf}^4 - T_i^4)}{T_{surf} - T_i}, \tag{4.13}$$

and where i represents the radiation component (ground, sky, or air), ε is the longwave emissivity of the surface, σ is the Stefan-Boltzmann constant ($Wm^{-2}K^{-4}$), Ψ_i is the view factor between the surface and the radiation component i, T_{surf} is the outside surface temperature, and T_i is the temperature of the radiation component i.

4.3.7. Shortwave radiation

The external shortwave radiation (Wm^{-2}) that is absorbed at a building surface is calculated as a combination of direct, diffuse, and reflected solar radiation, as follows:

$$q''_{\alpha,sol} = q''_{dir} + q''_{dif} + q''_{reflec}. \tag{4.14}$$

The reflected solar radiation term is described qualitatively in section 4.3.9. The absorbed direct solar radiation (Wm^{-2}) is given by:

$$q''_{dir} = \alpha I_{dir} \cos\theta \frac{A_{sun}}{A}, \tag{4.15}$$

where α is the solar absorptance of the surface, θ is the angle of incidence of the sun's rays, A is the area of the surface, A_{sun} is the sunlit area of the surface, and I_{dir} is the intensity of direct radiation (Wm^{-2}).

The absorbed diffuse solar radiation (Wm^{-2}) is expressed by:

$$q''_{dif} = \alpha I_{sky} \Psi_{sky}, \tag{4.16}$$

where I_{sky} is the intensity of sky diffuse radiation (Wm^{-2}) and Ψ_{sky} is the view factor between the surface and the sky.

If the surface is shaded, the program modifies the diffuse solar radiation from the sky based on isotropic shading factors as described below.

The diffuse solar radiation from the sky is calculated from the anisotropic radiance model of Perez et al. (1990). In this model, the radiance of the sky is determined by three distributions that are superimposed (Fig.4.5):

- An isotropic distribution that covers the entire sky dome.
- A circumsolar brightening centered at the position of the sun.
- A horizon brightening.

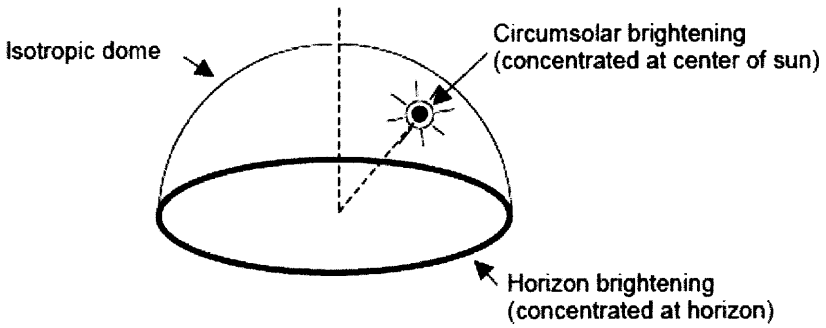

Fig.4.5: Schematic view of sky solar radiance distribution (*DOE, 2009*).

The proportions of these distributions depend on the sky condition, which are determined from the sun position and solar quantities from the weather file.

The anisotropic sky model uses the following expression to calculate the sky diffuse irradiance, I_{sky}, on a surface:

$$I_{sky} = R_{horizon} I_{horizon} + R_{dome} I_{dome} + R_{circumsolar} I_{circumsolar}, \tag{4.17}$$

where $I_{horizon}$ is the irradiance on the surface from sky horizon (Wm^{-2}), I_{dome} is the irradiance on the surface from sky dome, $I_{circumsolar}$ is the irradiance on the surface from circumsolar region, and $R_{horizon}$, R_{dome} and $R_{circumsolar}$ are factors that account for the shadowing from exterior obstructions. For the horizon source, the ratio $R_{horizon}$ is calculated by dividing the horizon line into 24 intervals of equal length, and summing the fractions of irradiance coming from each interval that reaches the surface. In the same way is calculated the corresponding ratio for the isotropic sky dome, R_{dome}, but dividing it into a grid of 144 points, 6 in altitude by 24 in azimuth. Finally, the circumsolar ratio $R_{circumsolar}$ is calculated assuming it is concentrated at the solar disk.

4.3.8. Shadowing

EP calculates the geometry of the shadows cast on building surfaces through a shadowing module based on coordinate transformation methods. First, a shadow is projected from the vertices of a shadowing polygon along the direction of the sun's rays to the plane of the receiving polygon. Then, the program determines the area of the overlap between the shadow polygon and the receiving polygon, using two-dimensional homogeneous coordinate

techniques. Partially transparent shadowing surfaces and shadow overlapping can also be modelled.

4.3.9. Reflections

EP is able to calculate the beam and sky solar radiation that is reflected from exterior surfaces and then strikes the building. The reflecting surfaces fall into three categories:

- Shadowing surfaces: overhangs, neighboring buildings, or other external obstructions. These surfaces can have diffuse and/or specular reflectance values.
- Exterior building surfaces: a building reflects solar radiation onto itself.
- The ground surface: beam solar and sky solar reflection from the ground is calculated, but in this case the ground plane is considered unobstructed.

A specular reflection method is used to calculate the beam-to-beam radiation from obstructions. The program assumes that specular reflection is only due to glazing; for example, the building's windows or a glazed façade of a neighbouring building. A ray-tracing method is used to calculate the diffuse reflection of beam solar and sky solar radiation from the ground and from obstructions. This calculation begins by generating a set of rays at each receiving point of a surface. Then, it determines whether each ray hits the sky, ground, or an obstruction (Fig.4.6). The radiance at the hit point from the reflection of incident beam or sky solar is determined; and the contribution of this radiance to the receiving surface is calculated, added to the contribution from other hit points, and averaged over the receiving points.

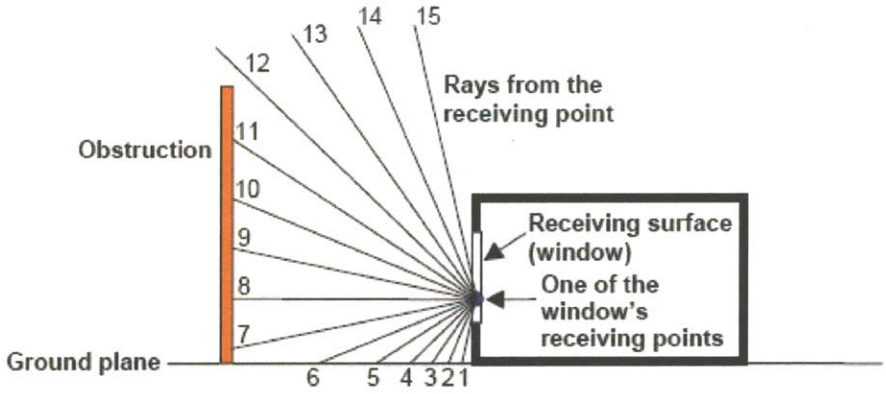

Fig.4.6: Schematic view of the ray-tracing method (*DOE, 2009*).

4.4. Daylighting

In building design and analysis, it is well known that buildings in urban environments can have reduced daylight access. A lack of daylight potential can have an impact on both the energy consumption of a building and the satisfaction of occupants. Usually, daylight access opposes the reduction of cooling loads associated with urban design and building façade design. For example, as a result of setting narrow streets in a hot climate to reduce solar gains, the daylight access will be also reduced. Lights can contribute significantly to the energy consumption of buildings, both directly and by adding heating load, affecting also the eventual waste heat released from HVAC systems. Therefore, it is important to include this parameter when studying the interactions between buildings and environment.

The UWG scheme, by using an advanced building simulation program as EP, is able to bring the daylighting analysis into the urban problem. This is an important contribution, since current building parameterizations usually ignore this issue.

4.4.1. Daylighting models

EP implements two different daylighting models, with different levels of complexity and computational cost.

The EnergyPlus Detailed model uses a split-flux method (DOE, 2009) to calculate the daylight reaching a reference point. In this method, the daylight transmitted through windows is split into two parts: a downgoing flux which falls on surfaces below the imaginary horizontal plane passing through the center of the window, and an upward-going flux that strikes the portions of surfaces above the window midplane. A fraction of these fluxes is absorbed by the room surfaces, and the remainder is reflected according to the area-weighted reflectances of the lower part and the upper part. To find the final average internally-reflected illuminance on the room surfaces, a flux balance is applied.

This procedure assumes that the room behaves like an integrating sphere with perfectly diffusing interior surfaces and with no internal obstructions. Therefore, it works best for rooms that are close to cubical in shape, have matte surfaces, and have no internal partitions. Deviations from these conditions can lead to substantial inaccuracies in the calculations.

The DElight model uses a radiosity method (DOE, 2009) to calculate the effect of interreflections among interior surfaces. This method subdivides each reflecting surface in the zone into nodal patches, and it uses the view factors between all nodal patch pairs to calculate the total contribution of reflected light within the zone, through an iterative process.

This method results in a more accurate calculation of the varied distribution of interreflected light throughout the zone. It allows inputting up to 100 reference points which supports a more complete assessment of this distribution, and accounts for interior obstructions between pairs of nodal patches. On the other hand, it is more computationally expensive than the Detailed model.

4.4.2. Daylighting calculations

The daylighting calculations in EP have three main stages:

1) Calculation and storage of daylight factors, which are defined as the ratio between the interior illuminance and the exterior horizontal iluminance.

   The Detailed model calculates the contribution of direct light from windows and light reflected on indoor surfaces to the illuminance at reference points. Daylight factors are calculated for hourly sun positions for representative days of the run period.

   The Delight model calculates the contribution of light transmitted through all simple and complex fenestration systems to the illuminance at reference points, as well as the illuminance at each nodal patch, for a given exterior luminous environment. Then, the effect of the interreflections between indoor surfaces is calculated, resulting in a total illuminance at each reference point. Finally, daylight factors are calculated.

2) Time-step interior daylighting calculation. A daylight calculation is performed at each heat-balance time step when the sun is up. The illuminance at reference points is found by interpolating the stored daylight factors, using the current time-step sun position and sky condition, and multiplying by the exterior horizontal illuminance.

3) Electric lighting control calculation. The electric light control system is simulated to determine the light energy needed to make up the difference between the daylighting illuminance level and the design illuminance at a given time step. The zone electric light reduction factor is passed to the thermal calculation to reduce the correspondent heat gain from lights.

The luminance distribution of the sky is represented as a superposition of four standard skies: clear sky, clear turbid sky, intermediate sky, and overcast sky. The exterior horizontal illuminance from the sun and the sky is calculated as described in section 4.3.7.

4.5. Interactions between building systems and environment

4.5.1. Passive systems

The first step to save energy in buildings, and help mitigate the UHI effect in urban areas, is to reduce the energy demand of buildings. This can be done by architectural design, applying so-called passive systems that take advantage of the sun, the wind, and environmental conditions to reduce the need of HVAC systems. Examples of passive systems are solar protections, heat storage walls, natural ventilation systems, radiant cooling, evaporative cooling, and earth tubes. In order to optimize the design of any of these systems, a detailed energy model of the building is required. Moreover, since all these systems have a close interaction with the environment, it is crucial to account for the actual microclimate around the buildings being simulated.

The UWG scheme constitutes an important contribution to the analysis and design of passive systems. For example, natural ventilation systems rely on a certain outdoor air temperature below the indoor air temperature to counteract cooling loads. Often, the range of suitable outdoor air temperatures is quite narrow, and the existence of an UHI effect may not allow the application of the natural ventilation system. The same is true for the wind speed inside the urban canopy layer. The suitability or not of a natural ventilation system has a great impact on the conception of a building; therefore, to have accurate information about the microclimate around the building is crucial in many cases. Another important example is the use of thermal mass in buildings. The benefits of building massive enclosures are usually related to the magnitude of the shift in outdoor air temperature between day and night. In an urban context, this shift can be reduced by the UHI effect at night affecting the performance of the thermal mass system.

4.5.2. HVAC systems

In many situations, passive systems are not enough to keep comfort conditions inside buildings, and an HVAC system is required. In cooling periods, HVAC systems are responsible for waste heat emissions, which can raise outdoor air temperature, provoking more cooling loads through the envelope of buildings, and ultimately increasing their energy consumption. In order to properly assess this negative effect, we have to be able to accurately

represent the energy performance of HVAC systems and their interactions with the outdoor environment.

EP implements detailed models of HVAC systems and their components. Depending on the purposes of the simulation, one can determine the required level of detail of the system definition. If one is only interested in a building load calculation, an idealized system with infinite capacity can be defined. In the same way, if one is interested in the overall or partial performance of a particular system and its response to the external environment, a complete or partial definition of all system components, from the air loop to the plant loop or the condenser loop, may be appropriate.

4.5.3. Waste heat released from HVAC systems into the environment

In current building parameterizations, the heat released from HVAC systems into the environment in cooling periods is calculated from the thermal loads of the building, applying a constant coefficient of performance (COP). This coefficient can be defined as:

$$COP = \frac{Q_{sys}}{Q_{elect}}, \tag{4.18}$$

where Q_{sys} is the energy supplied by the HVAC system to the zone (W), and Q_{elect} is the electric consumption of the system. Then, the heat released from HVAC systems into the environment (Q_{waste}) is calculated by the following simplified expression:

$$Q_{waste} = Q_{loads}\left(1 + \frac{1}{COP}\right), \tag{4.19}$$

where Q_{loads} is the thermal loads of the building, which has been equaled to the energy supplied by the system.

However, this formulation is only valid for ideal cases. Real HVAC systems supply energy not only to cover the thermal loads of the building, but also to counteract the thermal loses through the system. The capacity of the system depends on the conditions inside and outside the building, so there are situations where the system is not able to supply the required energy. Moreover, the COP of the system cannot be considered constant, since it also depends on the conditions inside and outside the building, and on the part load ratio of the cooling plant. Finally, an energy consumption evaluation must include the contribution of fans, pumps, and other electric equipment, which depend on the design of the HVAC system.

A detailed definition of HVAC systems allows an accurate evaluation of the impact of urban climate on the energy consumption of buildings, including the prediction of the actual waste heat released from HVAC systems. EP accounts for the dependence of HVAC systems on outdoor and indoor conditions, through the definition of characteristic energy performance curves. Each cooling plant type has a number of curves that determine its total cooling capacity and its overall energy efficiency.

The total cooling capacity of a cooling plant is calculated from the rated capacity, modified by two curves, one function of indoor and outdoor air temperatures, and another function of the flow rate. Thus, the total cooling capacity is given by:

$$Q_{total} = \phi_Q(T_{wb,i}, T_{c,i}) \cdot \psi_Q(ff) \cdot Q_{rated} . \tag{4.20}$$

where ϕ and ψ are characteristic curves that are functions of the wet-bulb temperature of the air entering the cooling coil, $T_{wb,i}$; the dry-bulb outdoor air temperature, in an air-cooled condenser (wet-bulb outdoor air temperature in an evaporative condenser), $T_{c,i}$; and the ratio between the actual air flow rate across the cooling coil and the rated air flow rate (*ff*).

The energy input ratio (EIR), which is defined as the inverse of the COP ($EIR = 1/COP$), is calculated from the rated EIR, modified by three curves, one function of indoor and outdoor air temperatures as described above, another function of the flow rate ratio, and the last one function of the part load ratio. Thus, the actual EIR is given by:

$$EIR_{total} = \phi_{EIR}(T_{wb,i}, T_{c,i}) \cdot \psi_{EIR}(ff) \cdot PLF \cdot \frac{1}{COP_{rated}} . \tag{4.21}$$

The part load fraction (PLF) correlation is a quadratic curve with the independent variable being the part load ratio (sensible cooling load / steady-state sensible cooling capacity). This correlation accounts for efficiency losses due to compressor cycling.

In order to assess the effect of the heat released from HVAC systems, it is also important to note that there are different types of HVAC systems, and each one can affect the environment in a different way. For example, unitary systems, in which there is one cooling machine per zone, generally have their condensers distributed on the façades; and therefore the waste heat is released directly into the canyon. In contrast, centralized systems supply several zones, and their big dimensions require locating them in an appropriate place, which often is at the roof of buildings. In this situation, the waste heat generated would be released on the roof, and depending on the wind direction and speed, part of this heat would contribute to the energy balance of the urban canyon, and part would be incorporated to the urban boundary layer.

Another important classification of cooling systems is based on the condensation fluid. In air-condensed systems, the condenser exchanges heat with the outdoor air through a fan; while in water-condensed systems, a condenser loop extracts heat from the condenser and releases it by evaporation in a cooling tower. As a result, the heat released by an air-condensed system has to be computed in the sensible heat balance of the urban canyon, while the heat released by a water-condensed system has to be introduced in the latent heat balance.

CHAPTER 5

The urban canopy model

5.1. Introduction

In chapter 3, we saw that the urban canopy model used in *step3* (Fig.3.1) is the Town Energy Balance (TEB) model (Masson, 2000). This model is coupled with the building simulation program presented in the previous chapter. In this chapter, the science behind the TEB model is described.

The TEB model is a physically based urban canopy model intended to represent the dynamic and thermodynamic effects of an urbanized area on the atmosphere. TEB is included in the super-program SURFEX (see section 3.2), together with the vegetation scheme (ISBA) used in *step1*, and two other surface schemes that account for the effects of lakes and oceans.

The original version of TEB has been validated with observations in various urban sites and weather conditions (Masson et al., 2002; Lemonsu et al., 2004; Pigeon et al., 2008). It calculates the drag force, the energy, and water fluxes of a town or neighborhood formed by identical urban canyons, where all the orientations are possible and all exist with the same probability. TEB considers a two-dimensional approximation of an urban canyon formed by three generic surfaces: a wall, a road, and a roof. It calculates the conditions inside the canyon and the sensible and latent heat exchanges between the canyon and the atmosphere by solving a heat balance among the heat fluxes from the canyon surfaces to the canyon air and from the canyon air to the atmosphere. Although the current version of the UWG scheme assumes that air inside the canyon is well mixed, the latest version of TEB introduces the possibility of vertically discretizing the urban canyon and applies conservation of mass, momentum, energy, and turbulent kinetic energy to represent the dynamics of the fluid variables inside the canyon (Hamdi and Masson, 2008).

The chapter starts with a description of the adapted version of TEB implemented in the UWG scheme. Then, the urban canyon energy balance used in TEB is presented. This energy balance leads to the calculation of the air temperature and air humidity inside the canyon. The chapter discusses the methods used in the scheme to calculate the surface to air heat transfer, which constitutes one of the interaction mechanisms between buildings and the environment. This includes the models implemented in the scheme to calculate the wind speed inside the canyon. The chapter closes with the algorithms used to calculate road temperatures.

5.2. The adapted version of TEB

As we saw in section 2.3.4, the TEB model includes a simple representation of the heat transfer processes that occur inside buildings. One of the contributions of the UWG scheme is incorporating into TEB the energy calculations carried out by a detailed building simulation program such as EnergyPlus™ (EP). The adapted version of TEB implemented in the UWG scheme is able to read hourly values of building exterior temperatures, surface convection heat transfer coefficients, and waste heat released from HVAC system generated by EP. Then, this information is introduced into the energy balance of the urban canyon, so TEB building calculations are no longer necessary. The roof surface energy balance of TEB does not contribute to the energy balance of the urban canyon, so it will be only used in *step2* of

the scheme to calculate the total heat flux from the urban area (see chapter 7). The roof energy balance will not be described here.

Another important difference between the original version of TEB and the UWG scheme is that the latter is interested in analyzing not only an average oriented urban canyon, but also a specific orientation of the urban canyon (see section 1.5.1). Therefore, in the following sections we will consider that there can be two different walls in terms of energy fluxes and surface temperatures, one for each side of the urban canyon, although the current version of TEB still considers a single generic wall. For the same reason, although TEB averages the solar radiation absorbed by the road for all possible orientations, in section 5.6.3, a solar radiation formulation for a specific orientation of the urban canyon will be presented. The next version of TEB is expected to include these features.

5.3. Energy balance of an urban canyon

The TEB model calculates the air temperature and air humidity inside an urban canyon applying sensible and latent heat balances to the canyon air (Eqs.5.1 and 5.2). The model computes the heat transfer between the canyon surfaces (road and walls) and the canyon air, and the heat exchange between the canyon air and the urban boundary layer (Fig.5.1).

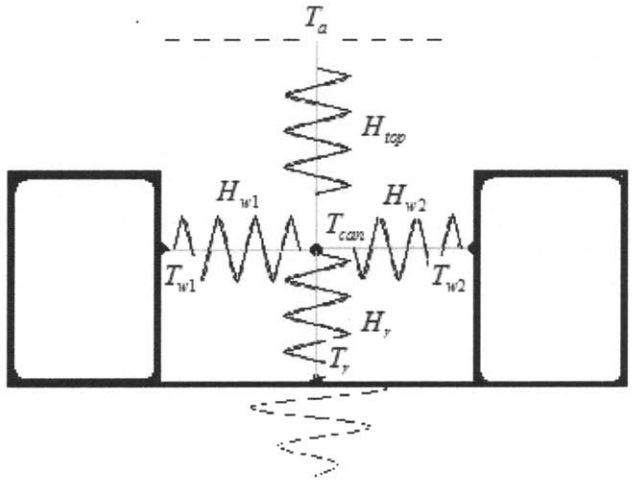

Fig.5.1: The sensible heat balance in an urban canyon.

The sensible and latent heat balances in the urban canyon can be expressed as:

$$H_{top} = H_r + (H_{w1} + H_{w2} + H_{waste}) \cdot h / w \tag{5.1}$$

and

$$E_{top} = E_r + (E_{w1} + E_{w2} + E_{waste}) \cdot h / w, \tag{5.2}$$

where H_{top} and E_{top} are the sensible and latent heat fluxes (Wm^{-2}) between the air inside the canyon and the urban boundary layer, H_r and E_r are the sensible and latent heat fluxes between the road and the canyon air, and H_{w1}, H_{w2}, E_{w1}, and E_{w2} are the sensible and latent heat fluxes between walls and the canyon air. The parameter h / w is the urban canyon aspect

ratio; and H_{waste} and E_{waste} are the sensible and the latent waste heat released by HVAC systems into the urban canyon.

The heat fluxes at the top of the canyon and at the road are calculated from an aerodynamic resistance formulation, also called a surface-layer formulation. This can be expressed as:

$$H_{top} = \rho c_p (T_{can} - T_a) / R_{top}, \tag{5.3}$$

$$E_{top} = \rho l (q_{can} - q_a) / R_{top}, \tag{5.4}$$

$$H_r = \rho c_p (T_r - T_{can}) / R_r, \tag{5.5}$$

and

$$E_r = \rho l (q_r - q_{can}) / R_r, \tag{5.6}$$

where c_p is the specific heat of air ($Jkg^{-1}K^{-1}$); ρ is the air density (kgm^{-3}); l is the latent heat of air (Jkg^{-1}); T_r, T_{can}, and T_a are the road temperature, the canyon air temperature, and the air temperature at the top of the canyon, respectively (K); q_r, q_{can}, and q_a are the road surface humidity content, the humidity content of the canyon air, and the humidity content of the air at the top of the canyon, respectively ($kgkg^{-1}$); and R_{top} and R_r are the aerodynamic resistances at the top of the canyon and at the road (sm^{-1}).

The surface heat fluxes at the walls are calculated from the building surface temperatures and convective heat transfer coefficients provided by the building energy model (see chapter 4). The latent heat flux from building surfaces is neglected for the purposes of the UWG scheme. This convective formulation can be written as:

$$H_w = h(T_w - T_{can}), \tag{5.7}$$

where h is a convection heat transfer coefficient ($Wm^{-2}K^{-1}$), and T_w is the surface temperature of a wall.

Substituting Eqs. 5.3-5.7 into Eqs. 5.1 and 5.2, we can obtain the air temperature and air humidity content inside the urban canyon.

5.4. Aerodynamic resistances

As we have seen in the previous section, the TEB model uses a surface-layer formulation for calculating the surface heat fluxes at the top of the canyon and at the road. The stability coefficients of Mascart et al. (1995) are used in the calculation of the aerodynamic resistances that appear in Eqs. 5.3-5.6. Lemonsu et al. (2003) expressed these aerodynamic resistances as function of the following relevant parameters:

$$R_{top} = f(Ri, z_{ref}, U_a, z_{oM}, z_{oH}) \tag{5.8}$$

and

$$R_r = f(Ri, h/2, U_{eff}, z_{oM,r}, z_{oH,r}), \tag{5.9}$$

where z_{ref} is a reference height above the urban canyon (m); h is the average building height (m); Ri is the Richardson number, either between the road surface and the canyon air or between the canyon and the urban boundary layer; U_a is the wind speed magnitude at z_{ref}; and U_{eff} is an effective wind speed of the canyon. $z_{oM,r}$ and $z_{oH,r}$ are the roughness lengths for momentum and heat of the road, respectively (m); and z_{oM} and z_{oH} are the characteristic roughness lengths for momentum and heat of the local-scale urban area (m).

The aerodynamic resistances can also be seen as the inverse of an exchange velocity. For example, Eq. (5.3) can be expressed as $H_{top} = \rho c_p U_{ex}(T_{can} - T_a)$, where the exchange velocity is calculated as the air velocity multiplied by a reduction factor, $U_{ex} = C_H U_a$. This factor C_H depends on atmospheric stability and can have values of around 0.05-0.1 at the top of the canyon.

In the absence of stability considerations, the aerodynamic resistance of the road used in Eq.5.9 can be related to the classical convective heat transfer coefficient. This relation is given by:

$$R = \rho c_p / h. \tag{5.10}$$

The application of a surface-layer formulation to the heat fluxes inside an urban canyon is not clear from the theoretical point of view. The surface-layer formulation was developed by Monin and Obukhov (1954) to estimate the heat exchange between a rough surface (e.g. field of crops) and the atmosphere, so the stability considerations in that case do not have to be the same as inside an urban canyon. Indeed, other urban studies are using the alternative convection correlations to calculate sensible heat fluxes from surfaces (e.g. Erell and Williamson, 2006; Kusaka et al., 2001).

In order to compare these two approaches, Fig.5.2 represents surface heat fluxes from a road, for different wind speeds and temperature gradients. The surface-layer formulation is the one found in Lemonsu et al. (2003), while the convection correlations are the ones used in the CAT model (see section 2.4.4).

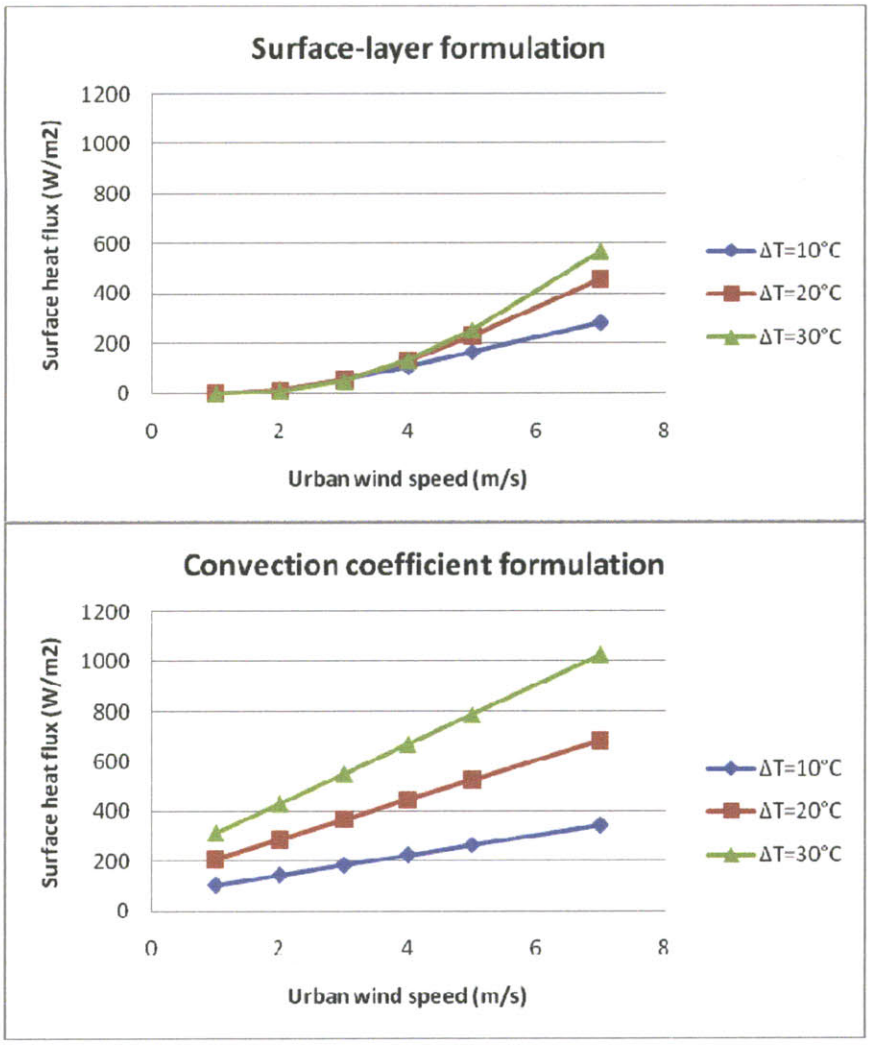

Fig.5.2: Road heat fluxes calculated from a surface-layer formulation (up) and from convective heat transfer coefficients (down).

As we saw in section 4.3.5, the convection correlations used in the CAT model can be overestimating the convective heat transfer, and this fact could explain why this formulation almost always predict higher values of surface heat fluxes than the surface-layer formulation. However, the constant term of the convection correlation (Eq.2.28) guarantees that the convective heat transfer coefficient never vanishes, even for very low wind speeds. In contrast, the surface-layer formulation predicts near zero values of surface heat flux when the wind speed is low, and this tends to markedly increase the surface temperature of the road.

These important differences show a lack of an agreement within the urban climate community to represent the convective heat transfer between urban surfaces and the air in a justified way. This fact leaves the door open for further research beyond the UWG scheme presented in this thesis, which relies on the formulation implemented in TEB.

5.4.1. Aerodynamic roughness length

In Masson (2000), the aerodynamic roughness length used for stability calculations (Eqs. 5.8, 5.12 and 5.13) is estimated as $z_{oM} = h/10$, where h is the average building height. Even so, the model allows this parameter to be specified independently, either from in-situ measurements or from more complex formulations. The literature shows a generalized disagreement about how to calculate the aerodynamic roughness length. Grimmond and Oke (1999b) made a comprehensive review and discussion of available methods. Hanna and Britter (2002) also made an interesting analysis of the meaning of this parameter and proposed methods to calculate it.

5.4.2. Thermal roughness length

The thermal roughness length parameter appears in the surface-layer formulation as an analogy of the aerodynamic roughness length. Usually, this parameter is approximated as a certain fraction of the aerodynamic roughness length, whose calculation is also ambiguous. For example, the TEB model uses the relation $z_{oH} = z_{oM}/200$.

Unlike a smooth surface, where there is an analogy between the loss of momentum and the heat transfer at the surface, at the rough surface, there is no such analogy because the drag force on a rough surface depends on the difference in pressure across the many roughness asperities while the heat transfer from the same surface depends on the molecular properties of the fluid such as thermal conductivity. This lack of analogy is the reason why the urban modelers must resort to various approximations.

it is not possible to relate the drag, which depends on the roughness of the surface and on the pressure form, and the heat transfer, which basically depends on the heat transfer surface area. That is the reason why urban modellers have to come up with these rough approximations.

Recent studies (Leroyer et al., 2009) argue that the relation between the thermal and the aerodynamic roughness lengths depends on the Reynolds number. This dependence is written as:

$$\ln(z_{oM}/z_{oH}) = a\,\mathrm{Re}^{0.25} - 2, \tag{5.11}$$

where a is a constant; Re is the Reynolds number, defined as $\mathrm{Re} = z_{oM}u_*/\nu$; u_* is the friction velocity; and ν is the kinematic viscosity of air.

5.5. Urban wind speeds

In TEB, the wind speed inside the canyon is divided into a horizontal or mean component and a vertical or turbulent component. The vertical component (W_{can}) is equalled to the friction velocity, as follows:

$$W_{can} = u_* = \sqrt{C_d}\,|U_a|, \tag{5.12}$$

where

u_* - Friction velocity (ms^{-1})

U_a - Wind speed magnitude at a reference height above the urban canyon (ms^{-1})

C_d - Drag coefficient, which is computed from the temperature and humidity in and above the canyon, and from the aerodynamic roughness length of the town (z_{oM}), taking into account stability effects according to Mascart et al. (1995).

The horizontal wind speed (U_{can}) is calculated applying a logarithmic-exponential profile, integrated over 360° to take into account all possible orientations of the canyon, and evaluated at half the height of the canyon. The final expression proposed by Lemonsu et al. (2003) reads as:

$$U_{can} = A\exp\left(-\frac{1}{4}\frac{h}{w}\right)\frac{\ln\left(\frac{h/3}{z_{oM}}\right)}{\ln\left(\frac{z_{ref}+h/3}{z_{oM}}\right)}|U_a|, \tag{5.13}$$

where A is a constant that depends on the aspect ratio (h/w).

Lemonsu et al. (2003) also proposed another component of wind speed that accounts for the buoyant effects inside the canyon. The free-convection velocity (w_*) assumes that the thermal production of turbulence is not negligible. The following expression was proposed:

$$w_* = \left(\frac{g}{T_{can}}Q_{r+w}h\right)^{1/3}, \tag{5.14}$$

where g is the gravitational acceleration (ms^{-2}), and the heat flux Q_{r+w} (Wm^{-2}) encompasses both road and wall turbulent heat fluxes.

Finally, an effective wind speed inside the canyon (U_{eff}) is calculated as a combination of horizontal and vertical components:

$$U_{eff} = \sqrt{U_{can}^2 + (u_* + w_*)^2}\,. \tag{5.15}$$

The formulation used in TEB assumes a uniform wind speed inside the urban canyon. In terms of the interactions between urban structures and an urban environment, the relevant wind speed is the air velocity near surfaces, where the convective heat transfer takes place. In real urban canyons, the wind speed has a great spatial variability. As an example, we can consider the case of a wind blowing transversely to a canyon with constant speed, so a vortex is formed inside the canyon (Fig.5.3).

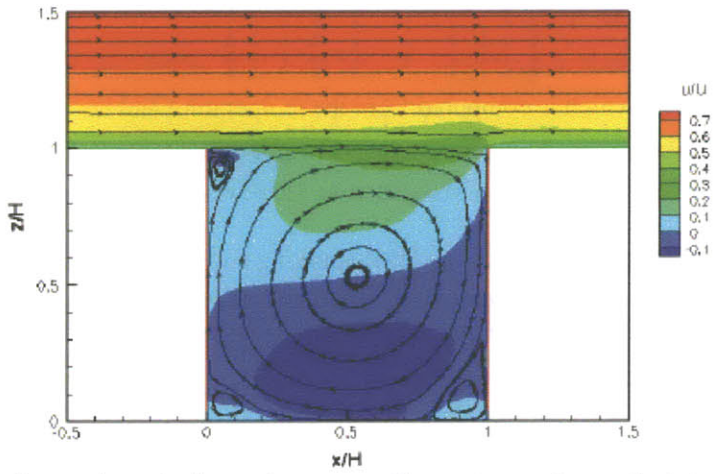

Fig.5.3: Example of vortex formation in an urban canyon. Flow patterns and normalized streamwise velocities *(Li et al., 2009).*

The vortex problem is being widely studied by different urban climate researchers. Taking advantage of the computational growth of computers, they are using computational fluid dynamic (CFD) techniques to simulate the phenomenon under different dynamical and thermal conditions.

The strong variability of velocities shown in Fig.5.3 introduces the problem of specifying the characteristic wind speed to be considered for energy calculations in an urban area. To further illustrate this problem, Fig.5.4 compares the profile of vertical wind speed in an urban canyon, applying the correlations used in the CAT model to represent the vortex formation (see section 2.4.5), with the vertical velocity calculated from TEB formulation (Eq.5.12), where the additional term w_* is neglected. In both cases, the wind speed above the canyon is 5m/s. As can be seen, near the wall, one formulation is predicting twice wind speed that the other, which directly affects the calculation of surface convective heat transfer.

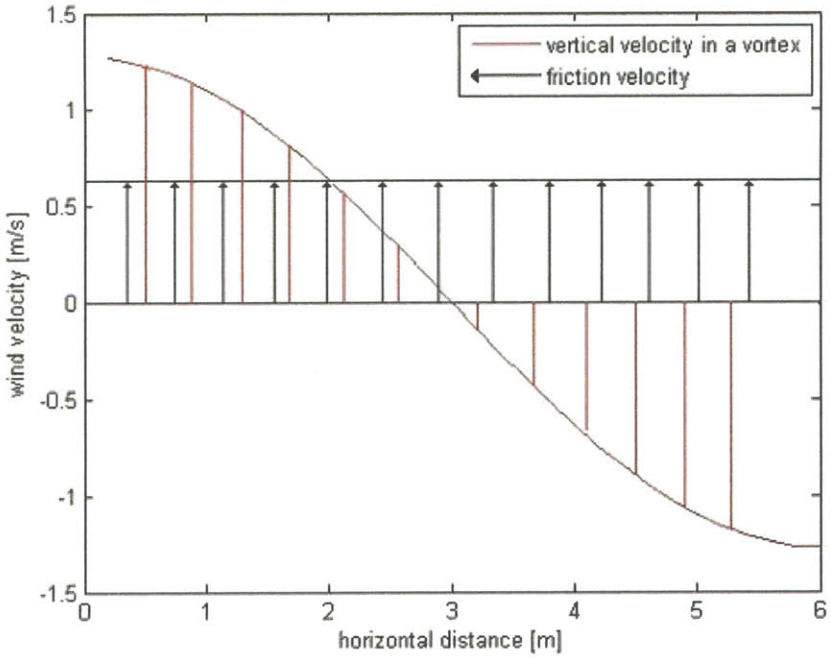

Fig. 5.4: vertical velocity in an urban canyon assuming vortex formation (red) and assuming it is equal to a characteristic friction velocity (black).

Furthermore, in real urban canyons, we do not have a constant wind speed blowing in one direction, which would form a clear vortex inside the canyon, but we have wind blowing in different directions with different intensities. Near the walls, even if the average wind velocities indicate a predominant vortex configuration, the heat transfer would not be characterized by these average velocities, since positive and negative wind directions do not cancel each other, but contribute together to convective heat transfer.

All these uncertainties in the calculation of urban wind speeds show another gap in current knowledge that is outside the scope of this thesis, which again relies on the formulation implemented in TEB.

5.6. Road surface temperatures

In TEB, the surface temperature of the road is calculated by solving numerically a transient conduction equation, taking into account the thermal properties of the various materials that compose the road. The lower boundary condition is represented as a zero flux lower boundary. As upper boundary condition, the following surface heat balance is applied:

$$-k\left.\frac{\partial T_r(x,t)}{\partial x}\right|_{x=0} = S_r^*(t) - L_r^*(t,T_{r1}) - H_r(t,T_{r1}), \tag{5.16}$$

where k is the thermal conductivity of the soil ($Wm^{-1}K$), T_r is the temperature of the soil, and T_{r1} is the surface temperature of the road. Longwave and solar net fluxes are represented by L_r^* and S_r^*, respectively (Wm^{-2}).

5.6.1. Longwave radiation

The net longwave radiation at the road is computed assuming that the road and walls are grey surfaces, and that the top of canyon behaves as a black body. Then, considering that both walls are at the same temperature, and taking into account the first reflection of solar radiation, the net longwave radiation absorbed by the road can be expressed as:

$$\begin{aligned} L_r^* &= -\varepsilon_r \sigma T_r^4 + \varepsilon_r \Psi_r L^{\downarrow} + \varepsilon_r \varepsilon_w (1-\Psi_r)\sigma T_w^4 \\ &+\varepsilon_r (1-\varepsilon_w)(1-\Psi_r)\Psi_w L^{\downarrow} + \varepsilon_r \varepsilon_w (1-\varepsilon_w)(1-\Psi_r)(1-2\Psi_w)\sigma T_w^4 , \\ &+\varepsilon_r (1-\varepsilon_w)(1-\Psi_r)\Psi_w \sigma \varepsilon_r T_r^4 \end{aligned} \tag{5.17}$$

where ε_w is the emissivity of a wall, ε_r is the emissivity of the road, Ψ_r is the sky view factor of the road, and Ψ_w is the sky view factor of a wall. From left to right, the terms on the right hand side of Eq.5.17 represent the longwave radiation emitted from the road, and the longwave radiation absorbed from the sky, from the walls, from the reflection of the sky onto the walls, from the reflection of the walls onto themselves, and from the reflection of the road onto the walls.

The sky view factors are computed for a two-dimensional representation of the canyon, as follows:

$$\begin{aligned} \Psi_r &= [(h/w)^2 + 1]^{1/2} - h/w, \\ \Psi_w &= \frac{1}{2}\left\{h/w + 1 - [(h/w)^2 + 1]^{1/2}\right\} / (h/w), \end{aligned} \tag{5.18}$$

where *h/w* is the aspect ratio of the urban canyon.

5.6.2. Solar radiation

As we have seen, TEB calculates the solar radiation averaged over all orientations, which represents the average conditions of a neighbourhood or town where all orientations are possible. This approach is described in this section.

TEB calculates the direct solar radiation by integrating with respect to all orientations of an urban canyon. The direct solar radiation that reaches the road ($S_r^{\Downarrow}$ (Wm^{-2})) then reads:

$$S_r^{\Downarrow} = S^{\Downarrow}\left[\frac{2\theta_o}{\pi} + \frac{2}{\pi}\frac{h}{w}\tan(\lambda)(1-\cos(\theta_o))\right], \tag{5.19}$$

where $S^{\Downarrow}$ is the incoming horizontal solar radiation (Wm^{-2}), λ is the solar zenith angle, and θ_o is the critical canyon orientation for which the road is no longer sunlit. The critical canyon orientation is given by:

$$\theta_o = \arcsin\left(\min\left[\frac{w}{h}\frac{1}{\tan(\lambda)};1\right]\right). \tag{5.20}$$

The diffuse solar radiation received by the road ($S_r^{\downarrow}(Wm^{-2})$) is directly deduced from the sky-view factor of the road (Ψ_r), as follows:

$$S_r^{\downarrow} = S^{\downarrow}\Psi_r, \tag{5.21}$$

where $S^{\downarrow}$ is the incoming sky radiation (Wm^{-2}).

The model also accounts for the multiple reflections that occur inside the canyon. The sum of the reflections against the road is expressed as:

$$M_r = \frac{R_r(0) + (1-\Psi_r)\varepsilon_r(R_w(0) + \Psi_w\varepsilon_w R_r(0))}{1-(1-2\Psi_w)\varepsilon_w + (1-\Psi_r)\Psi_w\varepsilon_r\varepsilon_w}, \tag{5.22}$$

where

$$R_w(0) = \varepsilon_w S_w^{\Downarrow} + \varepsilon_w S_w^{\downarrow} \tag{5.23}$$

and

$$R_r(0) = \varepsilon_r S_r^{\Downarrow} + \varepsilon_r S_r^{\downarrow}. \tag{5.24}$$

The total solar radiation absorbed by the road is the sum of the direct, diffuse and reflective components.

5.6.3. Solar radiation formulation for a specific canyon orientation

As mentioned before, the UWG scheme is interested in analyzing not only an average urban canyon, but also a specific urban canyon. Kusaka et al. (2001) developed an urban canopy model similar to TEB, but which includes a direct solar radiation formulation that considers a specific orientation of the urban canyon. This formulation is described here.

The information required for this model is hourly values of the solar zenith angle (θ_z) and the solar azimuth angle (θ_{sun}). Fig.5.5 represents the relevant solar angles for this model.

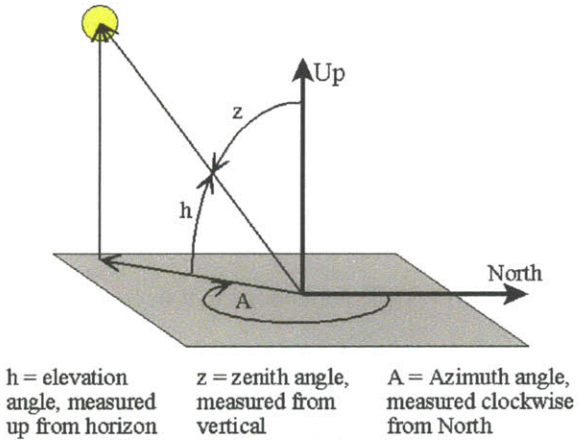

Fig.5.5: Representation of relevant solar angles.

The model defines a shadow length as the portion of the road shadowed by the buildings in a two-dimensional urban canyon (Fig.5.6).

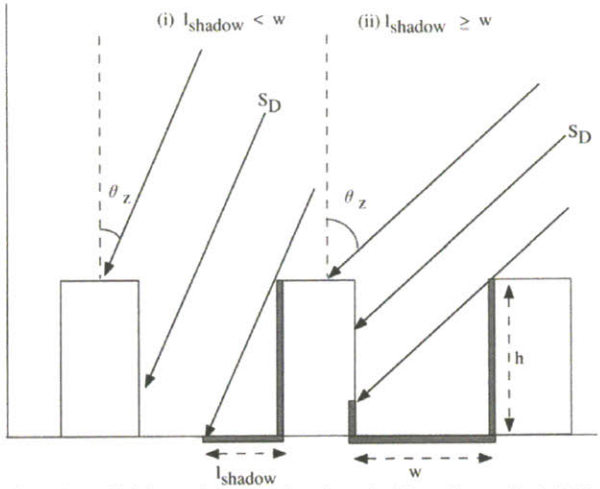

Fig.5.6: Definition of the shadow length (*Kusaka et al., 2001*).

The shadow length (l_{shadow}) is calculated as:

$$l_{shadow} = \begin{cases} 0 & 0 > l_{shadow} \\ h \cdot \tan\theta_z \cdot \sin\theta_n & 0 < l_{shadow} < w \\ w & l_{shadow} > w \end{cases}, \tag{5.25}$$

where h is the average building height, w is the canyon width, θ_n is the angle between the direction of the sun and the canyon axis, calculated as $\theta_n = \theta_{sun} - \theta_{can}$; and θ_{can} is the canyon orientation.

Then, the average direct solar radiation that reaches the road ($S_r^{\Downarrow}$) for a specific orientation of the urban canyon can be calculated with the following expression:

$$S_r^{\Downarrow} = S^{\Downarrow} \frac{w - l_{shadow}}{w}, \tag{5.26}$$

where $S^{\Downarrow}$ is the incoming horizontal solar radiation (Wm^{-2}).

CHAPTER 6

The vegetation model at the weather station

6.1. Introduction

In the last two chapters, we saw the energy interactions between buildings and an urban environment, which correspond to *step3* of the UWG scheme (Fig.3.1). Another critical part of the UWG scheme is the conversion of meteorological information at the weather station, from the measurement height (2m temperature and humidity; 10m wind speed) to a reference height above the station. In chapter 8, we will see an example of how vertical differences in air temperature at the weather station can be of the same order of magnitude as the vertical differences in the urban site. Therefore, the application of a vegetation scheme at the weather station is crucial in order to provide the boundary conditions at a reference height above the urban canyon that the urban canopy model requires.

This chapter describes the main concepts of the Interaction Soil Biosphere Atmosphere (ISBA) scheme, which is the model of choice for *step1* of the UWG scheme (Fig.3.1). The ISBA scheme was developed by Noilhan and Planton (1989), and updated by Noilhan and Mahfouf (1996), to predict the exchanges of heat and water between a vegetated surface or the soil, and the atmosphere. The ISBA scheme is implemented in the super-program SURFEX (CNRM, France), together with the TEB scheme described in chapter 5.

ISBA calculates the sensible and latent heat fluxes, as well as the mass transfer, between the surface of a rural site and the low-level atmosphere. These surface heat and mass fluxes are calculated from an aerodynamic formulation. The model also needs to calculate the evaporation of water, which is modeled by the α -method (Noilhan and Mahfouf, 1996). The initial version of the scheme used a force-restore method for computing the temperature and water content of the soil. This method has a lower computational cost than a numerical solution of the diffusion equations, but it requires the calibration of empirical coefficients. In the version of ISBA currently implemented in SURFEX, it is possible to choose a diffusion model to solve the heat and mass transfer in the soil, instead of the force-restore method. Finally, the scheme solves one more equation for the water intercepted by vegetation.

The objective of this chapter is to ensure that the reader understands the fundamentals behind *step1* of the UWG scheme. For a detailed definition of the equations implemented in the ISBA scheme see Le Moigne (2009).

6.2. The force-restore method

The force-restore method implemented in the initial version of the ISBA scheme solves five prognostic equations: the deep soil temperature equation, the deep soil water content equation, the surface soil/vegetation temperature equation, the top soil water content equation, and the interception water storage equation.

6.2.1. Calculation of soil heat content

In the force-restore method, the soil/vegetation surface temperature (T_s) evolves due to both the diurnal forcing ($G = Q^* - H - E$) and a restoring term towards the mean temperature of the soil (T_2). In contrast, the mean temperature of the soil varies only according to a slower relaxation towards T_s. This is expressed in Noilham et al. (1996) as:

$$\frac{\partial T_s}{\partial t} = \frac{1}{C_T}(Q^* - H - E) - \frac{2\pi}{\tau}(T_s - T_2) \tag{6.1}$$

and

$$\frac{\partial T_2}{\partial t} = \frac{1}{\tau}(T_s - T_2), \tag{6.2}$$

where H and E are the sensible and latent surface heat fluxes (Wm^{-2}), and Q^* is the net-radiation at the surface (Wm^{-2}). The parameter C_T is the surface soil/vegetation heat capacity ($Jm^{-2}K$), and τ is a characteristic time (s), which corresponds to a day period.

6.2.2. Calculation of soil water content

Similarly, the equations for top soil water content (w_s (m^3m^{-3})) and deep soil water content (w_2) are expressed as:

$$\frac{\partial w_s}{\partial t} = \frac{C_1}{\rho_w d_1}(P_s - V_s) - \frac{C_2}{\tau}(w_s - w_{seq}), \qquad 0 \le w_s \le w_{sat}; \tag{6.3}$$

and

$$\frac{\partial w_2}{\partial t} = \frac{1}{\rho_w d_2}(P_s - V_s - TR_s) - \frac{C_3}{d_2 \tau}\max[0,(w_2 - w_{fc})], \quad 0 \le w_2 \le w_{sat}, \tag{6.4}$$

where P_s is the precipitation water flux reaching the soil surface ($kg_w s^{-1} m^{-2}$), V_s is the evaporation at the soil surface ($kg_w s^{-1} m^{-2}$), TR_s is the transpiration rate ($kg_w s^{-1} m^{-2}$), ρ_w is the density of water ($kg_w m^{-3}$), d_1 and d_2 are the depths of top and deep soil (m), and w_{sat} is the total soil porosity ($m^3 m^{-3}$). The second term in Eq. (6.4) represents the drainage, which is proportional to the water amount exceeding the field capacity (i.e. $(w_2 - w_{fc})$), where w_{fc} is the field capacity volumetric moisture content. The coefficients C_1, C_2, and C_3 (m), as well as the equilibrium surface volumetric moisture (w_{seq}), were calibrated for different soil textures and moistures (Noilhan and Planton,1989).

6.2.3. The three-layer option

The standard two-soil layer version of ISBA does not differentiate between the root zone and the total soil water reservoir. The ISBA version currently implemented in SURFEX offers a three-layer model, where the bulk soil layer is divided into a root-zone layer and base-flow

layer. Like this, the deepest soil layer may provide water to the root zone, and the available water content for transpiration is modified accordingly.

6.2.4. Calculation of intercepted water

Rainfall and dew intercepted by the foliage feed a reservoir of water content W_r (kgm^{-2}). This amount of water evaporates from the fraction of the foliage covered with water, while the remaining part of the leaves transpires. In Noilham et al. (1996), the prognostic equation for the intercepted water is expressed as:

$$\frac{\partial W_r}{\partial t} = vegP_{veg} - (V_{veg} - TR_{veg}) - R_r, \qquad 0 \le W_r \le W_{r\max}, \qquad (6.5)$$

where *veg* is the fractional vegetation cover, P_{veg} is the precipitation rate at the top of the vegetation ($kg_w s^{-1} m^{-2}$), V_{veg} is the evaporation from the vegetation, TR_{veg} is the transpiration of the leaves, and R_r is the drainage from the reservoir. This drainage occurs when W_r exceeds a maximum value $W_{r\max}$, which depends on the density of the canopy.

6.2.5. Treatment of drainage

In its initial version, ISBA simulates surface drainage only when the soil is saturated. When the variability of drainage production is small, the soil almost never saturates according to the model. However, this approach neglects the surface drainage that can occur due to a partial saturation of the surface. The latest version of ISBA includes a drainage parameterization to account for sub-grid scale drainage (Le Moigne, 2009).

6.3. The diffusion method

As we have seen, the latest version of the ISBA scheme allows the user to choose between a force-restore approach and a diffusive approach for the calculation of the soil temperature and water content. The diffusion method solves the transient conduction and mass transfer equations downwards from the soil surface. In absence of sublimation processes, this can be expressed as:

$$\frac{\partial T_s}{\partial t} = \alpha \frac{\partial^2 T_s}{\partial z^2} \qquad (6.6)$$

and

$$\frac{\partial w_s}{\partial t} = -\frac{\partial F}{\partial z} - \frac{S_l}{\rho_w}, \qquad w_{\min} \le w \le w_{sat}, \qquad (6.7)$$

where α is the thermal diffusivity of the soil ($m^2 s^{-1}$), F is the vertical flow rate of water (ms^{-1}), S_l represents a external source/sink of water ($kgm^{-3}s^{-1}$), and $w_{\min}$ is a minimum liquid water threshold. The vertical flow rate of water (F) is calculated based on Darcy's law for liquid water transfer (see Le Moigne, 2009).

6.3.1. Boundary conditions

At the lowest layer, a zero-flux boundary condition is applied. The upper boundary condition of Eq.(6.6) can be expressed as:

$$C_T \frac{\partial T_s}{\partial t} = (Q^* - H - E) - G_1, \tag{6.8}$$

where $G_o = Q^* - H - E$ is the heat exchange (W) between the surface and the low-level atmosphere, and G_1 is the conduction heat flux coming from the soil. This definition can be seen as a prognostic equation of a force-restore method if G_1 is expressed as a restore term.

6.4. Surface heat fluxes

The surface heat fluxes Q^*, H, and E are calculated here in an analogous way to that in the TEB model (see chapter 5). The net-radiation (Q^*) is given by the sum of the absorbed fractions of incoming solar radiation and atmospheric longwave radiation, reduced by the emitted infrared radiation. The sensible and latent heat fluxes, H and E (Wm^{-2}), are calculated by means of a surface-layer formulation. The sensible heat flux is expressed as:

$$H = \rho c_p C_H U_{met} (T_s - T_{met}), \tag{6.9}$$

where U_{met} and T_{met} are the wind speed and the air temperature at the lowest atmospheric level; and C_H is a reduction factor that account for atmospheric stability (see section 5.4).

The water vapor flux is calculated as the sum of the evaporation of liquid water from the soil surface (V_s), and from the vegetation (V_{veg}). Then, the latent heat flux can be calculated as:

$$E = l_v (V_s + V_{veg}), \tag{6.10}$$

where

$$V_s = (1 - veg)\rho C_H U_{met} (h_u q_{sat}(T_s) - q_{met}) \tag{6.11}$$

and

$$V_{veg} = veg\,\rho C_H U_{met} h_v (q_{sat}(T_s) - q_a); \tag{6.12}$$

and where l_v is the specific heat of evaporation (Jkg^{-1}), $q_{sat}(T_s)$ is the saturated air humidity content at the temperature T_s, and q_a is the air humidity content at the lowest atmospheric level. The parameters h_u and h_v are the relative humidity at the soil surface and the Halstead coefficient (Le Moigne, 2009), respectively.

CHAPTER 7

Mesoscale correlations

7.1. Introduction

Previous chapters presented the models that compose *step1* and *step3* of the UWG scheme (Fig.3.1). This chapter discusses the possibilities and difficulties of finding a solution for *step2* of the scheme. *Step2* corresponds to a horizontal transformation that accounts for the UHI effect inside the urban boundary layer. The complexity of the meteorological phenomena that take place at this atmospheric level limits the application of simple solutions to this problem.

Urban canopy models use mesoscale models to obtain the boundary conditions they need above the urban canopy layer. Mesoscale models are 3-dimensional CFD models that are able to predict the meteorological phenomena at this atmospheric level. One of the most widely used mesoscale models is the Weather Research and Forecasting (WRF) model, which has already been coupled with the urban canopy model of Kusaka et al. (2001) and is in process of being coupled with TEB (Masson, 2000) and Martilli et al.'s model (2002). Unfortunately, the application of a complex 3-dimensional CFD model does not suit the needs of the current version of the UWG scheme, since the high computational cost of simulations prevents its application to an hour by hour annual simulation.

The solution proposed in this chapter is to find simplified correlations to estimate the UHI effect at this mesoscale level. The main idea is to apply similarity theory to obtain fundamental relations that would relate the UHI effect with known or calculable parameters of the problem. The chapter distinguishes two different situations:

(1) Natural convection dominated problem. When the wind speed is low, the urban boundary layer is dominated by buoyant air circulations.
(2) Forced convection dominated problem. When the wind speed is high enough, the urban boundary layer is dominated by the wind speed magnitude and direction.

In this chapter, we look in the literature for studies that can be applied to this problem. For the natural convection dominated problem, we analyze the works of Lu et al. (1997) and Hidalgo et al. (2009), who developed simplified correlations to calculate the temperature difference between a rural and an urban site at the mesoscale level in absence of wind. For the forced convection dominated problem, however, we have not found studies that can be directly applied to the problem. We analyze some simplified representations of the forced convection boundary layer and adapt the results from other studies to come up with a correlation for this situation. In any case, the proposed correlations still require validation with field data in order to be definitively implemented in the UWG scheme, so this analysis has to be seen as a first step in that direction.

7.2. Natural convection dominated problem

7.2.1. Structure of thermal boundary layers

The first step before making any simplified analysis to this problem is to have an idea of the structure of the thermal boundary layer that is formed above rural and urban areas. Hidalgo et

al. (2009) described this structure, differentiating between nighttime and daytime boundary layers.

During the night and in absence of large-scale wind speed, a stable layer inversion is formed in rural areas, due to the cooling of the surface by sky longwave radiation. Fig.7.1a represents the potential temperature profile associated with the UHI effect for this situation. This stable layer inversion reaches only few hundred meters, and it can be characterized by its potential ambient temperature gradient $\partial\theta / \partial z$, or alternatively, by its Brunt- Väisälä frequency $N = \left(g / \theta \cdot \partial\theta / \partial z\right)^{1/2}$. Above a city, however, the longwave radiation with the sky is less effective and there is a buoyant mixing of air that produces an UHI effect.

During the day and also in absence of wind speed, the rural surface is heated by the sun and the air is mixed to a much higher altitude (Fig.7.1b). The growth limit of this mixing layer varies typically between 500m in winter to 2000m during some hot days in summer. The presence of the city will have a similar effect on the atmosphere, producing an analogous mixing layer. An urban heat island effect will be formed depending on the differences between the upcoming heat fluxes from the city and from the rural surroundings.

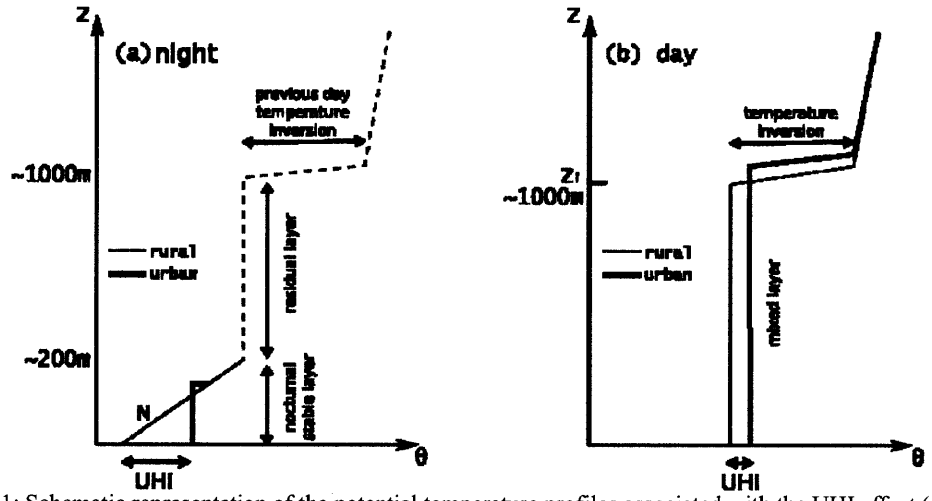

Fig.7.1: Schematic representation of the potential temperature profiles associated with the UHI effect (a) during the night and (b) during the day (*Hidalgo et al., 2009*).

7.2.2. Similarity theory

Hidalgo et al. (2009) developed a correlation for the UHI intensity during the day applying similarity theory to the thermal boundary layer problem described above. Here, the UHI intensity parameter is defined as the temperature difference between the air inside the urban boundary layer and the air inside the rural boundary layer.

The objective of similarity theory is to find scaling factors or laws for unknown variables (e.g. UHI intensity), which are a function of relevant scaling parameters. Once the scaling parameters are identified and the scaling factors are obtained, experiments or numerical analysis are used to calculate the coefficients of proportionality.

Consider the problem represented in Fig.7.2. Hidalgo et al. (2009) showed that the useful parameters in describing the UHI phenomenon at daytime are the following:

- Volumetric heat capacity of the air (ρc_p) $\left[Jm^{-3}K\right]$
- Buoyant coefficient of the air (βg) $\left[ms^{-2}K\right]$
- Characteristic air velocity (w) $\left[ms^{-1}\right]$
- Urban boundary layer thickness (z_i) $\left[m\right]$
- Turbulent heat flux difference between the urban and the rural sites (H_u - H_r) $\left[Js^{-1}m^{-2}\right]$

The fundamental units of each variable are contained in brackets.

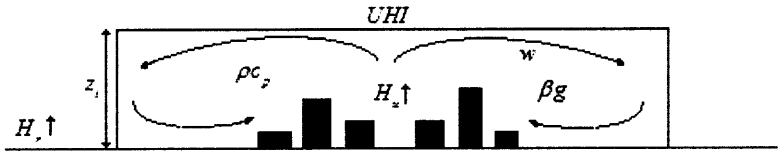

Fig.7.2: Schematic representation of the similarity problem associated with UHI intensity.

The dependence of the UHI intensity with the relevant parameters of the problem can be expressed as:

$$UHI = f(\rho c_p, \beta g, w, z_i, H_u - H_r). \tag{7.1}$$

Applying the Buckingham Pi theorem (e.g. Kundu and Cohen, 2008), we can obtain fundamental relations among these parameters. Since there are six variables and four fundamental units $\{J, m, s, K\}$, there will be two dimensional groups (or Pi groups). These can be written as:

$$\Pi_1 = \frac{w\left(\rho c_p\right)^{1/3}}{\left(g\beta\right)^{1/3} z_i^{1/3} (H_u - H_r)^{1/3}}, \tag{7.2}$$

and

$$\Pi_2 = \frac{UHI\left(\rho c_p\right)^{2/3} (g\beta z_i)^{1/3}}{\left(H_u - H_r\right)^{2/3}}. \tag{7.3}$$

According to the theorem, the Pi groups are invariant and can be represented as constants of proportionality. As a result, the following fundamental relations are obtained for the UHI intensity and the characteristic air velocity due to convective circulation (w):

$$UHI \propto (g\beta z_i)^{-1/3} \left(\frac{H_u - H_r}{\rho c_p}\right)^{2/3}, \tag{7.4}$$

and

$$w \propto \left(g\beta z_i \frac{H_u - H_r}{\rho c_p}\right)^{1/3}. \tag{7.5}$$

The coefficient of proportionality of Eq. (7.4) was obtained by Hidalgo et al. (2009) based on 3-dimensional high resolution mesoscale simulations. These calculations were performed assuming that the city was perfectly circular. Latent heat exchanges and external wind speed were not considered. The final correlation is given by:

$$UHI_{day} = 17.25\left(g\beta z_i\right)^{-1/3}\left(\frac{H_u - H_r}{\rho c_p}\right)^{2/3}. \qquad (7.6)$$

Fig.7.3 represents the UHI intensity as a function of the heat flux difference (H_u - H_r), according to Eq. (7.6). The values used for the other variables of the problem are ρ=1.2 kgm^{-3}, c_p=1000 $Jkg^{-1}K^{-1}$, β=1/300 K^{-1}, and z_i=*1000 m*.

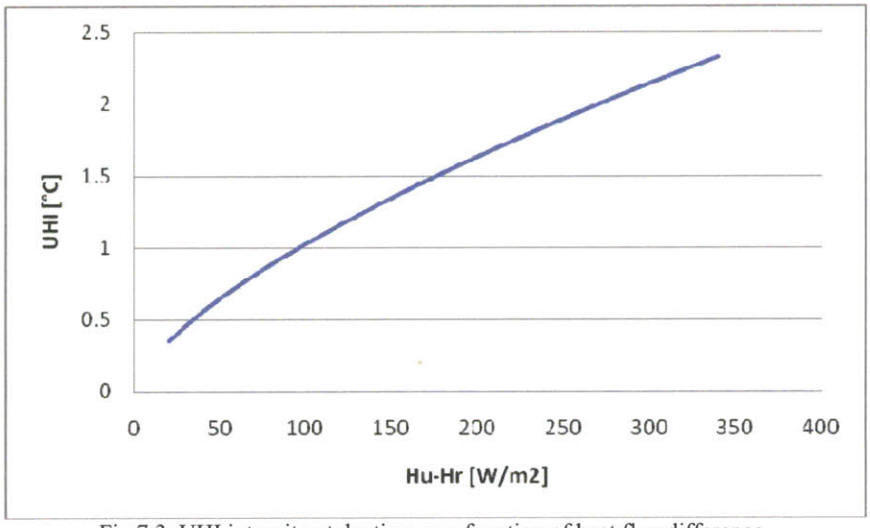

Fig.7.3: UHI intensity at daytime as a function of heat flux difference.

Note that theoretical procedure presented here assumes positive values of (H_u - H_r). Negative values would change the structure of the boundary layers and the resulting expressions would not be valid. Further research is required to evaluate the implications of this assumption.

7.2.3. Simplified physical relationships

Lu et al. (1997) developed a correlation for the UHI intensity at nighttime using a different approach. They considered a series of simplified physical relationships, representing the mass, momentum, and energy equations, from which they obtained scaling factors for the convective velocity (*w*) and UHI intensity. They showed that, under typical nighttime conditions and in absence of large-scale mean wind, the three relevant scaling parameters to calculate the UHI intensity were the characteristic diameter of the city (*D*), the ambient thermal stratification characterized by its Brunt- Väisälä frequency (*N*), and the turbulent heat flux from the city (H_u). Here, two different scales for the air velocity inside the urban boundary layer are considered: a mean radial velocity and an upward velocity.

A relation for the mean radial velocity (w_r) was obtained considering the idealized situation represented in Fig.7.4.

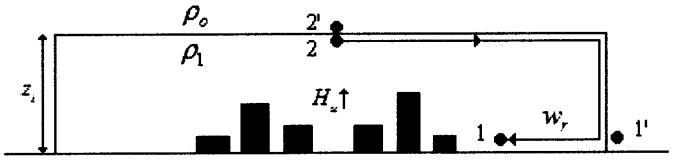

Fig.7.4: Schematic representation of the simplified physical problem used to calculate the mean radial velocity scale.

Assuming the streamline 1-2, where viscous effects are unimportant, we can apply the Bernoulli equation between the points 1 and 2:

$$p_1 + \frac{1}{2}\rho_i w_r^2 = p_2 + \rho_i g z_i, \tag{7.7}$$

where p_k is the thermodynamic pressure at the point k (Pa), ρ_i is the density of the air inside the urban boundary layer (kgm^{-3}), and z_i is the urban boundary layer thickness (m).

Assuming that the flow is static outside the boundary layer, we can apply hydrostatics between points 1' and 2':

$$p_1 = p_2 + \rho_o g z_i, \tag{7.8}$$

where ρ_o is the density of the air outside the urban boundary layer.

Subtracting Eqs. (7.7) and (7.8), and applying the Boussinesq approximation, the following fundamental relation is obtained for w_r:

$$w_r \propto (g\beta\Delta T z_i)^{1/2}, \tag{7.9}$$

where ΔT is the difference of air temperature inside and outside the urban boundary layer (UHI intensity).

A relation between the mean radial velocity (w_r) and the mean upward velocity (w_z) is obtained from the continuity equation:

$$\frac{\partial w_r}{\partial r} + \frac{\partial w_z}{\partial z} = 0 \rightarrow w_r z_i \propto w_z D, \tag{7.10}$$

where D is the diameter of the city (m).

A relation for the UHI intensity is obtained from the urban heat flux (H_u (Wm^{-2})) and the upward velocity (w_z), as follows:

$$UHI \propto \frac{H_u}{\rho c_p w_z}. \tag{7.11}$$

An additional relationship takes into account the air stratification through the Brunt- Väisälä frequency ($N\,(s^{-1})$), which is defined as:

$$N \propto (g\beta \cdot UHI / z_i)^{1/2} \ . \tag{7.12}$$

Eqs. (7.9) - (7.12) contain four unknowns, namely w_r, w_z, UHI, and z_i, and can be solved to obtain the following scaling factors for the convective air velocity (w) and the UHI intensity:

$$w_r = w \propto \left(g\beta D \frac{H_u}{\rho c_p} \right)^{1/3} \ , \tag{7.13}$$

and

$$UHI \propto N(g\beta)^{-2/3} \left(D \frac{H_u}{\rho c_p} \right)^{1/3} \ . \tag{7.14}$$

The coefficient of proportionality of Eq. (7.14) was obtained by Lu et al. (1997) based on experiments with a scale model, consisting of a water tank heated from a circular disk located at the bottom of the tank. The final correlation is given by:

$$UHI_{night} = 1.61N(g\beta)^{-2/3} \left(D \frac{H_u}{\rho c_p} \right)^{1/3} \ . \tag{7.15}$$

A closer look at Eqs. (7.6) and (7.15) shows that both expressions are equivalent if N is substituted by its definition (Eq.7.12) and the boundary layer thickness (z_i) is used as a length scale instead of the diameter of the city (D). The authors argue (Hidalgo, personal communication) that the different structure of the boundary layer varies the weight of the different physical parameters. At nighttime, D appears instead of z_i because the inversion height is small compared to the diameter of the city, so the most relevant length scale is the first one. During the day, however, the deciding length factor is the inversion height.

Fig.7.5 represents the UHI intensity as a function of the urban heat flux, according to Eq.(7.15). The values used for the other variables of the problem are ρ=1.2 kgm^{-3}, c_p=1000 $Jkg^{-1}K^{-1}$, β=1/300 K^{-1}, $N = 0.018\ s^{-1}$, and D=5000 m. Note that the Brunt-Väisälä frequency depends on the boundary layer thickness (z_i) and the UHI itself, so it is not trivial to find a value for it. The value used in Fig.7.5 has been obtained assuming z_i=200m and $\Delta T = 2K$.

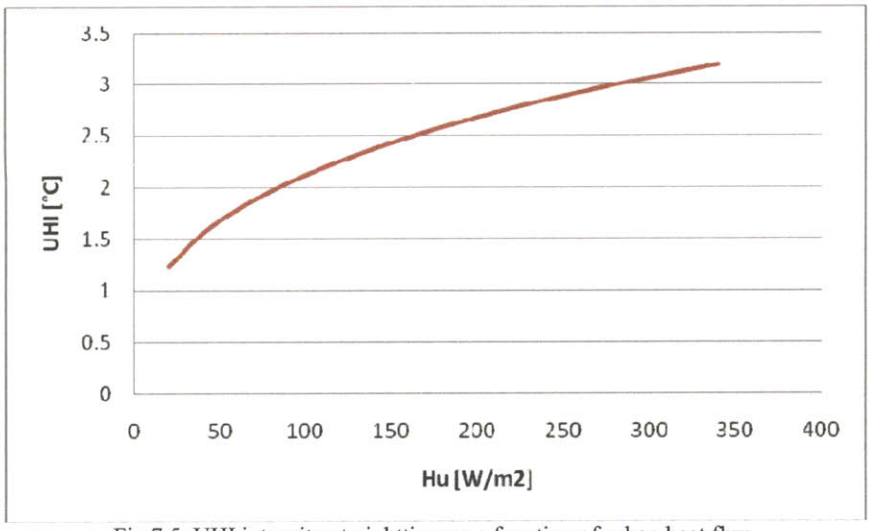

Fig.7.5: UHI intensity at nighttime as a function of urban heat flux.

7.2.4. City size and UHI

One of the frequently asked questions regarding the UHI effect is its relation with the size of cities. The works of Lu et al. (1997), Hidalgo et al. (2009), and Atkinson (2002) provide some discussion to this question.

As can be noted from Eq. (7.15), Lu et al. (1997) assumed that there is a relation between the UHI intensity and the diameter of the city (Fig.7.6).

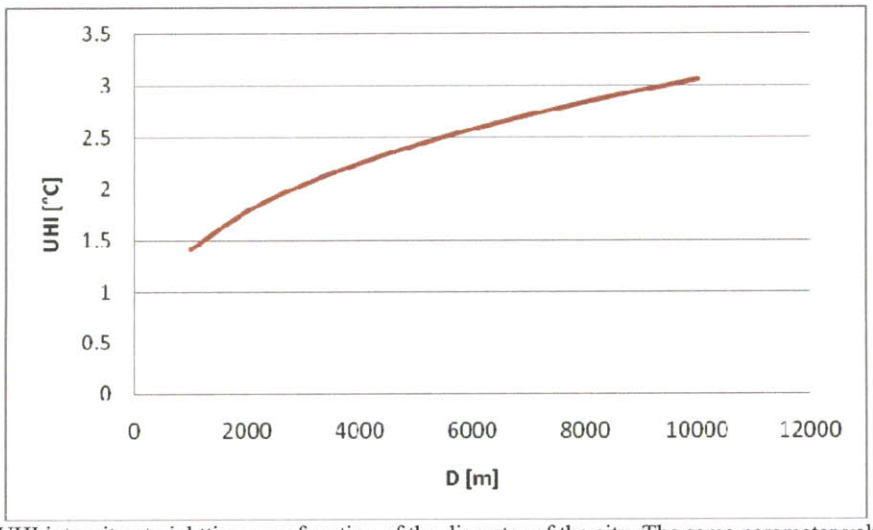

Fig.7.6: UHI intensity at nighttime as a function of the diameter of the city. The same parameter values as in Fig.7.5 have been used plus $H_u = 150\,Wm^{-2}$.

In contrast, Hidalgo et al. (2009) explicitly stated that the city size has a minimal effect on the UHI intensity. They showed that the UHI intensity depends on the relative position of the observer within the city, but not on the diameter of the city itself, which does not appear in Eq. (7.6). They stated that the highest UHI intensity is produced at the center of the city and it

decreases almost linearly. The correlation proposed in Hidalgo et al. (2009) can be very well approximated to:

$$\frac{UHI}{17.25\theta_s} = \frac{x}{D}, \tag{7.16}$$

where x is the distance from the periphery of the city to the center, D is the diameter of the city, and θ_s is the UHI scaling factor shown in Eq. (7.4).

Atkinson (2002) reviewed the different approaches in the literature that account for the relation between city size and UHI. In his paper, he simulates the UHI intensity of a city varying its horizontal dimension from 6 to 20 km in steps of 2 km. His results revealed only a small sensitivity of UHI intensity to city size. The maximum UHI intensity for the largest urban area was about 0.2 °C greater than for the smallest city.

Fig.7.7 shows one of Atkinson's results. He used a mesoscale model with a bulk urban parameterization to simulate a big city (London) for the first week of September. He also assumed an anthropogenic heat level of $100\ Wm^{-2}$.

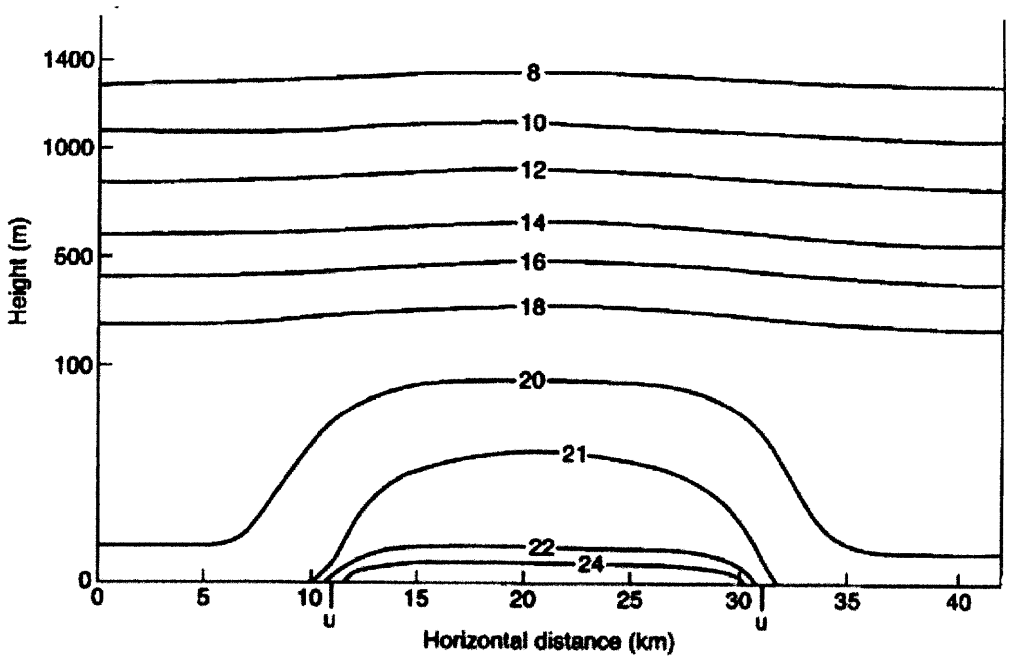

Fig.7.7: Isothermals (°C) resulted from mesoscale simulations of London during the first week of September (*Atkinson, 2002*).

If we now try to obtain the UHI intensity distribution by drawing a horizontal line in Fig.7.7 and calculating the temperature difference between inside and outside the city as a function of the distance, we will produce a curve like the one represented in Fig.7.8. This curve shows an approximately linear section, which agrees with Hidalgo et al.'s findings, but then it flattens nearby the center of the city.

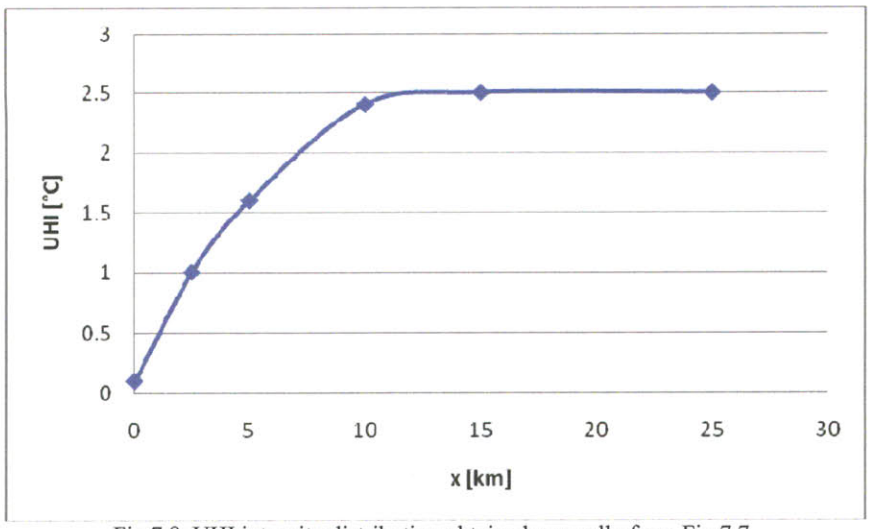

Fig.7.8: UHI intensity distribution obtained manually from Fig.7.7.

In summary, this section has shown different points of view about the relation between city size and UHI effect. We have not found an agreement about this relation, but assuming a weak dependence seems to be reasonable. This section has also given some insights about the distribution of UHI intensity along a city. These results will be used in section 7.3.2.

7.3. Forced convection problem

In previous sections, the main assumption underlying the theoretical approach was that the large-scale mean wind speed did not dominate the buoyant air velocities. In the following sections, we are interested in exploring different methods to account for the wind speed, which will have an attenuating effect on the UHI intensity.

Consider a 2-dimensional situation where the wind is blowing from the meteorological station toward the city (Fig.7.9). In this situation, a typical thermal boundary layer would be formed above the urban area. The problem will be to calculate the thermal conditions inside the boundary layer given the conditions at a reference height above the weather station (*step1*). Hanna and Britter (2002) stated that, at a certain height above the surface, we can assume that the wind speed does not vary in the horizontal direction. We will also assume that the reference height is high enough to neglect any vertical air velocity gradient.

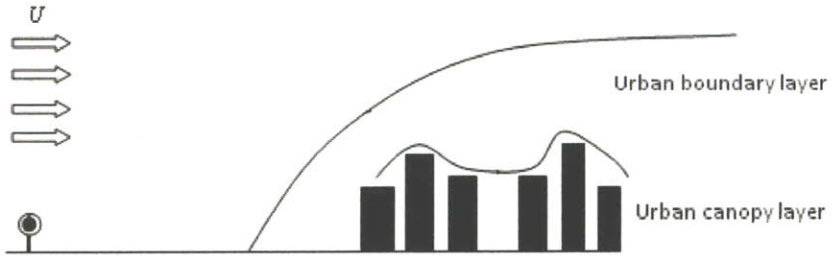

Fig.7.9: Schematic representation of the boundary layer problem in presence of wind speed.

Consider now the opposite situation where the wind is blowing in the other direction. In this case, the urban boundary layer can reach the weather station, and both locations would be

affected by the same mesoscale conditions. As a result, *step2* would not be necessary, and the results of *step1* could be directly used in *step3*. *Step2* can also be skipped if the weather station is close to the urban site, or if the wind speed is high enough, so the boundary layer thickness is small.

In summary, the objective of this section is to find simplified expressions for the UHI effect inside the urban boundary layer in presence of large-scale wind speed, when this not too high, but dominant over the convective buoyant velocities; and when the wind is blowing from the weather station toward the urban site. One could think that an approximate solution for this problem would be given by adapting the existing correlations of boundary layers over a rough flat plate to the thermal problem. However, the lack of an analogy between the dynamic and the thermal boundary layers in a rough surface prevented us from applying this approach.

7.3.1. Analogy with similarity theory

In section 7.2.2, similarity theory was applied to the UHI problem under the hypothesis of no dominant large-scale mean wind. When the wind is dominant, we can consider the same approach but using the wind speed (U) as a known scaling parameter.

Consider now the problem represented in Fig.7.10, where the heat flux from the urban canopy layer is constant and evenly distributed along the city.

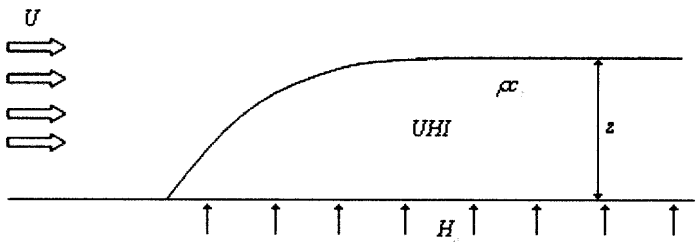

Fig.7.10: Schematic representation of the similarity theory problem in presence of wind speed.

Applying similarity theory to this problem, a dimensional analysis produces the following fundamental relation between the UHI intensity, the urban heat flux, and the external wind speed:

$$UHI \propto \frac{H_u}{\rho c_p U} \quad . \tag{7.17}$$

Note that the coefficient of proportionality can be a function of the boundary layer thickness (z_i).

7.3.2. Simplified heat transfer problem

Another approach that will give an equivalent result is to solve a simplified energy balance in the urban boundary layer. Consider the control volume represented in Fig.7.11.

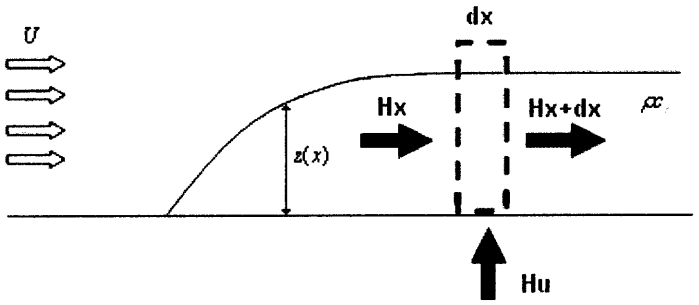

Fig.7.11: Energy balance to a control volume in the urban boundary layer.

The horizontal heat fluxes affecting the control volume can be expressed as:

$$H_x = U\rho c_p z_i(x)T(x), \tag{7.18}$$

and

$$H_{x+dx} = U\rho c_p z_i(x)\left(T(x)+\frac{dT}{dx}dx\right); \tag{7.19}$$

and they have units of *W/m*. *T(x)* represents the temperature of the boundary layer, which is a function of the horizontal coordinate *x*.

Applying an energy balance to the control volume, we obtain:

$$U\rho c_p z_i(x)T(x)+H_u dx = U\rho c_p z_i(x)\left(T(x)+\frac{dT}{dx}dx\right). \tag{7.20}$$

Simplifying and rearranging terms, we obtain the following differential equation:

$$\frac{dT}{dx} = \frac{H_u}{U\rho c_p z_i(x)}, \tag{7.21}$$

which can be solved to get:

$$T_u - T_r = \frac{H_u}{U\rho c_p}\int_0^x \frac{dx}{z_i(x)}, \tag{7.22}$$

Note that Eq. (7.22) has the same fundamental relation as Eq. (7.17), but considering the integral as a coefficient of proportionality.

Using Eq. (7.22), we can evaluate different distributions of UHI intensity along the city for different distributions of boundary layer thickness. In particular, the following three situations will be analyzed:

- Constant boundary layer thickness, which gives a linear growth of UHI intensity, as was suggested by Hidalgo et al. (2009) (see section 7.2.4).
- Linear boundary layer thickness, which produces a logarithmic growth of UHI intensity and approximates the distribution inferred in section 7.2.4 from Atkinson's results (Fig.7.8).

- Boundary layer growth with the square root of the distance, which corresponds to the typical boundary layer growth in the Blasius flat plate problem (e.g. Kundu and Cohen, 2008). This situation produces a UHI distribution that varies with the square root of the distance.

Fig.7.12 represents Eq. (7.22) for these three situations. The values for the different parameters of the equation are $\rho = 1.2\ kgm^{-3}$, $c_p = 1000\ Jkg^{-1}K^{-1}$, $H_u = 150\ Wm^{-2}$, and $U = 5\ ms^{-1}$. The constant of proportionality were selected so that for $x = 1\ km \rightarrow z_i = 100\ m$.

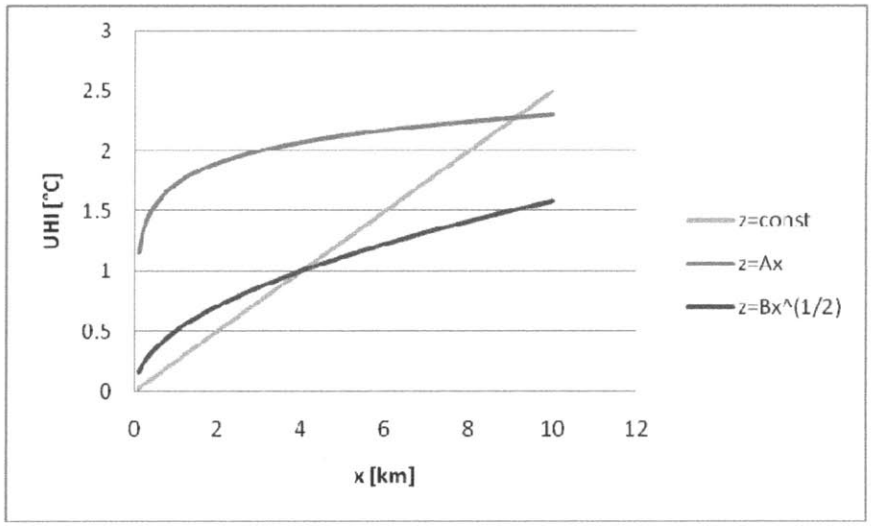

Fig.7.12: UHI intensity distribution as a function of the horizontal coordinate and for different distributions of boundary layer thickness.

7.3.3. Analogies with transport phenomena

In the last two sections, we have seen that the UHI intensity is directly proportional to the urban heat flux and inversely proportional to the wind speed. We still have to define the coefficient of proportionality, which can be a function of the boundary layer thickness. As we saw in section 7.2.1, the boundary layer thickness can vary by one order of magnitude from daytime to nighttime and depends also on the meteorological conditions (stability). To make some progress, we will now assume that the coefficient of proportionality is indeed constant, and we will seek values for it.

Looking at transport phenomena literature, we found a study (Gifford and Hanna, 1972) that stated that the air pollution concentration ($X\ (kgm^{-3})$) could be roughly estimated by the following simple area source formula:

$$X = c\frac{Q_X}{U}, \tag{7.23}$$

where Q_X is source strength per unit area ($kgs^{-1}m^{-2}$), U is the average wind speed, and the parameter c is a weak function of the city size and could be approximated as a constant. Performing a series of experiments to calibrate the parameter c, the authors found a value of

50 for SO_2 contaminants. Applying the existent analogy between transport and thermal phenomena in the atmosphere, we could use the same constant for our UHI problem (Britter, personal communication). Eq. (7.17) would therefore be expressed as:

$$UHI = 50\frac{H_u}{\rho c_p U}. \tag{7.24}$$

Fig.7.13 represents the UHI intensity as a function of the characteristic wind speed, according to Eq. (7.24). As can be seen, when the wind speed decreases below a certain value, the buoyant air velocity becomes dominant, and Eq. (7.24) produces unrealistic results. It can also be observed that when the wind speed is high, the UHI approaches zero as we discussed at the beginning of section 7.3.

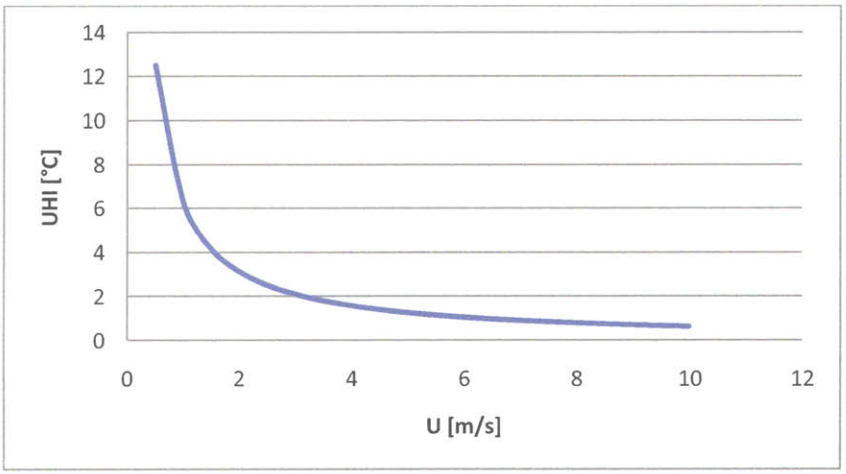

Fig.7.13: UHI intensity as a function of the wind speed according to Eq. (7.24) ($H_u = 150\,Wm^{-2}$).

7.3.4. Experimental data analysis of wind speed dependence

Although the theoretical analysis presented here for the forced convection problem has not been validated with experimental data, we have had access to experimental data that can support some of our findings. The results presented in this section correspond to the experimental campaign CAPITOL (Masson et al., 2008). In this campaign, measurement equipment was introduced in globes filled with gas. In each experiment, which was frequently repeated between March-04 and December-05, two of these globes were released into the atmosphere at the same time and from two different locations: one at the center of Toulouse (France), and another one in a rural site at 20 km north-west of the city. Fig.7.14 represents experimental values of temperature difference between the urban site and the rural site (UHI intensity) as a function of the wind speed measured at the rural site. The values correspond to a reference height of 50 m measured from Toulouse level.

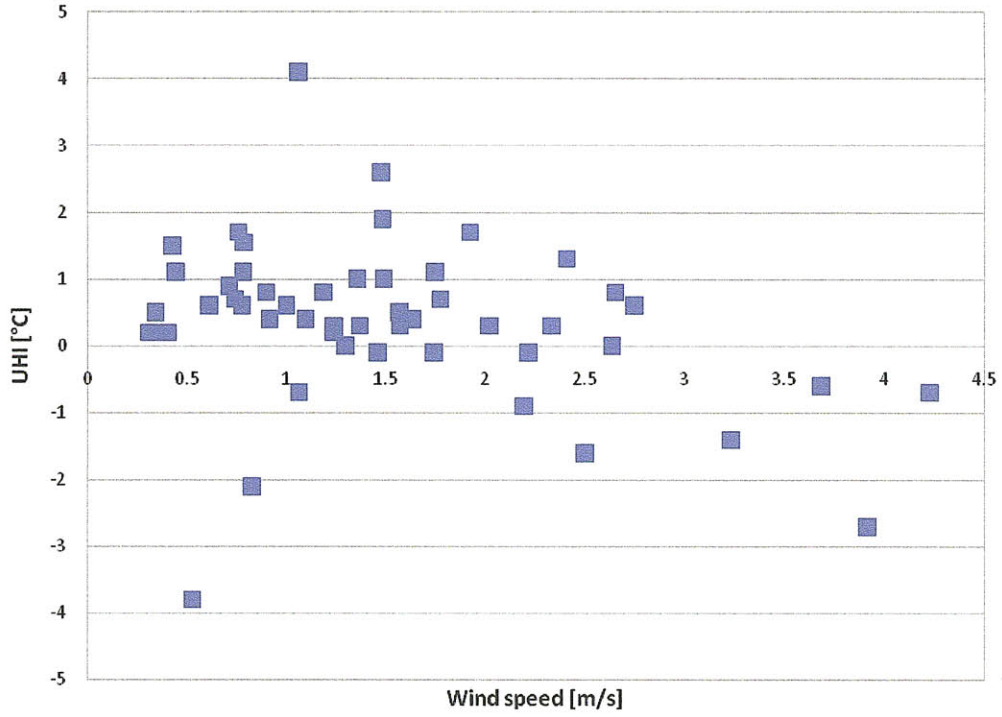

Fig.7.14: Experimental data points relating UHI intensity and wind speed.

At a first sight, no correlation between the UHI intensity and the wind speed seems to predominate. However, considering only the points that correspond to a wind speed larger than 1 *m/s* (forced convection dominated) and to an east-south wind direction (from the rural site toward the urban site) (Fig.7.15), we can observe an inversely proportional relation between the UHI intensity and the wind speed. Moreover, the slope of the regression curve is similar to the one obtained in Fig.7.13.

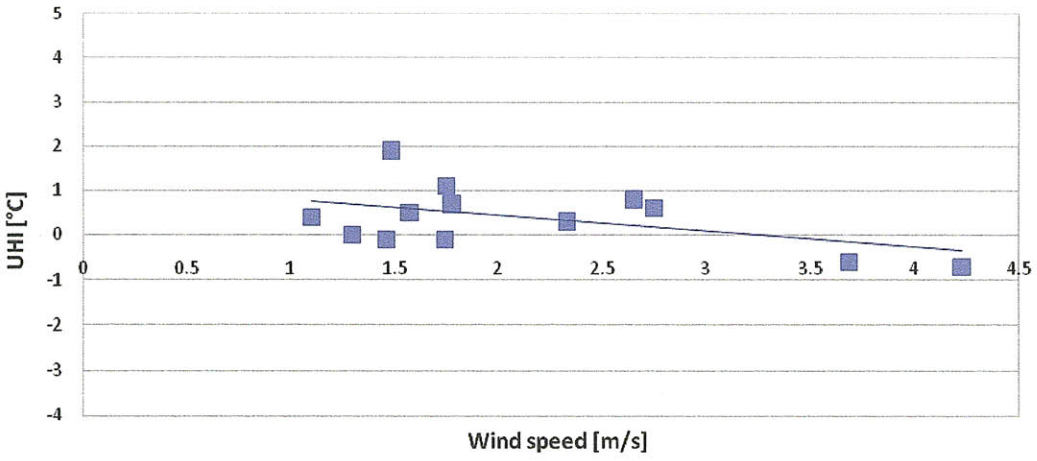

Fig.7.15: Experimental data points when the wind speed is higher than 1m/s and is blowing from the rural site toward the urban site.

7.4. Proposed correlations

The correlations proposed in this chapter still require validation with field data in order to be reliably applicable. The correlations of Hidalgo et al. (2009) and Lu et al. (1997) were both tested under simplifying hypotheses (see sections 7.2.2 and 7.2.3). The suitability of applying these correlations to predict the UHI effect of a real urban area is still undetermined. Eq. 7.24 has been theoretically obtained, and therefore, it needs to be tested with experimental data as well. The required validation procedure escapes from the scope of this thesis, but it will be performed in further developments of the UWG scheme. A draft of how these correlations could be implemented in the UWG scheme is presented here.

The first step would be to have a criterion to determine whether the UHI effect is dominated by natural or forced convection forces. The following non-dimensional wind speed is defined using the results of similarity theory obtained in section 7.2.2:

$$u^* = \frac{U}{(g\beta\Delta T z_i)^{1/2}}. \tag{7.25}$$

For $u^* < 1$, the problem would be dominated by buoyant air circulations and the correlations shown in section 7.2 would apply. The correlation of Hidalgo et al. (2009) would be used at daytime (Eq.7.6), while the correlation of Lu et al. (1997) would be used at nighttime (Eq.7.15). Note that these two correlations still have some parameters that are not completely defined. These are the cases of the Brunt- Väisälä frequency in Eq. (7.15) and the thermal boundary layer thickness (z_i) in Eq. (7.6). For these parameters, justified estimations based on the structure of the boundary layer discussed in this chapter would be required. For $u^* > 1$, the problem is forced convection dominated and Eq. (7.24) would apply.

All this is summarized in the following logic relations:

If $u^* < 1$ and night,

$$UHI_{night} = 1.61N(g\beta)^{-2/3}\left(D\frac{H_u}{\rho c_p}\right)^{1/3}.$$

If $u^* < 1$ and day,

$$UHI_{day} = 17.25\left(g\beta z_i\right)^{-1/3}\left(\frac{H_u - H_r}{\rho c_p}\right)^{2/3}.$$

If $u^* > 1$,

$$UHI = 50\frac{H_u}{\rho c_p U}.$$

Finally, if any of the following is true: $u^* >> 1$, or the wind is blowing from the urban site toward the weather station, or both locations are close together; then, we can assume that both locations have the same mesoscale conditions and *step2* can be skipped.

CHAPTER 8

Case study: Masdar, Abu Dhabi

8.1. Introduction

In this chapter, the application of the UWG scheme to a particular case of study is analyzed. The object of this study is a new urban area called Masdar that is being constructed in Abu Dhabi (United Arab Emirates). The Masdar Project aims to create an energy-efficient urban environment and has promoted various research initiatives in this direction. These initiatives include applying energy-efficient strategies at both building and urban levels to this particular urban area and climate. The evaluation and modeling of these strategies constitute appropriate applications of the UWG scheme.

This case study will focus on explaining how to use the scheme and on showing its potential as compared to a standard building simulation analysis. The importance of considering the Urban Heat Island (UHI) effect in building energy simulations, as well as the importance of including building energy analysis into UHI calculations, will be highlighted. In some cases, a net-energy analysis will be performed. It is not an objective of this study, however, to find optimal design parameters for this urban area.

The chapter will start with a qualitative overview of the content and scope of this case study. Then, the chapter is divided in three main parts. The first part will present the simulation of *step1*. This part will describe the boundary conditions of the problem, the inputs used in the ISBA model, the ISBA iterative procedure, and the analysis of results of *step1*. The second part will describe the simulation of *step3*. This section will analyze the inputs used in EP and TEB, the EP-TEB iterative procedure, and the results obtained for the reference case. The third part is a study of cases. It will analyze the sensitivity of different parameters of the problem, such as the occupation schedule, the amount of waste heat injected into the canyon, and the canyon aspect ratio. The last two studies analyze the effect of applying energy efficiency strategies at the building level and at the urban level. The chapter closes with a summary and an overall evaluation of the UWG scheme as applied to this case study.

8.3. Description of the problem

In this case study, we will analyze the Urban Heat Island (UHI) effect and the Urban Cool Island (UCI) effect produced in a hot and arid climate by an urban canyon configuration. We will also evaluate the impact of these phenomena on the energy performance of buildings. It will be seen that during the day, an UCI effect may be produced due to the shadowing effect from building surfaces. When the buildings are actively conditioned, they act as sinks of heat from the canyon. This heat, together with internal heat sources, can be re-injected into the canyon producing the UHI effect. Other causes of UHI in urban canyons are the trap of radiation due to reduced sky view factors, and the reduction of advective heat removal associated with the loss of momentum of the wind around buildings.

The following metrics will be used to compare and analyze cases: first, the UHI intensity defined as the difference between the air temperature predicted at the urban canyon and the air temperature measured at the weather station; and second, the error in the predicted energy performance of HVAC systems as compared to an EP simulation that uses an *epw* file.

The *epw* file used in this case study corresponds to the weather station of the International Airport of Abu Dhabi. Fig.8.1 shows a satellite image of this airport and the urban site under study (Masdar City). Since both locations are very close to each other, it will be assumed that they are affected by the same mesoscale conditions. In this situation, *step2* of the UWG scheme (Fig.3.1) is not applicable (see section 7.3).

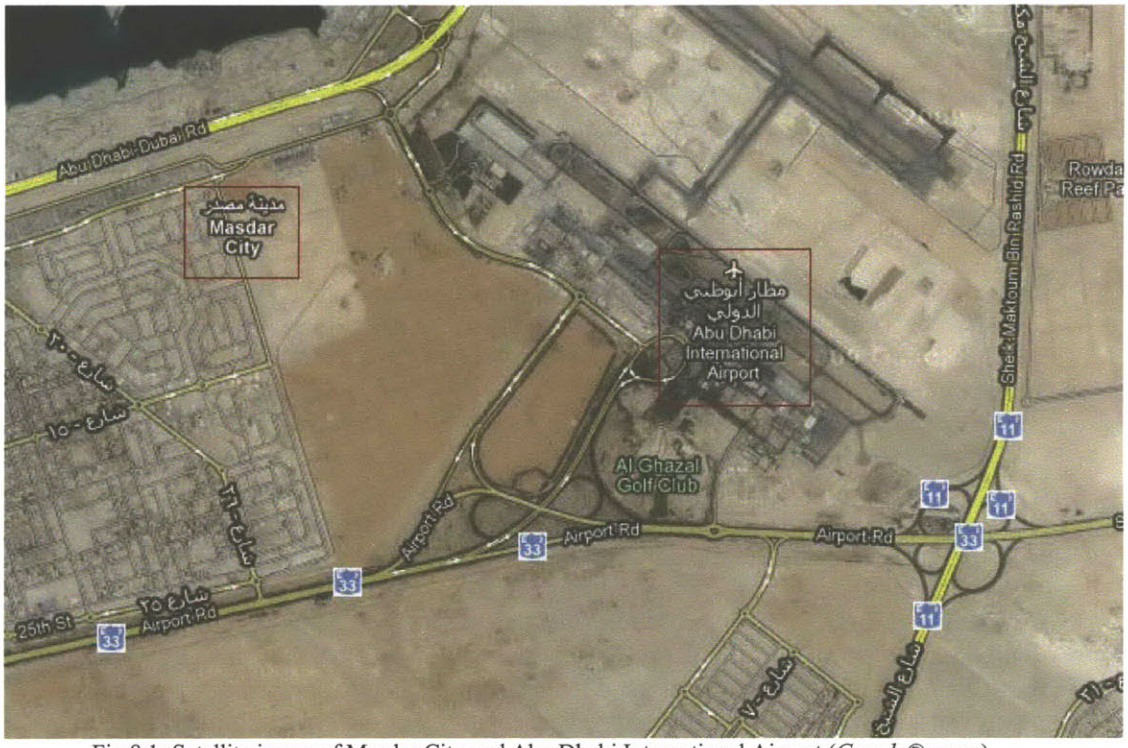

Fig.8.1: Satellite image of Masdar City and Abu Dhabi International Airport (*Google® maps*).

We will analyze an average urban canyon (section 3.5.2) formed by four-story office buildings. For the reference case, buildings are assumed to be in continuous operation and all the heat released by HVAC systems is injected into the canyon. As expected, this case will yield the largest UHI effect. In later sections, some of these hypotheses will be relaxed to represent more realistic situations. We will evaluate an office schedule from 8am to 6pm and different fractions of waste heat released into the canyon.

Then, the effect of varying the aspect ratio (*h/w*) of the urban canyon will be analyzed. In this study, we will keep the geometry of the buildings constant. This means that we are not considering a constant building area ratio, where different aspect ratios and building volumes take place. In addition, a net-energy analysis as a function of the canyon aspect ratio will be performed, considering both HVAC and electric lighting contributions.

The study of cases includes the application of the UWG scheme to the evaluation of building energy efficiency strategies. In some cases the suitability of a building energy strategy can be compromised by the existence of the UHI effect. Reciprocally, the calculation of the UHI effect can be also affected by the application of a building energy efficiency strategy. Two measures will be analyzed: increasing the insulation thickness of external facades, and adding an economizer to HVAC systems.

One of the measures at the urban level proposed in the Masdar Project is to install shadowing surfaces at the top of urban canyons to reduce solar gains. In the last section, some modeling approximations to this situation will be also analyzed.

8.3. Step1 of the UWG scheme

8.3.1. Abu Dhabi weather conditions

Abu Dhabi (United Arab Emirates) is located at 24° 25'N latitude and 54°39'E longitude. Its average elevation above the sea is 27m. Abu Dhabi has a hot arid climate, in which clear skies can be expected throughout the year.

The meteorological information used in this case study is taken from the *epw* file ARE_Abu.Dhabi.412170_IWEC, which correspond to the WMO station at the Abu Dhabi International Airport. The measured data has been processed through the International Weather for Energy Calculations (IWEC) method to obtain a Typical Meteorological Year (TMY) (see section 3.2).

Fig.8.2 shows the dry-bulb air temperatures for this TMY. As can be seen, maximum temperatures reach above 40°C and minimum temperatures are rarely lower than 10°C. Considering office buildings as the reference case, only cooling loads will be obtained throughout the year.

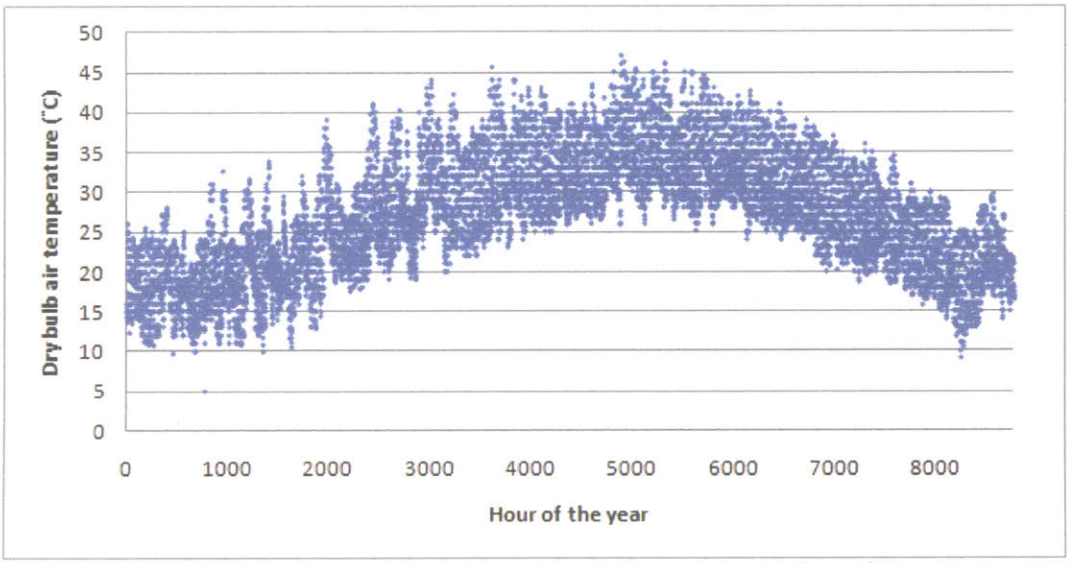

Fig.8.2: Annual evolution of dry-bulb air temperatures at the weather station.

Fig.8.3. represents the relative humidity (RH) of the air. Abu Dhabi has a relatively humid climate, in spite of the lack of precipitation. This fact can be attributed to the proximity of the sea. Although the UWG scheme includes the latent calculations of ISBA and TEB, this analysis will focus only on the sensible heat balance.

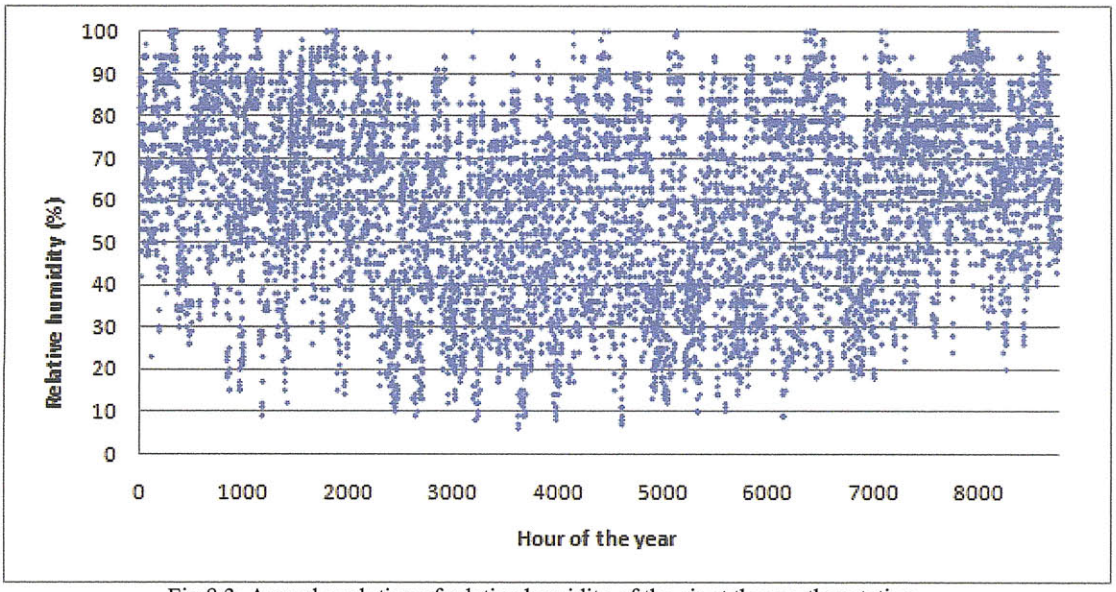

Fig.8.3: Annual evolution of relative humidity of the air at the weather station.

Finally, Fig.8.4 shows the variations in wind speed magnitude throughout this TMY. It can be observed that the wind speed is relatively low. This fact suggests that the reduction of advective heat removal at the urban site will not dominate the UHI effect.

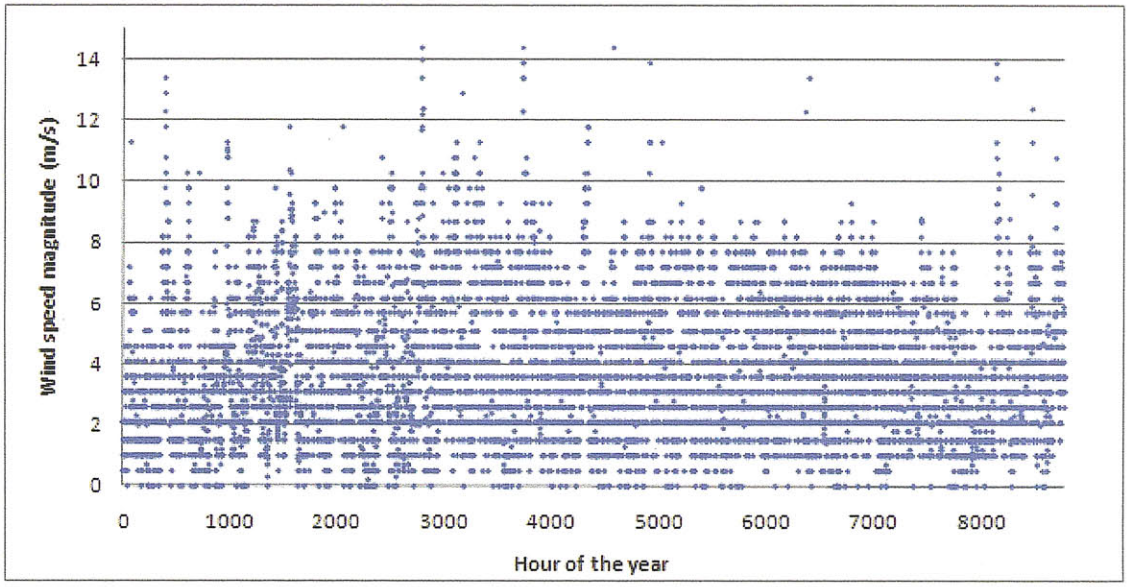

Fig.8.4: Annual evolution of wind speed magnitude at the weather station.

8.3.2. ISBA inputs

Fig.8.1 shows an arid terrain surrounding the weather station, with no appreciable vegetation. ISBA inputs were selected to represent this situation. The surface cover fractions were taken from a predefined configuration that corresponds to a desert terrain. The material composition of the terrain was unknown, so the defaults of the model were selected. The force-restore method with three layers for hydrology was chosen for the type of soil

discretization and physics in ISBA (see section 6.2.3). The reference height was defined as 25 m, following the criterion of twice the average building height. Section 8.4.6 studies the sensitivity of the model to this parameter.

8.3.3. Iterative procedure

The iterative procedure required in *step1* was described in section 3.5.1. Fig.8.5 represents the error evolution for this case study. The error is represented as the differences in air temperature and wind speed between consecutive iterations. Here, convergence is assumed to be reached after eight iterations.

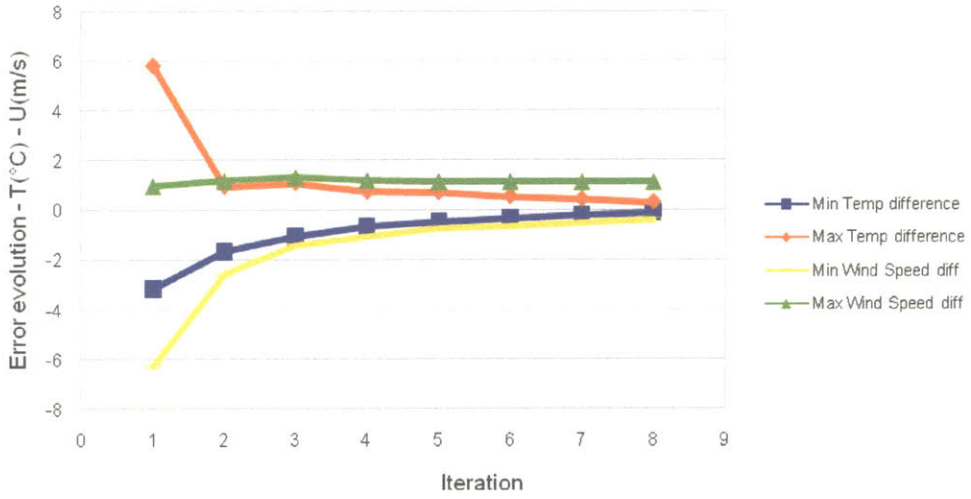

Fig.8.5: Error evolution in ISBA iterative procedure

8.3.4. Step1 results and analysis

Fig.8.6 contains the frequency distribution of air temperature difference between *epw* and *step1*. The term *epw* represents the conditions at measurement height and the term *step1* refers to the conditions at the reference height. This graph represents the fraction of hours of the year that a temperature difference ranged between its two abscissa values.

It can be observed that the difference in air temperature between *epw* and *step1* is positive most of the time, although it is also negative for a significant number of hours. The average positive difference is 2.6°C, while the average negative difference is -1.1°C. This behavior is explained by the fact that the air next to ground is warmed up at daytime and cooled down at night faster than the air at a certain height above the ground. The predominance of positive differences is related to high surface temperatures at daytime due to solar radiation. Fig.8.7 illustrates this phenomenon by comparing the time-evolution of air temperatures at both heights. The high frequency changes in air temperature at reference height are probably related to changes in wind speed.

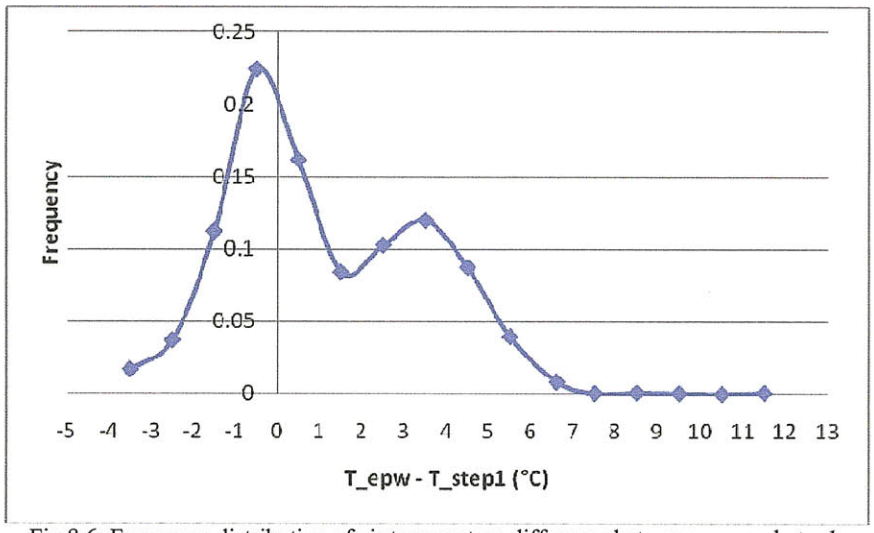

Fig.8.6: Frequency distribution of air temperature difference between *epw* and *step1*.

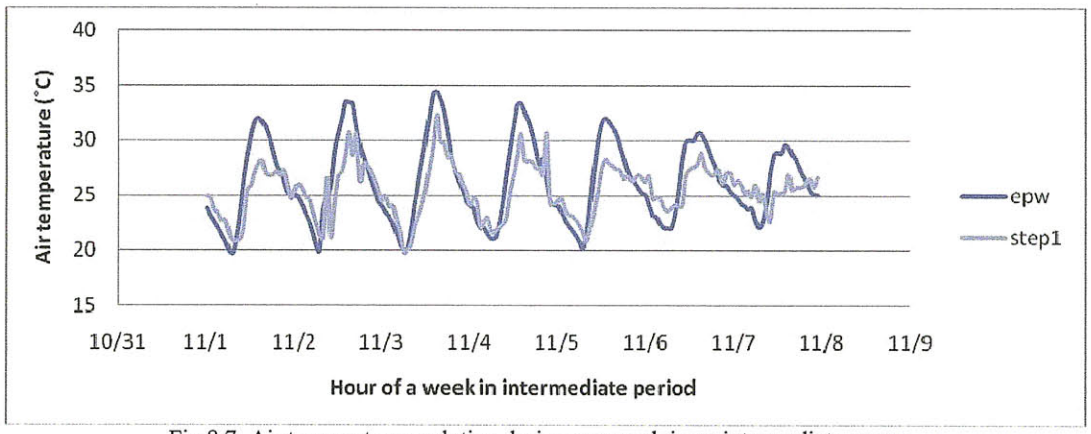

Fig.8.7: Air temperature evolution during one week in an intermediate season.

8.4. Step3 of the UWG scheme

8.4.1. Description of the reference urban canyon

This case study will consider an average urban canyon, as described in section 3.5.2. The urban canyon is formed by four-story office buildings, and it has an aspect ratio *h/w=1.5*. The reference building has standard internal gains corresponding to an office building. The operation schedule is always on. External facades are composed of 100 mm of heavyweight concrete and 50 mm of insulation board. The glazing ration is 0.3, and windows are double-pane glazed.

8.4.2. EP inputs

The following lists summarize the inputs used in EP for the reference case. The EP input data file (*idf*) is included in Appendix C.

Geometry
A single zone is considered at a medium height of the urban canyon. The zone has two exterior facades opposing each other. All the other surfaces are assumed to be adiabatic (see section 3.5.2).

- Zone height: 3 m.
- Zone length: 10 m.
- Zone depth: 18.67 m.
- Z origin of the zone: 4.5 m.
- Windows: one window per exterior façade (9 m x 0.9 m).
- Shading surfaces: located on both sides of the building representing the effect of adjacent urban canyons (height: 12 m, length: 100 m).
- Distance between shading surfaces and the zone (urban canyon width): 8 m.

Construction
Outside layer: 100 mm heavyweight concrete.

- Roughness: medium rough.
- Thickness: 0.1 m.
- Thermal conductivity: 1.95 $Wm^{-1}K^{-1}$.
- Density: 2240 kgm^{-3}
- Specific heat: 900 $Jkg^{-1}K^{-1}$.
- Thermal absorptivity: 0.9.
- Solar absorptivity: 0.7.

Inside layer: I02 50 mm insulation board.

- Thickness: 0.05 m.
- Thermal conductivity: 0.03 $Wm^{-1}K^{-1}$
- Density: 43 kgm^{-3}.
- Specific heat: 1210 $Jkg^{-1}K^{-1}$

Double-pane (6 mm x 6 mm x 6 mm) clear windows

Schedules

- Standard office building in terms of internal gains (people: 12.63 m^2 / $person$; lights: 13.46 W / m^2; equipment: 16.15 W / m^2).
- AlwaysON: offices are operative 24h per day, during all days of the year.

Daylight

- EP Detailed model. This choice has a lower computational cost than the alternative DElight model (see section 4.4.1) and produces similar results for this case study.
- Reference point: one reference point in the middle of the zone, and at working height (0.8 m).
- Illuminance threshold: 500 lux.
- Light control method: linear dimming. The fractional electric lighting input power is a linear function of the electric lighting required to fulfill the illuminance threshold.

HVAC

- System type: Unitary System (Fig.8.8).
- Thermal set points: 20 °C – 25 °C.

- Outdoor air: 2.5 $l/(s \cdot person)$.
- Dimension: autosized by EP.
- Cooing coil type: single-speed DX.
- Rated COP: 2.5.
- Energy efficiency strategies: None.

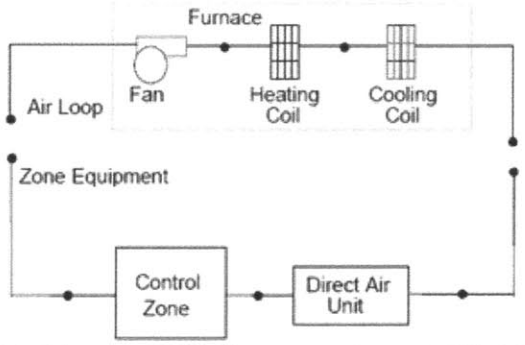

Fig.8.8: Schematic of EP unitary system furnace (DOE, *2009c)*.

8.4.3. TEB inputs

TEB inputs are based on geometric parameters relatives to an urban area, instead of relative to an urban canyon. Although the energy balance unit is still the urban canyon, it uses these inputs to represent more heterogeneous urban configurations. As a result, the inputs relative to the urban canyon and the buildings must be converted into TEB inputs by the following relations:

$$H/V = 2h/w\left(1-a_{bld}\right), \tag{8.1}$$

and

$$a_{bld} = W/(w+W), \tag{8.2}$$

where H/V is the horizontal to vertical surface ratio, h/w is the aspect ratio of the urban canyon, a_{bld} is the building area ratio, W is the building depth, and w is the canyon width.

The following lists summarize the inputs used in the TEB model for the reference case:

Geometry

- Building height: 12 m.
- Building area ratio: 0.7.
- Horizontal to vertical surface ratio: 0.9.
- Roughness length: 1.2 m.

Road construction

- Albedo: 0.08.
- Emissivity: 0.94
- Outer layer:
  - Thickness: 0.24 m.
  - Thermal conductivity: 1.95 $Wm^{-1}K^{-1}$.

- Volumetric specific heat: 2016000 $Jm^{-3}K^{-1}$.

– Inner layer:
  - Thickness: 1.00 m.
  - Thermal conductivity: 0.40 $Wm^{-1}K^{-1}$.
  - Volumetric specific heat: 1400000 $Jm^{-3}K^{-1}$.

8.4.4. Iterative procedure

The iterative procedure between EP and TEB required in *step3* was explained in section 3.5.2. Fig.8.9 shows the iteration error evolution for the reference case. The iteration error is defined here as the maximum difference in air temperature between iterations, normalized by the average air temperature. In step3, convergence is assumed to be reached after 5 iterations.

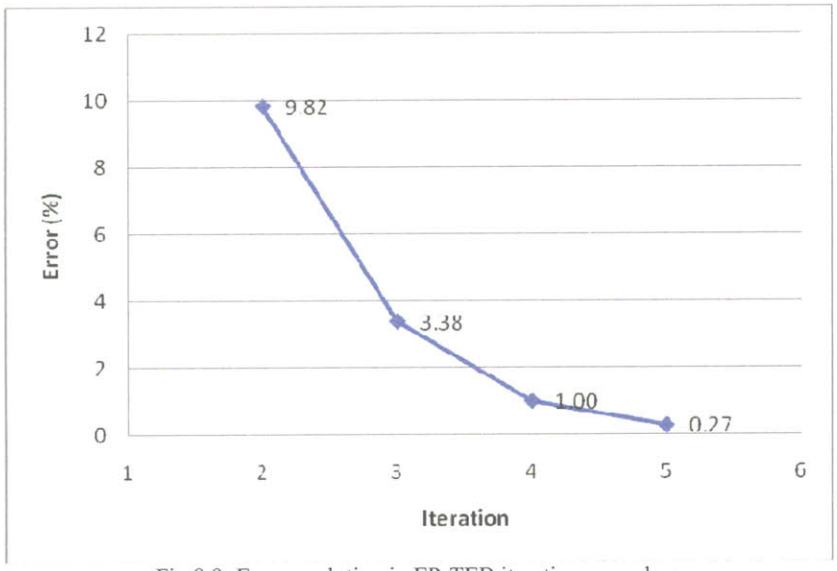

Fig.8.9: Error evolution in EP-TEB iterative procedure

8.4.5. Step3 results and analysis

This section summarizes the results of UWG simulations for the reference case described before. Fig.8.10 represents the frequency distribution of UHI intensities. The UHI intensity is defined in this analysis as the air temperature difference between the urban conditions predicted by the UWG scheme and the meteorological conditions contained in the *epw* file. This type of graph, which will be used throughout this chapter, allows comparing the annual distribution of UHI intensity for various cases in a very compact form.

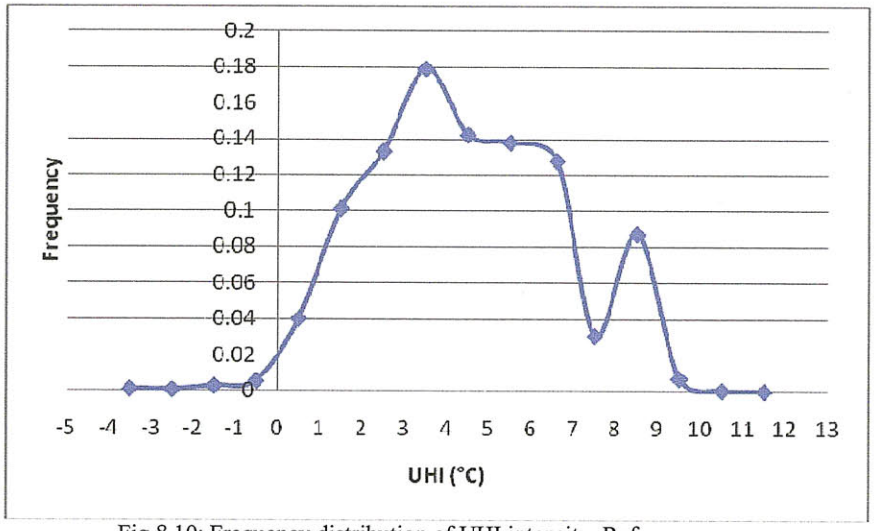

Fig.8.10: Frequency distribution of UHI intensity. Reference case.

It is observed the UHI intensity is significantly high for the reference case, reaching a maximum of 11.2°C and an average of 4.8°C. It is relevant that almost no UCI effect is produced, which could have been expected at daytime due to the shadowing effect of the urban canyon. To check the validity of the UHI intensity obtained, the following order of magnitude analysis will be performed. Consider that all the waste heat released into the canyon is leaving the canyon air volume through the top of the canyon. Then, the increase in air temperature can be calculated equaling the waste heat released and the sensible heat flux at the top of the canyon, as follows:

$$Q_{waste} \cdot 2h / w = \rho c_p C_H U_a \Delta T \,. \tag{8.3}$$

From the simulation results, the average waste heat flux is $Q_{waste} = 261\ Wm^{-2}$ and the average wind speed is $U_{can} = 3.1\ ms^{-1}$. Considering a heat exchange factor of $C_H = 0.05$ (see section 5.4), the increase in air temperature calculated from Eq.(8.3) is $\Delta T = 4.2\ ^{\circ}C$. This result agrees with the average UHI intensity obtained from simulations.

The following figures illustrate the time evolution of UHI intensity. Fig.8.11 compares the evolution of air temperature at the meteorological station (*epw*) with that at the urban site (*uwg*) during one week in winter. In this case, the UHI effect is mainly produced at night, when the waste heat released by the HVAC system is added to the nocturnal longwave trapping. At daytime, however, the shadowing effect is probably counteracting the waste heat release, so the UHI intensity is lower.

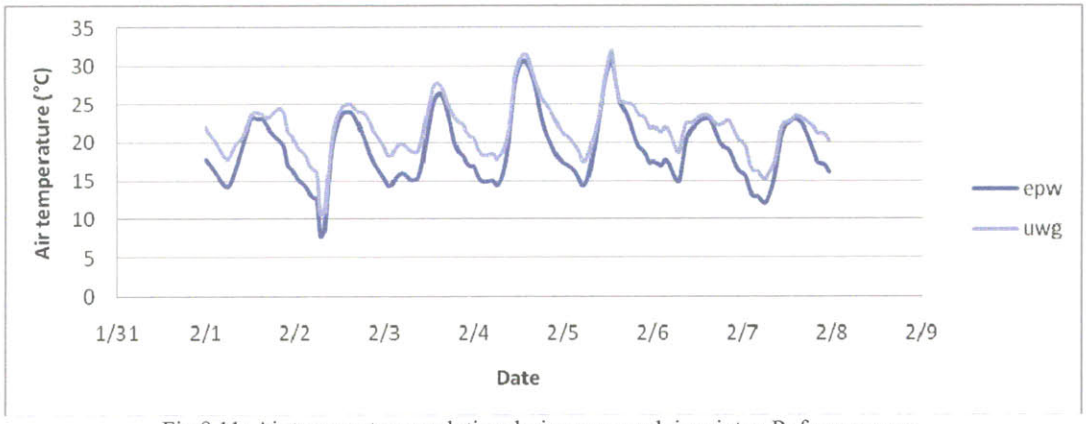

Fig.8.11: Air temperature evolution during one week in winter. Reference case.

Fig 8.12 is analogous to Fig.8.11, but it represents one week in summer. As can be observed, the UHI intensity becomes accentuated in summer. The higher outdoor temperatures and solar radiation increase building cooling loads, which are converted into more waste heat released into the environment. The increase in solar radiation can also have a direct impact on the UHI effect through the heating of urban surfaces.

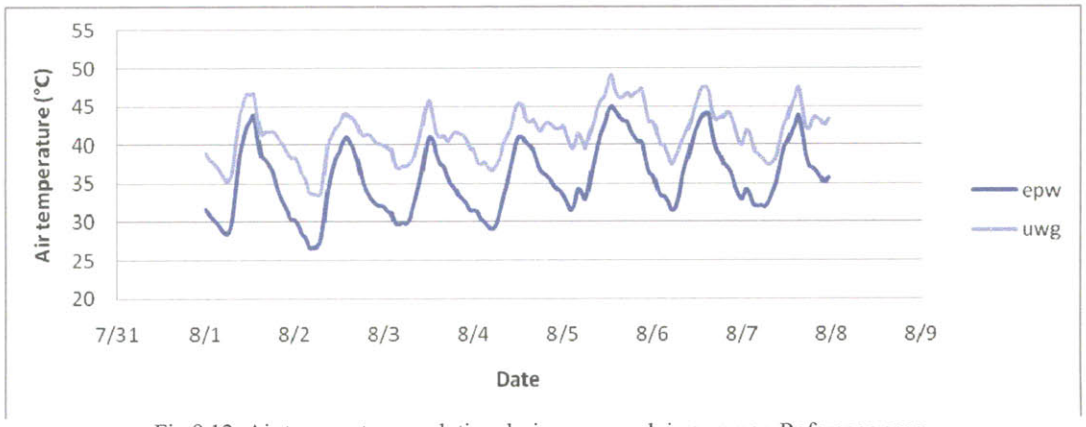

Fig.8.12: Air temperature evolution during one week in summer. Reference case.

This increase in urban air temperature leads to an increase in the annual energy consumption of HVAC systems of 10.24% and to an increase in the annual peak load of 4.07%. It is important to note that these percentages are calculated relative to the first EP simulation using the *epw* file, so they are only associated with the UHI effect. They should not be confused with the increase in energy consumption or peak load of a building by being in an urban context as compared to the same building isolated. For example, the first EP simulation has already into account the shadowing from the urban canyon.

8.4.6. Reference height sensitivity analysis

Before moving forward, it is important to check the sensitivity of the model to the reference height at which the boundary conditions of TEB are calculated. As discussed in section 3.3, this parameter is not completely defined, although a general value of twice the building height is usually recommended. Fig.8.13 shows the frequency distribution of UHI intensities for four different reference heights. The associated energy parameters are listed in Table 8.1.

The results indicate that the model is relatively insensitive to the reference height, and therefore the criterion of using approximately twice the building height will be maintained.

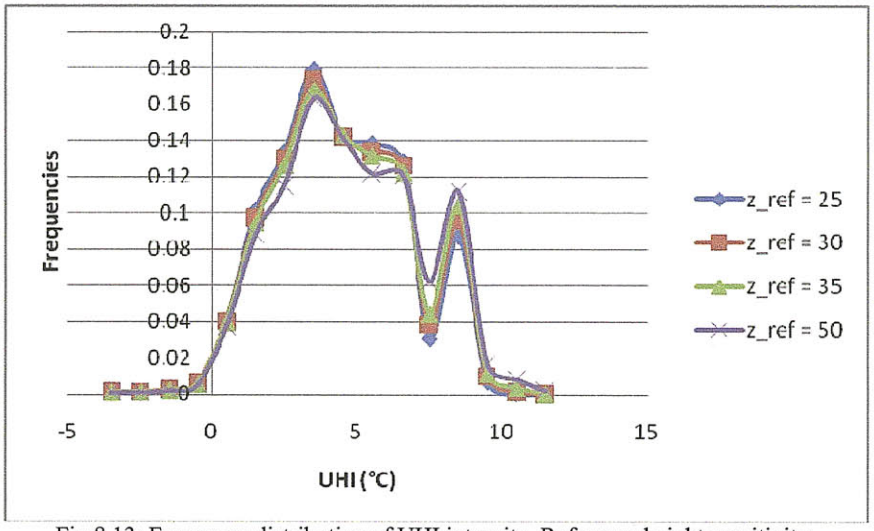

Fig.8.13: Frequency distribution of UHI intensity. Reference height sensitivity.

TABLE 8.1: Energy performance error associated with the UHI effect. Reference height sensitivity.

Reference height (m)	Annual consumption (%)	Peak load (%)
25	10.24	4.07
30	10.33	3.97
35	10.39	3.77
50	10.48	3.35

8.4.7. Comparison with the original TEB

As a validation of the *step3* iterative procedure, a comparison with the original TEB is presented in this section. For that purpose, the building model defined in EP will be adjusted to emulate the simplified building model implemented in TEB. In the TEB building model, the indoor air temperature is allowed to fluctuate with a minimum thermal set point of 19°C, the effects of windows and internal gains are not considered, and the external convection coefficient is calculated as $h = 11.8 + 4.2U_{eff}$, where U_{eff} is the wind speed in the canyon.

Fig.8.14 compares the resulting urban air temperatures calculated by the original TEB with those calculated by *step3* of the UWG scheme when the building definition corresponds to TEB's. The error between both calculations has an average of 0.04°C and a standard deviation of 0.7°C. Differences can be related to the different heat transfer models used in EP and TEB.

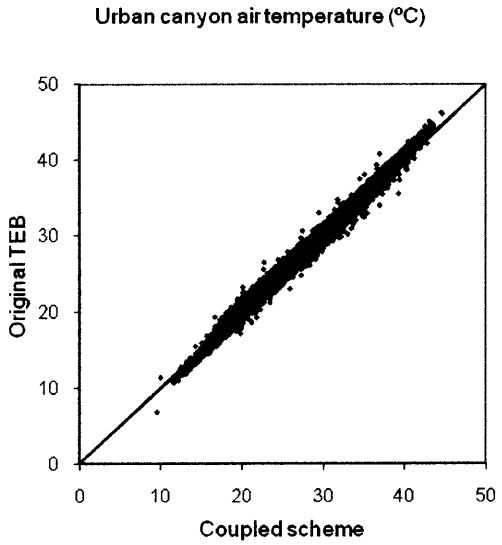

Fig.8.14: Comparison between the Original TEB and *step3* of the UWG scheme when the building is represented as in TEB.

8.5. Parametric study

In this section, the effect of different geometric and operational parameters of the urban canyon and the reference building will be analyzed.

8.5.1. Effect of building occupation

In the reference case analyzed before, the building was operative 24h per day, rejecting heat into the environment all the time. This constituted an upper limit in terms of UHI generation. In order to study a more realistic situation, an operation schedule from 8am to 6pm will be now considered. This schedule affects both internal gains and HVAC operation, so the waste heat is only released during this period of the day.

Fig.8.15 compares the frequency distribution of UHI intensities between a schedule AlwaysOn and a schedule 8-18. As can be seen, the reduction of UHI intensity is significant. The maximum is moved from 11.2°C to 7.1°C and the average from 4.8°C to 1.9°C. Note that in this case as well, no UCI effect is produced.

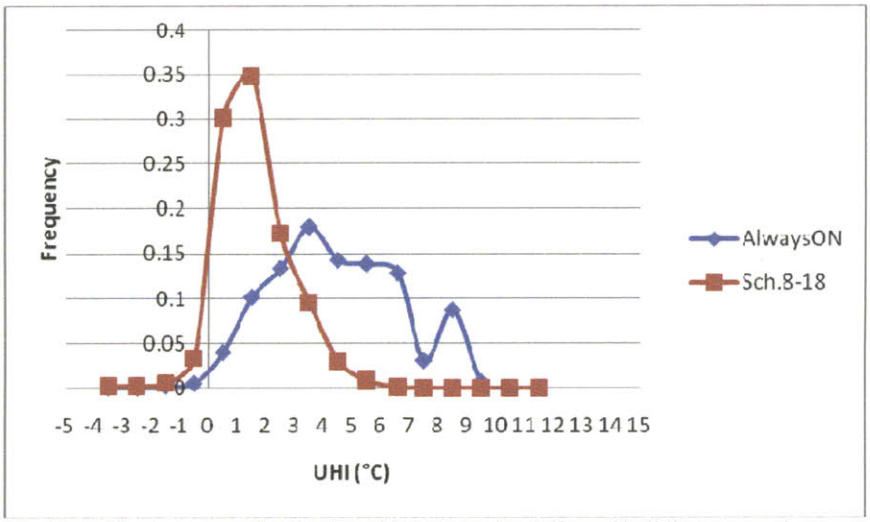

Fig.8.15: Frequency distribution of UHI intensity. Effect of building occupation.

The impact on the annual consumption and the peak load of buildings associated with this UHI effect is summarized in Table 8.2. Correlated with the UHI intensity distributions, there is an important reduction in both annual consumption and peak load for the schedule 8-18. It can be surprising that the model is predicting a lower peak load than the EP simulation, even if almost no UCI is produced. Changes in peak load are sometimes difficult to assess due to the number of factors that can be involved (latent calculations, changes in system efficiency, transient phenomena, etc.). Therefore, a detailed analysis of this pathology will not be included here.

TABLE 8.2: Energy performance error associated with the UHI effect. Effect of building occupation.

Occupation schedule	Annual consumption (%)	Peak load (%)
Always ON	10.24	4.07
Occupation 8h-18h	4.74	-3.62

8.5.2. Effect of waste heat released from HVAC system

In this case, we will analyze the sensitivity of the problem to the fraction of waste heat rejected into the canyon. Consider the case in which the external HVAC equipment is located at the roof of a building and where the heat released by this equipment is mixed in the urban boundary layer without re-circulating into the urban canopy layer. This would represent a case where the fraction of waste heat that participates into the energy balance of the urban canyon is zero, although, in practice, some of this heat will likely be brought back into the canyon.

Fig.8.16 shows the effect of reducing the fraction of waste heat released into the canyon (f) on the frequency distribution of UHI intensity. The upper graph represents the schedule AlwaysOn, while the bottom graph represents the schedule 8-18 considered in the previous case. It can be observed that both cases converge in the absence of waste heat release. This means that the occupation is only affecting the environmental conditions through the waste heat rejected into the canyon. The significant dependence of the UHI intensity on the waste

heat release highlights the importance of considering anthropogenic heat fluxes into the energy balance of the urban canyon in urban canopy models.

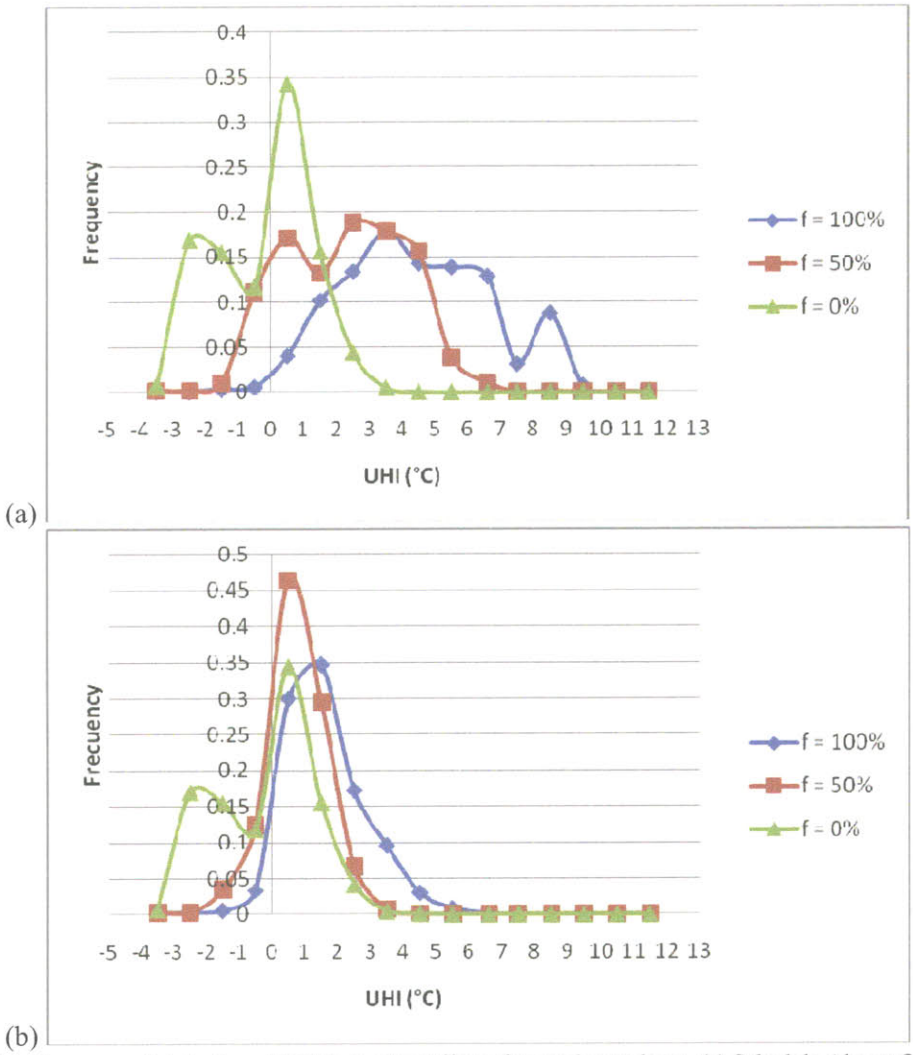

Fig.8.16: Frequency distribution of UHI intensity. Effect of waste heat release. (a) Schedule AlwaysON; (b) schedule 8-18.

For the case of no waste heat rejected into the canyon ($f = 0\%$), a noticeable UCI effect is produced. The distribution of UHI intensity for this case resembles the classical situation of a dominant UHI effect at night and an UCI effect at daytime. Fig.8.17 illustrates this situation by representing the evolution of UHI intensity during a week in an intermediate season for the case $f = 0\%$.

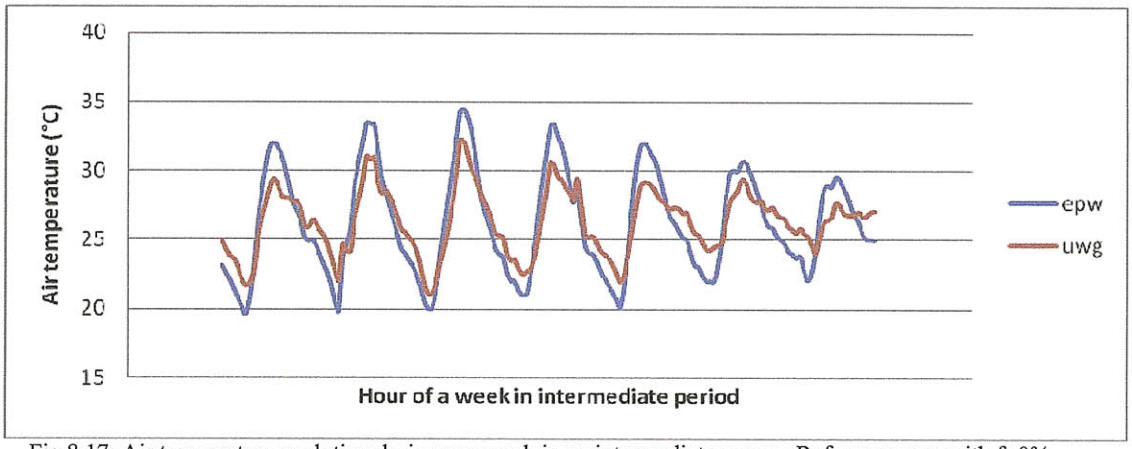

Fig.8.17: Air temperature evolution during one week in an intermediate season. Reference case with f=0%.

Table 8.3 lists the effect of these UHI intensity distributions on the energy performance of buildings. There is a direct relation between the amount of waste heat released and the energy consumption associated with UHI intensity. This direct relation is also observed for the peak load of the schedule AlwaysON. However, when a schedule 8-18 is defined, an inverse relation between peak load and waste heat released appears.

TABLE 8.3: Energy performance error associated with the UHI effect.
Effect of waste heat release for different schedules.

Fraction of waste heat released into the canyon f	Schedule AlwaysON		Schedule 8-18	
	Annual consumption (%)	Peak load (%)	Annual consumption (%)	Peak load (%)
0%	-1.89	-4.18	-3.99	-0.71
50%	4.79	1.99	1.06	-2.32
100%	10.24	4.07	4.74	-3.62

8.5.3. Aspect ratio analysis

In this case, the effect of varying the aspect ratio of the urban canyon will be analyzed. The geometry of the reference building will be kept constant, so the differences in the energy performance of buildings will only depend on outdoor conditions and not on differences in the volume of the space. As a result, inputs of the TEB model for the building area ratio or the vertical to horizontal area ratio (see section 8.4.3) will vary from case to case.

Fig.8.18 contains the frequency distributions of UHI intensity for aspect ratios ranging from 0.5 to 4. The four graphs represent four different scenarios of schedule and waste heat fraction: (a) AlwaysON - $f = 100\%$; (b) AlwaysON - $f = 0\%$; (c) Schedule 8-18 - $f = 100\%$; and (d) Schedule 8-18 - $f = 0\%$.

In Fig.8.18a, the UHI intensity increases significantly as the aspect ratio increases. This result can be explained by the fact that when the aspect ratio is high, the urban canyon has less volume, so the same amount of heat rejected into it has a greater impact on the energy balance. In addition, the increase in UHI intensity contributes to the generation of more waste

heat that produces an even larger increase in air temperature. The same effect is observed in Fig8.18b, although moderated by the fact that the waste heat is only released at daytime when the UHI effect is lower.

Scenarios (c) and (d) produce similar results to each other, which agree with the previous finding that the operation schedule has an effect only through the waste heat released. Notice that in these cases, when the aspect ratio increases, not only the UHI effect increases, but also the UCI effect does. In absence of waste heat, it can be observed that reduced aspect ratios increase the longwave trapping at night producing UHI effect, and they shade the canyon more efficiently in daytime, generating the UCI effect.

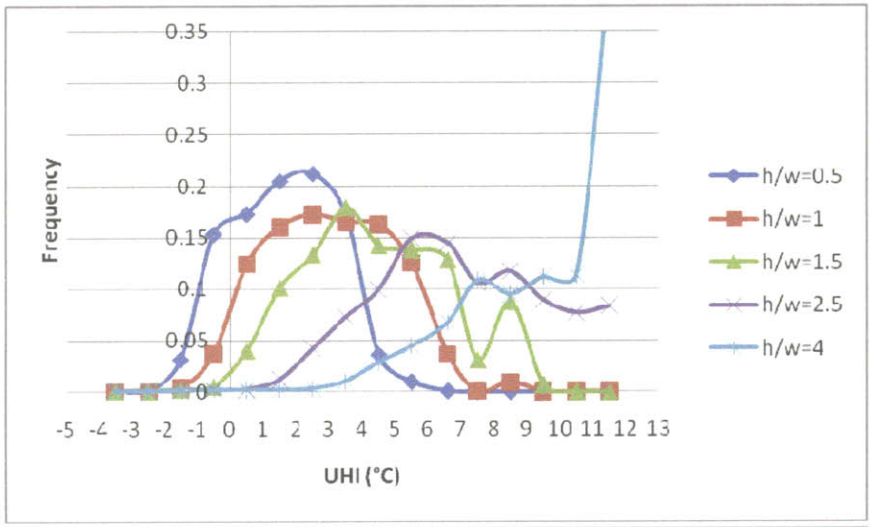

(a)

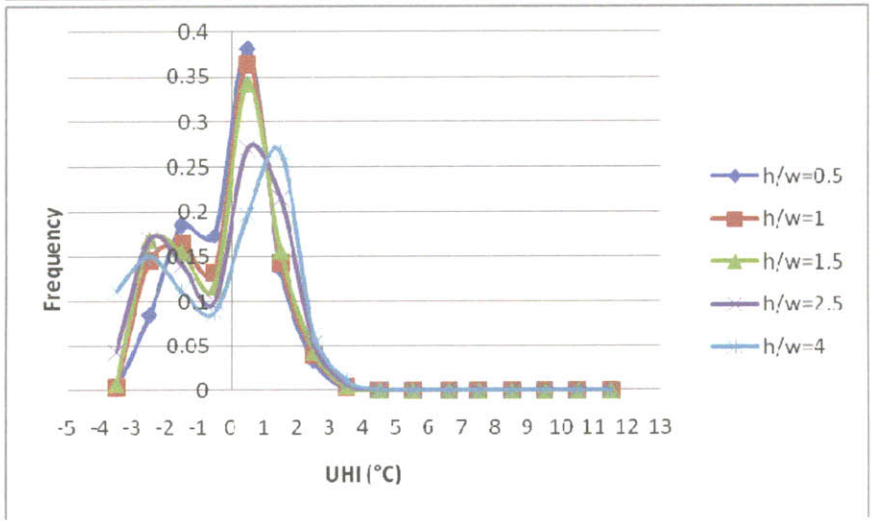

(b)

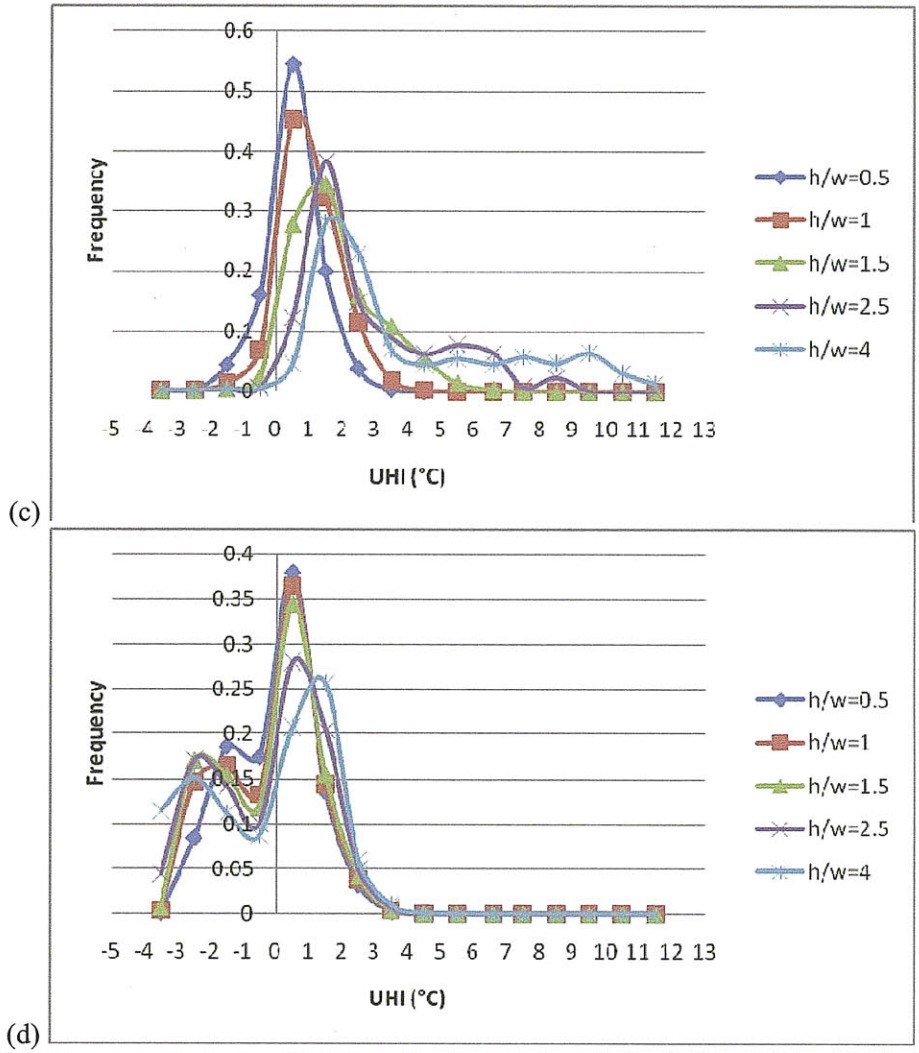

Fig.8.18: Frequency distribution of UHI intensity. Aspect ratio analysis. (a) AlwaysON - $f = 100\%$; (b) AlwaysON - $f = 0\%$; (c) Schedule 8-18 - $f = 100\%$; and (d) Schedule 8-18 - $f = 0\%$.

Table 8.4 contains the annual energy consumption increase as compared to EP simulations. In scenarios (a) and (c), the error in annual consumption increases as the aspect ratio does, reaching significantly high values for high aspect ratios. This result is expected since the UHI intensity is increasing with the aspect ratio and there is no appreciable UCI effect. In contrast, scenarios (b) and (d) show an inverse relation between annual consumption error and aspect ratio. This fact is explained by the existence of the UCI effect, which becomes more intense as the aspect ratio grows. Still, error values remain small in those scenarios, since there is an increase in annual consumption associated with the UHI as well.

TABLE 8.4: Energy performance error associated with the UHI effect.
Effect of waste heat release for different schedules. (a) AlwaysON - $f = 100\%$;
(b) AlwaysON - $f = 0\%$; (c) Schedule 8-18 - $f = 100\%$; and (d) Schedule 8-18 - $f = 0\%$.

Aspect ratio (h/w)	Annual consumption (%)			
	Scenario a	Scenario b	Scenario c	Scenario d
0.5	2.93	-1.68	0.09	-3.01
1	6.66	-1.85	2.37	-3.63
1.5	10.24	-1.89	5.43	-3.99
2.5	17.07	-2.03	8.84	-4.53
4	24.67	-2.32	13.28	-5.43

Net-energy analysis

Throughout this section, we have been analyzing the UHI effect and its impact on the energy performance of buildings. In this case, we will look at the overall electric energy consumption of buildings as a function of the aspect ratio of the urban canyon, including both HVAC and electric lighting contributions.

Fig.8.19 shows the annual electric consumption for different aspect ratios due to HVAC systems, lighting systems, and the sum of both. A zero aspect ratio represents the same building but isolated from other buildings or shading obstructions. In this case, the environmental conditions correspond to the *epw* file. All the energy consumption values have been normalized with the total electric consumption of the zero aspect ratio case. Both graphs correspond to an operation schedule 8-18. Fig.8.19a represents the case where there is not waste heat released into the canyon ($f = 0\%$), whereas Fig.8.19b includes this waste heat ($f = 100\%$).

(a)

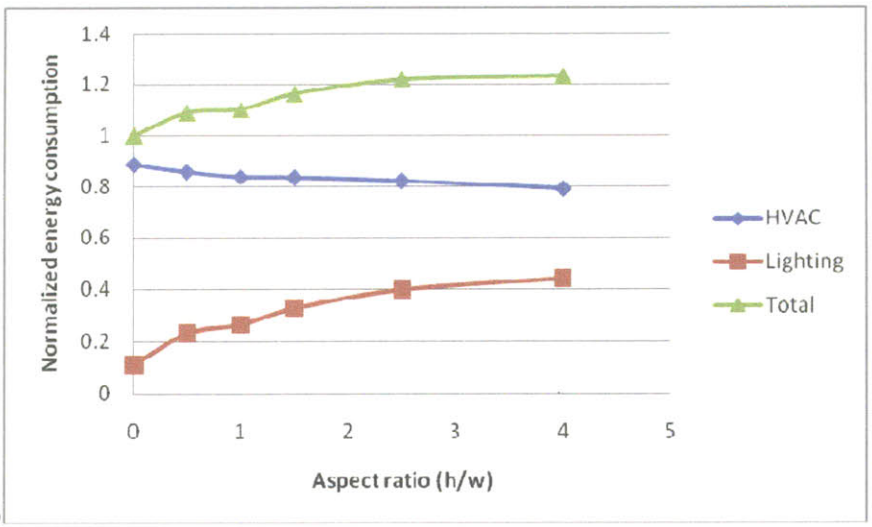

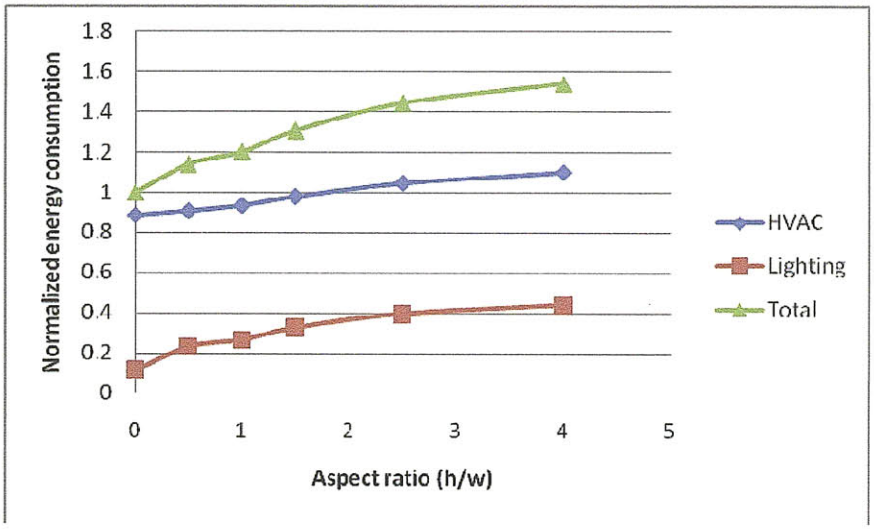

(b)

Fig.8.19: Annual electric energy consumption as a function of the aspect ratio of the urban canyon. (a) Schedule 8-18 - $f = 0\%$; (b) Schedule 8-18 - $f = 100\%$;

In Fig.8.19a, it is seen that the HVAC consumption decreases slowly as the aspect ratio increases. This circumstance was also observed in the previous analysis (Table 8.3). However, the lighting consumption increases at a higher rate with the aspect ratio; and therefore, the total electric consumption presents a monotonic growth. The increase in lighting consumption is explained by the reduced sky view factors and daylight access associated with high aspect ratios. As a result, the total energy consumption can be increased up to 20% by being in an urban canyon as compared to an isolated building.

Fig.8.19b describes an even worse scenario where the energy consumption due to HVAC systems also increases as the aspect ratio does. The waste heat released avoids the production of UCI and the UHI dominates the energy performance of buildings. As a result, the total energy consumption can rise up to 50% in this case.

8.5.4. Effect of building energy efficiency strategies

This case is intended to show the UWG scheme's potential in evaluating building energy efficiency strategies as compared to a standard building simulation. We will analyze two different measures applied to the reference case described in section 8.4. The first one is doubling the insulation thickness of exterior walls from 0.05m to 0.1m. The second measure is adding an economizer to the HVAC system, so it allows outside air to enter the building whenever the outdoor air temperature is below room temperature.

Fig.8.20 compares the frequency distribution of UHI intensity of each of these measures with the reference case. Table 8.4 shows the error in the energy performance of buildings associated with the UHI intensity. Notice again that this error is not related to the measure itself, which is also included in the EP simulation. It is clear that doubling the insulation of external façades does not introduce any advantage in terms of UHI effect. Since office buildings are often dominated by internal gains, the conduction through walls constitutes a negligible component of the building thermal loads, so it does not contribute to the waste heat rejection. This is also observed in the energy parameters indicated in Table 8.4, which are approximately the same as in the reference case.

Adding an economizer to the HVAC system, however, does have an impact on the UHI intensity. The presence of an economizer reduces the energy consumption of buildings, so the amount of waste heat released is lower. As a result, the UHI distribution moves to lower values of UHI intensity. Note that the distribution of high UHI intensities is the same as for the reference case, since they correspond to the warmest periods of the year when the economizer is not operative. On the other hand, the increase in urban air temperatures reduces the amount of time the economizer can be operative, and therefore reduces the energy savings associated with it. This fact is suggested in Table 8.5 by having significantly higher energy consumption when considering the UHI effect.

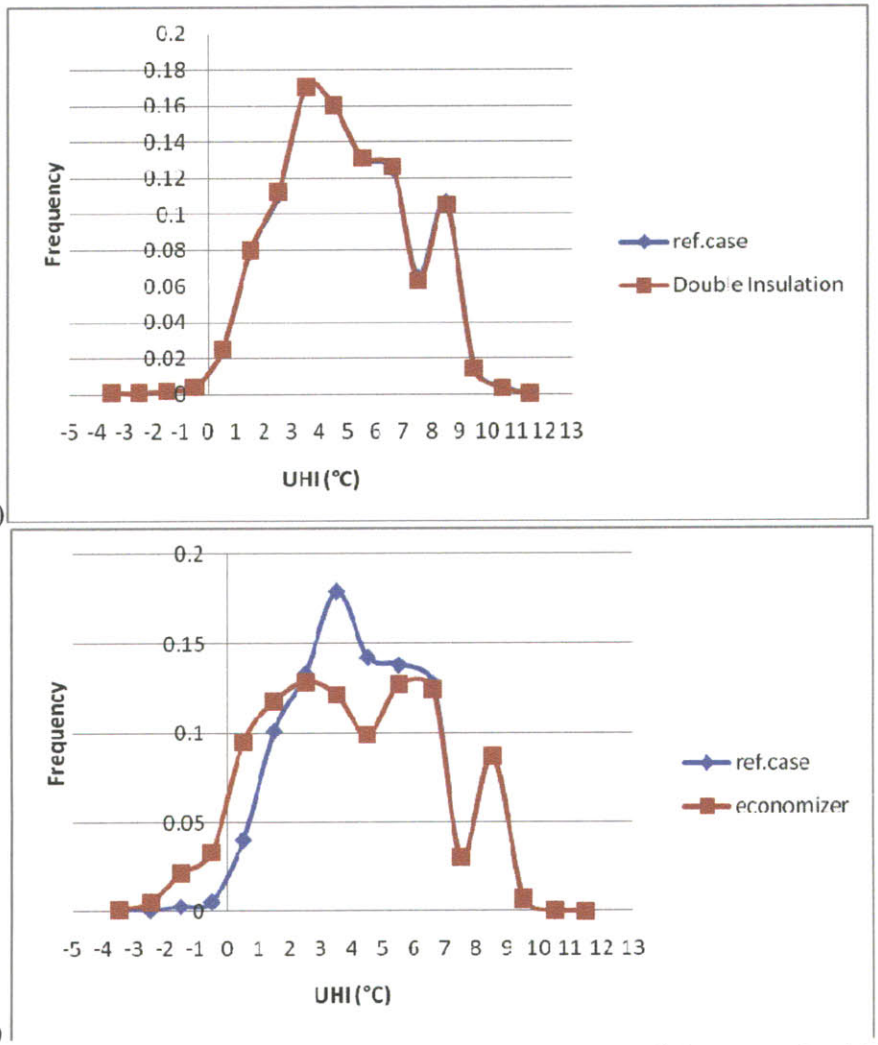

Fig.8.20: Frequency distribution of UHI intensity. Effect of building energy efficiency strategies: (a) double insulation, and (b) economizer.

TABLE 8.5: Energy performance error associated with the UHI effect.
Effect of building energy efficiency strategies.

	Annual consumption (%)	Peak load (%)
Ref.case	10.24	4.07
Double insulation	9.83	4.27
Economizer	14.55	-11.10

8.5.5. Approximations to the effect of road shadowing

This case analyzes the effect of adding road shadowing surfaces at the top of the urban canyon.
Road shadowing surfaces reduce the solar radiation entering the canyon, but they can contribute to the UHI effect. For example, they can prevent the heat loss at night due to longwave radiation exchange with the sky, and they limit the advective heat exchange between the canyon and the atmosphere. Furthermore, road shadowing surfaces can reduce daylight access, increasing the electric lighting consumption of buildings.

In this analysis, we will consider the reference case of a schedule AlwaysON and no waste heat rejection ($f = 0\%$). The shadowing effect will be approximated by two actuations. First, external shadowing surfaces are defined in EP with a transmisivity of 0.5. Second, the absortivity of the road in TEB is reduced from 0.92 to 0.5. The effect on the advective heat exchange at the top of the canyon is represented by adding a factor of 0.5 to the aerodynamical conductance. No approximation is made to the reduction of longwave radiation exchange with the sky.

Fig.8.21 compares the distributions of UHI intensity between the reference case and two approximations to the road shadowing surfaces. In the first one, only the shadowing effect of the surfaces is considered; while in the second one, the reduction factor is also applied to the aerodynamic conductance at the top of the canyon. Note that these approximations are not intended to represent the real effect of road shadowing surfaces, but to study the sensibility of some of the problem parameters.

The first approximation produces almost the same UHI intensity distribution as the reference case. This means that the road is not having a dominant contribution to the energy balance of the urban canyon. The differences in cooling loads due to solar gains are absorbed by HVAC systems without affecting the environment, since there is no waste heat rejection. However, these differences produce a reduction in the annual energy consumption of HVAC systems of 18%.

The second approximation does have an impact on the UHI effect. The UHI intensity distribution is moved up, reproducing the effect of reducing the heat exchange between the canyon and the atmosphere. The effect of the second approximation on the annual energy consumption of HVAC systems is still positive due to the shadowing effect, leading to an overall reduction of 17%.

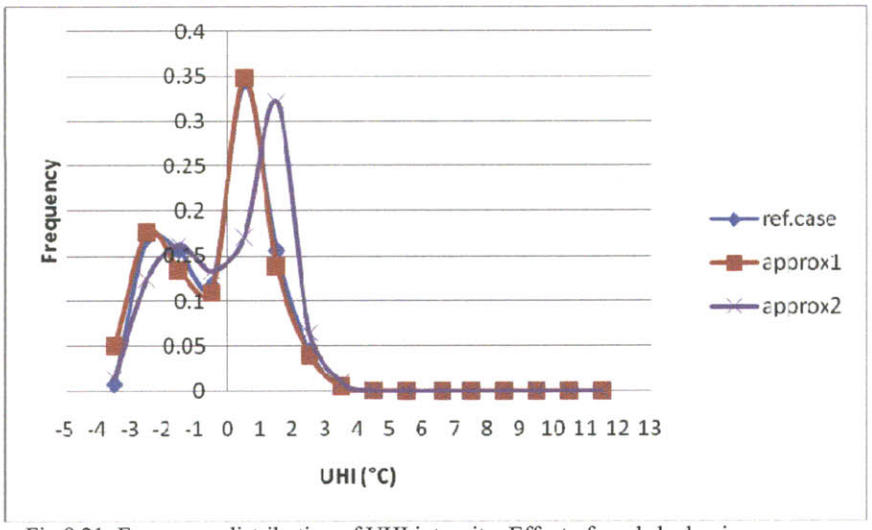

Fig.8.21: Frequency distribution of UHI intensity. Effect of road shadowing.

8.6. Conclusion

In this chapter, the UWG scheme has been applied to a particular case study. The object of the study was an urban area in a hot and arid climate. The reference urban canyon was formed by 4-story office buildings. The high air temperatures of the site and the internal gains of buildings produced only cooling loads into the system.

The reference building had a continuous operation schedule and all the waste heat from HVAC systems was released into the urban canyon. The simulations predicted high UHI intensities and significant increases in the energy consumption of buildings. These results highlight the importance of considering both the UHI effect in the energy simulation of buildings and anthropogenic heat emissions in UHI calculations.

Then, different scenarios were simulated and analyzed. The parametric variables were the fraction of waste heat rejected into the canyon, the occupation schedule, and the aspect ratio of the urban canyon. It was observed that the fraction of waste heat had the greatest impact on the UHI effect. The occupation schedule also had an important effect, mainly because of the amount of time the waste heat was released into the canyon. It was also seen that higher aspect ratios of the urban canyon produced not only a higher UHI effect, but also a higher UCI effect. In absence of waste heat released, the combination of these two effects led to a decrease in the annual consumption of buildings for higher aspect ratios. However, when waste heat was released into the canyon, the annual consumption of buildings increased with the aspect ratio.

A net-energy analysis was carried out as a function of the canyon aspect ratio, computing both HVAC and electric lighting contributions. As the aspect ratio of urban canyons increases, the daylight access of buildings is reduced, and the energy consumption of electric lighting rises. As a result, the total energy consumption can grow with the aspect ratio, even if the HVAC contribution decreases.

This chapter also analyzed the suitability of two building energy efficiency strategies in presence of the UHI effect. For this particular case study, improving the insulation of external façades did not have an effect on either the energy consumption of buildings or the urban

conditions. Adding an economizer to the HVAC system, however, had a significant impact on the UHI effect and on the energy consumption associated with it. This example showed again the importance of considering the UHI effect in building energy performance evaluations. This is even more relevant for building systems with a close interaction with the environment, such as economizers or natural ventilation systems.

The last case study analyzed the effect of installing road shadowing surfaces at the top of the urban canyon. Different approximations to this situation were simulated and analyzed. The results were not intended to represent the real performance of this measure, but to analyze the sensitivity of different parameters of the model. The results showed a moderate dependence of the UHI effect on the aerodynamic resistance between the canyon and the atmosphere.

This analysis also showed that the error in energy consumption associated with the UHI effect was always higher than the error in peak load. This fact indicates the predominance of the UHI effect at night, when the absolute temperatures are lower; and in some situations, it also indicates the presence of an UCI effect.

An important conclusion of this analysis is that one of the major differences between the UWG scheme and the original TEB model is the introduction of the waste heat from HVAC systems into the energy balance of the urban canyon. This effect can be of the same order of magnitude as the other urban heat fluxes ($50 - 300 W / m^2$), and therefore it is crucial to be able to model it accurately. The UWG scheme constitutes a step forward in this direction due to a detailed representation of HVAC systems.

However, since the waste heat rejection was not included in the original TEB model, the validations carried out to the original formulation may no longer be valid. Phenomena as the buoyant plumes produced from HVAC equipments could compromise the assumption of well mixed air inside the canyon. These effects could also invalidate the formulation used to calculate heat exchanges between the urban canyon and the atmosphere. A more detailed representation of the fluid dynamics inside urban canyon and validation with experimental data are required to solve some of these questions. This leaves the door opened to further research and development of the UWG scheme.

CHAPTER 9

Final remarks

9.1. Conclusion

The UWG scheme presented in this thesis constitutes a step forward in modelling the interactions between buildings and the urban environment. The scheme combines the building energy and urban climate studies for the first time, coupling a building energy program and an urban canopy model, which are both the state-of-the-art in their respective fields.

This thesis fulfils two important needs. On one hand, it proposes a methodology that allows simulating the energy performance of buildings in an urban context taking into account site-specific weather conditions. On the other hand, it proposes a building parameterization for urban canopy models that takes advantage of all the modeling capability of an advanced building simulation program such as EnergyPlus.

The case study analyzed in this thesis highlights the importance of considering both the UHI effect in the energy simulation of buildings and anthropogenic heat emissions in UHI calculations. This is especially relevant when analyzing building systems with an inherent close interaction with the environment, such as economizers.

Still, the current version of the UWG scheme presents some limitations that require further development and understanding of the models implemented. These limitations are summarized in the following list:

- Any urban area under study is assumed to be formed by urban canyons that are infinitely long and homogeneous in one dimension. Heterogeneities in real urban configurations inevitably introduce errors to urban climate calculations, whose extent is still undetermined.
- The external longwave radiation model implemented in EnergyPlus assumes that external obstructions and the road are at outdoor air temperature. The longwave radiation between two facing buildings can be important when one of them is sunlit and the other one is not. In general, the longwave radiation between buildings and the road is significant and should not be neglected.
- Some of the inputs required for the vegetation scheme at the weather station, such as the type and composition of the terrain, are not always available.
- There are some uncertainties related to the effect of the airport (i.e. asphalt, buildings, and planes) on the meteorological conditions at the weather station.
- The horizontal transformation from the weather station to the urban site (*step2)* has not been implemented in the UWG scheme yet. The mesoscale correlations presented in chapter 7 must be validated with field data in order to be reliably applicable.
- Current weather data files (unless for US cities) lack precipitation information, which affects the latent heat calculations of the scheme.

9.2. Future work

The research carried out in this thesis revealed many unsolved questions about the interactions between buildings and the urban environment. Further research would include:

- Propose an improvement of the longwave radiation model in the next version of EnergyPlus.
- Find appropriate expressions for the convective heat transfer between urban surfaces and the air inside the urban canopy layer. This thesis has shown inconsistencies among published correlations applied to this problem. In general, there is a need to identify and appropriately represent the dominant heat and mass transfer processes that occur inside the urban canopy layer.
- Represent the effect of waste heat released from HVAC systems into the urban environment. HVAC outdoor equipments act as concentrated sources of heat that, in a stratified environment, can create a thermal plume above them. The hypothesis of well mixed air may not be valid in those situations. A more detailed representation of the fluid dynamics inside the urban canyon and validation with experimental data are required to properly asses these phenomena.
- Investigate the latent heat calculations implemented in SURFEX. Latent heat exchanges play a critical role in situations with water-condensed building systems, vegetation, or large bodies of water close to an urban area.
- Validate and further analyze the simplified methods presented in chapter 7 for the horizontal transformation between the weather station and the urban site (*step2*).
- Investigate the possibility of a three-model coupling among EnergyPlus, TEB, and the mesoscale model WRF.

Once we obtain a comprehensive and fully operative program that integrates surface modelling in weather prediction and building energy calculations, we will have a powerful tool for the design and analysis of urban areas. The prediction of urban weather conditions and the analysis of the interactions between buildings and an urban environment can be applied to a number of different problems, such as architectural design, material selection, building system design, and urban planning.

References

Atkinson B.W., 2002. Numerical modelling of urban heat-island intensity. *Boundary-Layer Meteorology,* 109, 285-310.

Chow, W.T.L., M. Roth, 2006. Temporal dynamics of the urban heat island of Singapore. *International Journal of Climatology*, 26, 2243-2260.

de Bruin, H.A.R., A.A.M. Holtslag, 1982. A simple parameterization of surface fluxes of sensible and latent heat during daytime compared with the Penman–Monteith concept. *Journal of Applied Meteorology,* 21, 1610–1621.

Elnahas, M.M., T.J. Williamson, 1997. An improvement of the CTTC model for predicting urban air temperatures. *Energy and Buildings,* 25, 41-49.

Erell E., 2005. Predicting air temperatures in city streets on the basis of measured reference data. PhD. Thesis, University of Adelaide.

Erell, E., T. Williamson, 2006. Comments on the correct specification of the analytical CTTC model for predicting the urban canopy layer temperature. *Energy and Buildings*, 38, 1015-1021.

Erell, E., T. Williamson, 2006b. Simulating air temperature in an urban street canyon in all weather conditions using measured data at a reference meteorological station. *International Journal of Climatology,* 26, 1671–1694.

Gifford, F.A., S.R. Hanna, 1972. Technical note modelling urban air pollution. Atmospheric Environment, 7, 131-136.

Grimmond, C.S.B, H.A. Cleugh, T.R. Oke, 1991. An objective heat storage model and its comparison with other schemes. *Atmospheric Environment,* 25B, 311–326.

Grimmond, C.S.B. T.R. Oke, 1999b. Aerodynamic properties of urban areas derived from analysis of surface form. *Journal of Applied Meteorology,* 38, 1262–1292.

Grimmond, C.S.B. T.R. Oke, 2002. Turbulent heat fluxes in urban areas: observations and a Local-scale Urban Meteorological Parameterization Scheme (LUMPS). *Journal of Applied Meteorology,* 41, 792–810.

Hagishima, A, J. Tanimoto, 2003. Field measurements for estimating the convective heat transfer coefficient at building surfaces. *Building and Environment,* 38, 873–881.

Hamdi, R., V. Masson, 2008. Inclusion of a Drag Approach in the Town Energy Balance (TEB) Scheme: Offline 1D Evaluation in a Street Canyon. *Journal of Applied Meteorology and Climatology*, 47, 2627-2644.

Hanna, S.R., R.E. Britter, 2002. *Wind flow and vapour cloud dispersion at industrial and urban sites*. American Institute of Chemical Engineers.

Hidalgo, J., V. Masson, L. Gimeno, 2009. Scaling the daytime urban heat island and urban-breeze circulation. *Journal of Applied Meteorology and Climatology*, doi: 10.1175/2009JAMC2195.1

Kikegawa, Y., Y. Genchi, H. Yoshikado, H. Kondo, 2003. Development of a numerical simulation system for comprehensive assessments of urban warming countermeasures including their impacts upon the urban building's energy-demands. *Applied Energy*, 76, 449–66.

Kundu, P.K., I.M. Cohen, 2008. *Fluid Mechanics*. 4th ed. Burlington, MA: Elsevier.

Kusaka, H., H. Kondo, Y. Kikegawa, F. Kimura, 2001. A simple single-layer urban canopy model for atmospheric models: comparison with multi-layer and slab models. *Boundary-Layer Meteorology,* 101, 329–358.

Kuttler, W., 2008. The urban climate: basic and applied aspects. *Urban ecology*, 233-248.

Le Moigne, P., 2009. *SURFEX Scientific Documentation.*

Lemonsu, A., C.S.B. Grimmond, V. Masson, 2003. Modeling the surface energy balance of the core of an old Mediterranean city: Marseille, *Journal of Applied Meteorology*, 43, 312–327.

Leroyer S., J. Mailhot, S. Belair, A. Lemonsu, I.B. Strachan, 2009. Influence of the thermal roughness length parameterization in the TEB scheme on the simulation of the surface energy budget during the thawing period of the Montreal urban snow experiment. Poster session, International Conference of Urban Climate (Yokohama, 2009).

Li, X.X., R.E. Britter, T.Y. Koh, L.K. Norford, C.H. Liu, D. Entekhabi, D.Y.C. Leung, 2009. Large-eddy simulation of flow and pollutant transport in urban street canyons with ground heating. Submitted to Boundary-Layer Meteorology.

Lu, J., P. Arya, W.H. Snyder, R.E. Lawson, 1997.A laboratory study of the Urban Heat Island in a calm and stably stratified environment. Part I: Temperature field. *Journal of Applied Meteorology*, 36, 1377-1391.

Lu, J., P. Arya, W.H. Snyder, R.E. Lawson, 1997.A laboratory study of the Urban Heat Island in a calm and stably stratified environment. Part II: Velocity field. *Journal of Applied Meteorology*, 36, 1392-1402.

Martilli, A., A. Clappier, M.W. Rotach, 2002. An urban surface exchange parameterization for mesoscale models. *Boundary-Layer Meteorology,* 104, 261–304.

Mascart, P., J. Noilhan, H.Giordani, 1995. A modified parameterization of flux-profile relationship in the surface layer using different roughness length values for heat and momentum. *Boundary-Layer Meteorology,* 72, 331–344.

Masson, V., 2000. A physically-based scheme for the urban energy budget in atmospheric models. *Boundary-Layer Meteorology,* 94, 357–397.

Masson V., C.S.B. Grimmond, T.R. Oke, 2002. Evaluation of the Town Energy Balance (TEB) scheme with direct measurements from dry districts in two cities. *Journal of Applied Meteorology,* 41, 1011-1026.

Masson V., L. Gomes, G. Pigeon, C. Liousse, V. Pont, J.P. Lagouarde, J. Voogt, J. Salmond, T.R. Oke, J. Hidalgo, D. Legain, O. Garrouste, C. Lac, O. Connan, X. Briottet, S. Lacherade, P. Tulet, 2008. The Canopy and Aerosol Particles Interactions in Toulouse Urban Layer (CAPITOUL) experiment. *Meteorology and Atmospheric Physics,* 102, 135–57.

Noilhan, J. S. Planton, 1989. A simple parameterization of land surface processes for meteorological models. *Monthly Weather Review*, 117, 536-549.

Noilhan, J., J.F. Mahfouf, 1996. The ISBA land surface parameterization scheme. *Global and Planetary Change*, 13, 145-159.

Oke, T.R., 1988. The urban energy balance. *Progress in Physical Geography*, 12- 4, 471-508.

Pigeon G., A.M. Moscicki, J.A. Voogt, V. Masson, 2008. Simulation of fall and winter surface energy balance over a dense urban area using the TEB scheme. *Meteorology and Atmospheric Physics,* 102, 159-171.

Pon, B., D.M. Stamper-Kurn, C.K. Smith, H. Akbari. Existing climate data sources and their use in heat island effect. LBNL. http://eetd.lbl.gov/HeatIsland/

Priestly, C.H.B., R.J. Taylor, 1972. On the assessment of surface heat flux and evaporation using large-scale parameters. *Monthly Weather Review*, 106, 81-92.

Priyadarsini, R., N.H. Wong, C.K.W. David, 2008. Microclimatic modeling of the urban thermal environment of Singapore to mitigate Urban Heat Island. *Solar Energy*, 82, 727-745.

Rizwan, A.M., Y.C.L Dennis, C. Liu, 2008. A review on the generation, determination and mitigation of Urban Heat Island. *Journal of Environmental Sciences,* 20, 120-128.

Robert, S.M., T.R. Oke, C.S.B. Grimmond, J.A. Voogt, 2006. Comparison of Four Methods to Estimate Urban Heat Storage. *Journal of Applied Meteorology*, 45, 1766-1781.

Salamanca, F., A. Krpo, A. Martilli, A. Clappier, 2009. A new building energy model coupled with an urban canopy parameterization for urban climate simulations. —Part I. Formulation, verification and a sensitive analysis of the model. *Theoretical Applied Climatology*, doi: 10.1007/s00704-009-0142-9.

Shashua-Bar, L., M.E. Hoffman, 2002. The green CTTC model for predicting the air temperature in small urban wooded sites. *Building and Environment,* 37, 1279-1288.

Swaid H., M.E. Hoffman, 1989. The prediction of impervious ground surface temperature by the surface thermal time constant (STTC) model. *Energy and Buildings*, 13, 149-157

Swaid H., M.E. Hoffman, 1990. Prediction of air temperature variations using the analytical CTTC model. *Energy and Buildings*, 14, 313-324.

United States Department of Energy, 2009. *EnergyPlus Manual, Engineering Reference.*

United States Department of Energy, 2009b. *EnergyPlus Manual, Auxiliary Programs.*

United States Department of Energy, 2009c. *EnergyPlus Manual, Input Output Reference.*

Walton, G.N., 1983. *Thermal Analysis Research Program Reference Manual*, NBSSIR 83-2655, National Bureau of Standards.

Yamartino RJ, G. Wiegand, 1986. Development and evaluation of simple models for the flow, turbulence and pollutant concentration fields within an urban street canyon. *Atmospheric Environment,* 20, 2137–2156.

Appendix A: Input data format conversion from *csv* to SURFEX

```
#==============================
# Routine csv_to_surfex
#==============================
#
# Routine to transform EnergyPlus outputs into boundary conditions for the
adapted version of TEB
#
# EnergyPlus variables to be transformed are surface temperatures (walls
and windows),
# surface convection coefficients (walls and windows), and energy consumed
be the cooling coil,
# electric energy consumed by the HVAC system.
#
# TEB inputs are wall temperature (1 generic), surface convection
coefficient (1 generic),
# and waste heat from HVAC system.
#
#--Routine-----------------------

# Import python functions
import csv
from numpy import *
from string import *

# Read EnergyPlus output file
try:
 fichier=open('../EP/Output/UWG2.csv','r')
 heading = list()
 heading.append(fichier.readline())
 data = csv.reader(fichier)
 mydata = list()
 for row in data:
  mydata.append(row)
 fichier.close
 M=array(mydata)

# Define variables
 TS1 = list() # Temperature of surface 1
 CC1 = list() # Convection coefficient of surface 1
 TS2 = list() # Temperature of surface 2
 CC2 = list() # Convection coefficient of surface 2
 TS3 = list() # Temperature of surface 3
 CC3 = list() # Convection coefficient of surface 3
 TS4 = list() # Temperature of surface 4
 CC4 = list() # Convection coefficient of surface 4
 LOAD  = list() # Cooling load of the HVAC system
 ELEC  = list() # Electric consumption of the HVAC system

# Assign variables
 line_ts1 = atof(M[8759,6])
 TS1.append(line_ts1)
 line_cc1 = atof(M[8759,7])
 CC1.append(line_cc1)
 line_ts2 = atof(M[8759,8])
 TS2.append(line_ts2)
 line_cc2 = atof(M[8759,9])
 CC2.append(line_cc2)
 line_ts3 = atof(M[8759,10])
```

```
 TS3.append(line_ts3)
 line_cc3 = atof(M[8759,11])
 CC3.append(line_cc3)
 line_ts4 = atof(M[8759,12])
 TS4.append(line_ts4)
 line_cc4 = atof(M[8759,13])
 CC4.append(line_cc4)
 line_load = atof(M[8759,14])
 LOAD.append(line_load)
 line_elec = atof(M[8759,15])
 ELEC.append(line_elec)
 for i in range(8760):
  line_ts1 = atof(M[i,6])
  TS1.append(line_ts1)
  line_cc1 = atof(M[i,7])
  CC1.append(line_cc1)
  line_ts2 = atof(M[i,8])
  TS2.append(line_ts2)
  line_cc2 = atof(M[i,9])
  CC2.append(line_cc2)
  line_ts3 = atof(M[i,10])
  TS3.append(line_ts3)
  line_cc3 = atof(M[i,11])
  CC3.append(line_cc3)
  line_ts4 = atof(M[i,12])
  TS4.append(line_ts4)
  line_cc4 = atof(M[i,13])
  CC4.append(line_cc4)
  line_load = atof(M[i,14])
  LOAD.append(line_load)
  line_elec = atof(M[i,15])
  ELEC.append(line_elec)
 TS1=array(TS1)
 CC1=array(CC1)
 TS2=array(TS2)
 CC2=array(CC2)
 TS3=array(TS3)
 CC3=array(CC3)
 TS4=array(TS4)
 CC4=array(CC4)
 LOAD=array(LOAD)
 ELEC=array(ELEC)

# Calculate a generic wall temperature, weighting according to area and
transforming to Kelvin
 TS = array((0.7*TS1[:]+0.3*TS2[:]+0.7*TS3[:]+0.3*TS4[:])/2+273.16)

# Calculate a generic convection coefficient, weighting according to area
 CC = array((0.7*CC1[:]+0.3*CC2[:]+0.7*CC3[:]+0.3*CC4[:])/2)

# Calculate waste heat from HVAC systems. The following expression is used:
# Qwaste[W/m2] = ( Qload[W] + Qelectric[W] )/(2walls * Wall_area[m2])
 WASTE = ( LOAD[:] + ELEC[:] )/2/3/10 #*0.001 (corresponding to f=0%)

# Assign outputs
 TSW = list()
 CCW = list()
 WASTEW = list()
 for i in range(8761):
  TSW.append(str(TS[i]))
  CCW.append(str(CC[i]))
```

```
  WASTEW.append(str(WASTE[i]))
 TSW = array(TSW)
 CCW = array(CCW)
 WASTEW = array(WASTEW)

# Write outputs into files
 ficwrite = open('EP_TWALL.txt','w')
 ficwrite2 = open('EP_CHTC.txt','w')
 ficwrite3 = open('EP_HEAT.txt','w')
 for i in range(8761):
  ficwrite.write(TSW[i])
  ficwrite.write('\n')
  ficwrite2.write(CCW[i])
  ficwrite2.write('\n')
  ficwrite3.write(WASTEW[i])
  ficwrite3.write('\n')
 ficwrite.close()
 ficwrite2.close()
 ficwrite3.close()

# Control messages
 print '=========================='
 print '  EP to surfex completed  '
 print '=========================='
except:
 print "erreur d'ouverture"
```

Appendix B: Input data format conversion SURFEX to *epw*

```
#==============================
# Routine surfex_to_epw
#==============================
#
# Routine to transform Surfex outputs into an EnergyPlus weather file (epw)
#
# Surfex variables to be transformed:
# -two components of wind velocity
# -canyon air temperature
# -canyon air humidity
#
# Epw variables modified by the routine:
# -Air temperture
# -Air dew point temperature
# -Air relative humidity
# -Wind speed
#
# Psychrometric transformations have been obtained from 2001 ASHRAE
Fundamentals Handbook, Chapter 6;
# unless otherwise indicated
#
#--Routine-----------------------

# Import python functions
import csv
from numpy import *
from string import *

# Read epw file
try:

fichier=open('../EXPORT_v5.1/EXP/Data/abudhabi/ARE_Abu.Dhabi_IWEC.epw','r')
 heading = list()
 for l in range(8):
  heading.append(fichier.readline())
 data = csv.reader(fichier)
 mydata = list()
 for row in data:
  mydata.append(row)
 fichier.close
 M=array(mydata)

# Wind speed conversion
# The wind speed in epw is calculated as the modulus of the two components
of wind velocity
# obtained from surfex
 fichier=open('../EXPORT_v5.1/EXP/rundir/abudhabi/ZON10M_TEB.TXT','r')
 U_ZON = list()
 for line in fichier.readlines():
  line_vel = atof(replace(line,"D","e"))
  U_ZON.append(line_vel)
 fichier.close
 U_ZON = array(U_ZON)
 fichier=open('../EXPORT_v5.1/EXP/rundir/abudhabi/MER10M_TEB.TXT','r')
 U_MER = list()
 for line in fichier.readlines():
  line_vel = atof(replace(line,"D","e"))
  U_MER.append(line_vel)
```

```
 fichier.close
 U_MER = array(U_MER)
 U_CAN = list()
 for i in range(8760):
  U_CAN.append(str(round(sqrt(U_ZON[i]**2+U_MER[i]**2),1)))
 U_CAN = array(U_CAN)
 M[:,21] = U_CAN[:]

# Air temperature conversion
# Air temperature is directly converted, transforming from Kelvin to
Celsious
 fichier=open('../EXPORT_v5.1/EXP/rundir/abudhabi/T_CANYON.TXT','r')
 T_VEC = list()
 T_CAN = list()
 for line in fichier.readlines():
  line_temp = atof(replace(line,"D","e"))-273.15
  T_VEC.append(line_temp)
  T_CAN.append(str(round(line_temp,2)))
 fichier.close
 T_VEC = array(T_VEC)
 T_CAN = array(T_CAN)
 M[:,6] = T_CAN[:]

# Air pressure
# Obtained from epw file
 P_CAN = list()
 for i in range(8760):
  line_p = atof(M[i,9])
  P_CAN.append(line_p)
 P_CAN = array(P_CAN)

# Saturation pressure
# Calculated from air temperature using a Surfex function
 A=10.79574
 B=1.50475E-4
 C=-8.2969
 D=0.42873E-3
 E=4.76955
 F=0.78614
 G=5.028
 T1=273.16
 T2=273.15
 TST1=array((T_VEC[:]+T2)/T1)
 T1ST=array(T1/(T_VEC[:]+T2))
 Z=array(log(10.)*(A*(1.-T1ST[:])+B*(1.-exp(log(10.)*C*(TST1[:]-
1.)))+D*(exp(log(10.)*E*(1.-T1ST[:]))-1.)+F)+G*log(T1ST[:]))
 ZEW=array(100.*exp(Z[:]))

# Saturated humidity content
# Calculated from saturation pressurea and air pressure
 Q_SAT=array(0.62198*ZEW[:]/(P_CAN[:]-ZEW[:]))

# Humidity content
# Obtained from epw file
 fichier=open('../EXPORT_v5.1/EXP/rundir/abudhabi/Q_CANYON.TXT','r')
 Q_CAN = list()
 for line in fichier.readlines():
  line_hum = atof(replace(line,"D","e"))
  Q_CAN.append(line_hum)
 fichier.close
 Q_CAN = array(Q_CAN)
```

```
# Saturated humidity ratio
# Calculated from humidity content and saturated humidity content
 MU=array(Q_CAN[:]/Q_SAT[:])

# Relative Humidity conversion
# Calculated from saturated humidity ratio, saturation pressure, and air
pressure
 RH=array((MU[:]/(1-(1-MU[:])*(ZEW[:]/P_CAN[:])))*100)
 RH_CAN = list()
 for i in range(8760):
  RH_CAN.append(str(round(RH[i],0)))
 RH_CAN = array(RH_CAN)
 M[:,8] = RH_CAN[:]

# Vapour pressure
# Obtained from air temperature and humidity content
 PW=array(P_CAN[:]*Q_CAN[:]/((0.62198+Q_CAN[:])*1000))

# Dew point temperature conversion
# Calculated from vapour pressure
 C1=6.54
 C2=14.526
 C3=0.7389
 C4=0.09486
 C5=0.4569

TD=array(C1+C2*log(PW[:])+C3*(log(PW[:]))**2+C4*(log(PW[:]))**3+C5*(PW[:])*
*0.1984)
 TD_CAN = list()
 for i in range(8760):
  TD_CAN.append(str(round(TD[i],1)))
 TD_CAN = array(TD_CAN)
 M[:,7] = TD_CAN[:]

# Write into epw file
 ficwrite = open('new_urban_weather_file.epw','w')
 for l in range(8):
  ficwrite.write(heading[l])
 datawrite = csv.writer(ficwrite)
 datawrite.writerows(M)
 ficwrite.close()

# Control messages
 print '=========================='
 print '  surfex to EP completed  '
 print '=========================='
except:
 print "erreur d'ouverture"
```

Appendix C: IDF case study

```
!-   ===========  DESCRIPTION ===========

!- Idf file of the case study. Reference case

!-   ===========  ALL OBJECTS IN CLASS: VERSION ===========

Version,
    3.1;                    !- Version Identifier


!-   ===========  ALL OBJECTS IN CLASS: BUILDING ===========

BUILDING,
    BaseCase,               !- Building Name
    45,                      !- North Axis {deg}
    Urban,                 !- Terrain
    0.04,                   !- Loads Convergence Tolerance Value
    0.25,                   !- Temperature Convergence Tolerance Value
{deltaC}
    FullInteriorAndExteriorWithReflections,  !- Solar Distribution
    25;                     !- Maximum Number of Warmup Days


!-   ===========  ALL OBJECTS IN CLASS: TIMESTEP IN HOUR ===========

Timestep,
    4;                      !- Number of Timesteps per Hour


!-   ===========  ALL OBJECTS IN CLASS: INSIDE CONVECTION ALGORITHM
===========


SurfaceConvectionAlgorithm:Inside,
    Detailed;               !- Algorithm


!-   ===========  ALL OBJECTS IN CLASS: OUTSIDE CONVECTION ALGORITHM
===========


SurfaceConvectionAlgorithm:Outside,
    Detailed;               !- Algorithm


!-   ===========  ALL OBJECTS IN CLASS: SOLUTION ALGORITHM ===========

HeatBalanceAlgorithm,
    ConductionTransferFunction;  !- Algorithm


!-   ===========  ALL OBJECTS IN CLASS: SHADOWING CALCULATIONS ===========

SHADOWCALCULATION,
    20;                     !- PeriodForCalculations
```

```
!-   ===========  ALL OBJECTS IN CLASS: ZONE VOLUME CAPACITANCE MULTIPLIER
===========

ZONECAPACITANCEMULTIPLIER,
    1.0;                      !- Capacitance Multiplier


!-   ===========  ALL OBJECTS IN CLASS: RUN CONTROL ===========

SimulationControl,
    Yes,                       !- Do Zone Sizing Calculation
    Yes,                       !- Do System Sizing Calculation
    No,                       !- Do Plant Sizing Calculation
    No,                      !- Run Simulation for Sizing Periods
    Yes;                      !- Run Simulation for Weather File Run Periods


!-   ===========  ALL OBJECTS IN CLASS: RUNPERIOD ===========

RunPeriod,
    1,                        !- Begin Month
    1,                        !- Begin Day Of Month
    12,                       !- End Month
    31,                       !- End Day Of Month
    ,                         !- Day Of Week For Start Day
    ,                         !- Use WeatherFile Holidays/Special Days
    ,                         !- Use WeatherFile DaylightSavingPeriod
    ,                         !- Apply Weekend Holiday Rule
    ,                         !- Use WeatherFile Rain Indicators
    ,                         !- Use WeatherFile Snow Indicators
    1;                        !- Number of times runperiod to be done


!-   ===========  ALL OBJECTS IN CLASS: LOCATION ===========

Site:Location,
    ABU DHABI_ARE Design_Conditions,  !- LocationName
    24.43,                    !- Latitude {deg}
    54.65,                    !- Longitude {deg}
    4.00,                     !- TimeZone {hr}
    27.00;                    !- Elevation {m}


!-   ===========  ALL OBJECTS IN CLASS: DESIGNDAY ===========

! ABU DHABI_ARE Annual Heating Design Conditions Wind Speed=2m/s Wind
Dir=110
! Coldest Month=JAN
! ABU DHABI_ARE Annual Heating 99.6%, MaxDB=11.2°C
SizingPeriod:DesignDay,
    ABU DHABI Ann Htg 99.6% Condns DB,  !- DesignDayName
    11.2,                     !- Maximum Dry-Bulb Temperature {C}
    0.0,                      !- Daily Temperature Range {deltaC}
    11.2,                     !- Humidity Indicating Conditions at Max Dry-
Bulb
    101001.,                  !- Barometric Pressure {Pa}
    2,                        !- Wind Speed {m/s}
    110,                      !- Wind Direction {deg}
    0.00,                     !- Sky Clearness
    0,                        !- Rain Indicator
    0,                        !- Snow Indicator
```

```
    21,                       !- Day Of Month
    1,                        !- Month
    WinterDesignDay,          !- Day Type
    0,                        !- Daylight Saving Time Indicator
    WetBulb;                 !- Humidity Indicating Type

! ABU DHABI_ARE Annual Cooling (DB=>MWB) 2%, MaxDB=42°C MWB=23.6°C
SizingPeriod:DesignDay,
    ABU DHABI Ann Clg 2% Condns DB=>MWB,  !- DesignDayName
    42,                       !- Maximum Dry-Bulb Temperature {C}
    12.5,                     !- Daily Temperature Range {deltaC}
    23.6,                     !- Humidity Indicating Conditions at Max Dry-
Bulb
    101001.,                  !- Barometric Pressure {Pa}
    4.3,                      !- Wind Speed {m/s}
    320,                      !- Wind Direction {deg}
    1.00,                     !- Sky Clearness
    0,                        !- Rain Indicator
    0,                        !- Snow Indicator
    21,                       !- Day Of Month
    8,                        !- Month
    SummerDesignDay,          !- Day Type
    0,                        !- Daylight Saving Time Indicator
    WetBulb;                 !- Humidity Indicating Type


!-   ===========  ALL OBJECTS IN CLASS: GROUNDTEMPERATURES ===========

Site:GroundTemperature:BuildingSurface,
    20,                       !- January Ground Temperature {C}
    20,                       !- February Ground Temperature {C}
    20,                       !- March Ground Temperature {C}
    20,                       !- April Ground Temperature {C}
    20,                       !- May Ground Temperature {C}
    20,                       !- June Ground Temperature {C}
    20,                       !- July Ground Temperature {C}
    20,                       !- August Ground Temperature {C}
    20,                       !- September Ground Temperature {C}
    20,                       !- October Ground Temperature {C}
    20,                       !- November Ground Temperature {C}
    20;                       !- December Ground Temperature {C}


!-   ===========  ALL OBJECTS IN CLASS: MATERIAL:REGULAR ===========

MATERIAL,
    G01a 19mm gypsum board,  !- Name
    MediumSmooth,             !- Roughness
    0.019,                    !- Thickness {m}
    0.16,                     !- Conductivity {W/m-K}
    800,                      !- Density {kg/m3}
    1090,                     !- Specific Heat {J/kg-K}
    0.9000000,                !- Thermal Absorptance
    0.6500000,                !- Solar Absorptance
    0.6500000;                !- Visible Absorptance

MATERIAL,
    M01 100mm brick,          !- Name
    MediumRough,              !- Roughness
    0.1016,                   !- Thickness {m}
    0.89,                     !- Conductivity {W/m-K}
```

```
    1920,                    !- Density {kg/m3}
    790,                     !- Specific Heat {J/kg-K}
    0.9000000,               !- Thermal Absorptance
    0.6500000,               !- Solar Absorptance
    0.6500000;               !- Visible Absorptance

MATERIAL,
    M14a 100mm heavyweight concrete,  !- Name
    MediumRough,             !- Roughness
    0.1,                  !- Thickness {m}
    1.95,                    !- Conductivity {W/m-K}
    2240,                    !- Density {kg/m3}
    900,                     !- Specific Heat {J/kg-K}
    0.9000000,               !- Thermal Absorptance
    0.700000,               !- Solar Absorptance
    0.6500000;               !- Visible Absorptance

MATERIAL,
    F16 Acoustic tile,       !- Name
    MediumSmooth,            !- Roughness
    0.0191,                  !- Thickness {m}
    0.06,                    !- Conductivity {W/m-K}
    368,                     !- Density {kg/m3}
    590,                     !- Specific Heat {J/kg-K}
    0.9000000,               !- Thermal Absorptance
    0.6500000,               !- Solar Absorptance
    0.6500000;               !- Visible Absorptance

MATERIAL,
    I02 50mm insulation board,  !- Name
    MediumRough,             !- Roughness
    0.05,                 !- Thickness {m}
    0.03,                    !- Conductivity {W/m-K}
    43,                      !- Density {kg/m3}
    1210,                    !- Specific Heat {J/kg-K}
    0.9000000,               !- Thermal Absorptance
    0.6500000,               !- Solar Absorptance
    0.6500000;               !- Visible Absorptance


!-   ===========  ALL OBJECTS IN CLASS: MATERIAL:AIR ===========

MATERIAL:AIRGap,
    F04 Wall air space resistance,  !- Name
    0.15;                    !- Thermal Resistance {m2-K/W}

MATERIAL:AIRGap,
    F05 Ceiling air space resistance,  !- Name
    0.18;                    !- Thermal Resistance {m2-K/W}


!-   ===========  ALL OBJECTS IN CLASS: MATERIAL:WINDOWGLASS ===========

WINDOWMaterial:Glazing,
    CLEAR 6MM,               !- Name
    SpectralAverage,         !- Optical Data Type
    ,                        !- Name of Window Glass Spectral Data Set
    0.006,                   !- Thickness {m}
    0.775,                   !- Solar Transmittance at Normal Incidence
    0.071,                   !- Solar Reflectance at Normal Incidence:
Front Side
```

```
    0.071,                  !- Solar Reflectance at Normal Incidence: Back
Side
    0.881,                  !- Visible Transmittance at Normal Incidence
    0.08,                   !- Visible Reflectance at Normal Incidence:
Front Side
    0.08,                   !- Visible Reflectance at Normal Incidence:
Back Side
    0,                      !- IR Transmittance at Normal Incidence
    0.84,                   !- IR Hemispherical Emissivity: Front Side
    0.84,                   !- IR Hemispherical Emissivity: Back Side
    0.9;                    !- Conductivity {W/m-K}


!-   ===========  ALL OBJECTS IN CLASS: MATERIAL:WINDOWGAS ===========

WINDOWMaterial:Gas,
    AIR 6MM,                !- Name
    Air,                    !- Gas Type
    0.0063;                 !- Thickness {m}


!-   ===========  ALL OBJECTS IN CLASS: CONSTRUCTION ===========

CONSTRUCTION,
    ExtWallConst,           !- Name
    M14a 100mm heavyweight concrete,  !- Outside Layer
    I02 50mm insulation board;  !- Layer #2

CONSTRUCTION,
    RoofConst,              !- Name
    M14a 100mm heavyweight concrete,  !- Outside Layer
    F05 Ceiling air space resistance,  !- Layer #2
    F16 Acoustic tile;      !- Layer #3

CONSTRUCTION,
    PartitionConst,         !- Name
    G01a 19mm gypsum board,  !- Outside Layer
    F04 Wall air space resistance,  !- Layer #2
    G01a 19mm gypsum board;  !- Layer #3

CONSTRUCTION,
    FloorConst,             !- Name
    F16 Acoustic tile,      !- Outside Layer
    F05 Ceiling air space resistance,  !- Layer #2
    M14a 100mm heavyweight concrete;  !- Layer #3

CONSTRUCTION,
    WindowConst,            !- Name
    CLEAR 6MM,              !- Outside Layer
    AIR 6MM,                !- Layer #2
    CLEAR 6MM;              !- Layer #3


!-   ===========  ALL OBJECTS IN CLASS: ZONE ===========

ZONE,
    zone1,                  !- Zone Name
    0,                      !- Relative North (to building) {deg}
    0,                      !- X Origin {m}
    0,                      !- Y Origin {m}
    4.5,                      !- Z Origin {m}
```

```
    1,                        !- Type
    1,                        !- Multiplier
    autocalculate,            !- Ceiling Height {m}
    autocalculate;            !- Volume {m3}


!-   ===========  ALL OBJECTS IN CLASS: SURFACEGEOMETRY ===========

GlobalGeometryRules,
    UpperLeftCorner,          !- SurfaceStartingPosition
    CounterClockWise,         !- VertexEntry
    Relative;                 !- CoordinateSystem


!-   ===========  ALL OBJECTS IN CLASS: SURFACE:HEATTRANSFER ===========

! ==========================
! ZONE 1 SURFACES
! ==========================
BuildingSurface:Detailed,
    SouthWall1,               !- User Supplied Surface Name
    WALL,                     !- Surface Type
    ExtWallConst,             !- Construction Name of the Surface
    zone1,                    !- Zone Name
    Outdoors,                 !- Outside Boundary Condition
    ,                         !- Outside Boundary Condition Object
    SunExposed,               !- Sun Exposure
    WindExposed,              !- Wind Exposure
    0.5,                      !- View Factor to Ground
    4,                        !- Number of Surface Vertex Groups -- Number
of (X,Y,Z) groups in this surface
    0,                        !- Vertex 1 X-coordinate {m}
    0,                        !- Vertex 1 Y-coordinate {m}
    3,                      !- Vertex 1 Z-coordinate {m}
    0,                        !- Vertex 2 X-coordinate {m}
    0,                        !- Vertex 2 Y-coordinate {m}
    0,                        !- Vertex 2 Z-coordinate {m}
    10,                       !- Vertex 3 X-coordinate {m}
    0,                        !- Vertex 3 Y-coordinate {m}
    0,                        !- Vertex 3 Z-coordinate {m}
    10,                       !- Vertex 4 X-coordinate {m}
    0,                        !- Vertex 4 Y-coordinate {m}
    3;                      !- Vertex 4 Z-coordinate {m}

BuildingSurface:Detailed,
    EastWall1,                !- User Supplied Surface Name
    WALL,                     !- Surface Type
    PartitionConst,           !- Construction Name of the Surface
    zone1,                    !- Zone Name
    Surface,                  !- Outside Boundary Condition
    EastWall1,                !- OutsideFaceEnvironment Object
    NoSun,                    !- Sun Exposure
    NoWind,                   !- Wind Exposure
    0.5,                      !- View Factor to Ground
    4,                        !- Number of Surface Vertex Groups -- Number
of (X,Y,Z) groups in this surface
    10,                       !- Vertex 1 X-coordinate {m}
    0,                        !- Vertex 1 Y-coordinate {m}
    3,                      !- Vertex 1 Z-coordinate {m}
    10,                       !- Vertex 2 X-coordinate {m}
    0,                        !- Vertex 2 Y-coordinate {m}
```

```
    0,                        !- Vertex 2 Z-coordinate {m}
    10,                       !- Vertex 3 X-coordinate {m}
    18.67,                     !- Vertex 3 Y-coordinate {m}
    0,                        !- Vertex 3 Z-coordinate {m}
    10,                       !- Vertex 4 X-coordinate {m}
    18.67,                     !- Vertex 4 Y-coordinate {m}
    3;                      !- Vertex 4 Z-coordinate {m}

BuildingSurface:Detailed,
    NorthWall1,               !- User Supplied Surface Name
    WALL,                     !- Surface Type
    ExtWallConst,             !- Construction Name of the Surface
    zone1,                    !- Zone Name
    Outdoors,                 !- Outside Boundary Condition
    ,                         !- Outside Boundary Condition Object
    SunExposed,               !- Sun Exposure
    WindExposed,              !- Wind Exposure
    0.5,                      !- View Factor to Ground
    4,                        !- Number of Surface Vertex Groups -- Number
of (X,Y,Z) groups in this surface
    10,                       !- Vertex 1 X-coordinate {m}
    18.67,                     !- Vertex 1 Y-coordinate {m}
    3,                      !- Vertex 1 Z-coordinate {m}
    10,                       !- Vertex 2 X-coordinate {m}
    18.67,                     !- Vertex 2 Y-coordinate {m}
    0,                        !- Vertex 2 Z-coordinate {m}
    0,                        !- Vertex 3 X-coordinate {m}
    18.67,                     !- Vertex 3 Y-coordinate {m}
    0,                        !- Vertex 3 Z-coordinate {m}
    0,                        !- Vertex 4 X-coordinate {m}
    18.67,                     !- Vertex 4 Y-coordinate {m}
    3;                      !- Vertex 4 Z-coordinate {m}

BuildingSurface:Detailed,
    WestWall1,                !- User Supplied Surface Name
    WALL,                     !- Surface Type
    PartitionConst,           !- Construction Name of the Surface
    zone1,                    !- Zone Name
    Surface,                  !- Outside Boundary Condition
    WestWall1,                !- OutsideFaceEnvironment Object
    NoSun,                    !- Sun Exposure
    NoWind,                   !- Wind Exposure
    0.5,                      !- View Factor to Ground
    4,                        !- Number of Surface Vertex Groups -- Number
of (X,Y,Z) groups in this surface
    0,                        !- Vertex 1 X-coordinate {m}
    18.67,                     !- Vertex 1 Y-coordinate {m}
    3,                      !- Vertex 1 Z-coordinate {m}
    0,                        !- Vertex 2 X-coordinate {m}
    18.67,                     !- Vertex 2 Y-coordinate {m}
    0,                        !- Vertex 2 Z-coordinate {m}
    0,                        !- Vertex 3 X-coordinate {m}
    0,                        !- Vertex 3 Y-coordinate {m}
    0,                        !- Vertex 3 Z-coordinate {m}
    0,                        !- Vertex 4 X-coordinate {m}
    0,                        !- Vertex 4 Y-coordinate {m}
    3;                      !- Vertex 4 Z-coordinate {m}

BuildingSurface:Detailed,
    Floor1,                   !- User Supplied Surface Name
    FLOOR,                    !- Surface Type
```

```
    FloorConst,               !- Construction Name of the Surface
    zone1,                    !- Zone Name
    Surface,                  !- Outside Boundary Condition
    Floor1,                   !- OutsideFaceEnvironment Object
    NoSun,                    !- Sun Exposure
    NoWind,                   !- Wind Exposure
    1.000000,                 !- View Factor to Ground
    4,                        !- Number of Surface Vertex Groups -- Number
of (X,Y,Z) groups in this surface
    0,                        !- Vertex 1 X-coordinate {m}
    0,                        !- Vertex 1 Y-coordinate {m}
    0,                        !- Vertex 1 Z-coordinate {m}
    0,                        !- Vertex 2 X-coordinate {m}
    18.67,                     !- Vertex 2 Y-coordinate {m}
    0,                        !- Vertex 2 Z-coordinate {m}
    10,                       !- Vertex 3 X-coordinate {m}
    18.67,                     !- Vertex 3 Y-coordinate {m}
    0,                        !- Vertex 3 Z-coordinate {m}
    10,                       !- Vertex 4 X-coordinate {m}
    0,                        !- Vertex 4 Y-coordinate {m}
    0;                        !- Vertex 4 Z-coordinate {m}

BuildingSurface:Detailed,
    Ceiling1,                 !- User Supplied Surface Name
    CEILING,                  !- Surface Type
    RoofConst,                !- Construction Name of the Surface
    zone1,                    !- Zone Name
    Surface,                  !- Outside Boundary Condition
    Ceiling1,                 !- OutsideFaceEnvironment Object
    NoSun,                    !- Sun Exposure
    NoWind,                   !- Wind Exposure
    0.0,                      !- View Factor to Ground
    4,                        !- Number of Surface Vertex Groups -- Number
of (X,Y,Z) groups in this surface
    0,                        !- Vertex 1 X-coordinate {m}
    0,                        !- Vertex 1 Y-coordinate {m}
    3,                      !- Vertex 1 Z-coordinate {m}
    10,                       !- Vertex 2 X-coordinate {m}
    0,                        !- Vertex 2 Y-coordinate {m}
    3,                      !- Vertex 2 Z-coordinate {m}
    10,                       !- Vertex 3 X-coordinate {m}
    18.67,                     !- Vertex 3 Y-coordinate {m}
    3,                      !- Vertex 3 Z-coordinate {m}
    0,                        !- Vertex 4 X-coordinate {m}
    18.67,                     !- Vertex 4 Y-coordinate {m}
    3;                      !- Vertex 4 Z-coordinate {m}


!-   ===========  ALL OBJECTS IN CLASS: SURFACE:HEATTRANSFER:SUB
===========

! ====================
! ZONE1 WINDOWS
! ====================

FenestrationSurface:Detailed,
    NorthWindow,              !- User Supplied Surface Name
    WINDOW,                   !- Surface Type
    WindowConst,              !- Construction Name of the Surface
    NorthWall1,               !- Base Surface Name
    ,                         !- OutsideFaceEnvironment Object
```

```
    0.5,                     !- View Factor to Ground
    ,                        !- Name of shading control
    ,                        !- WindowFrameAndDivider Name
    1,                       !- Multiplier
    4,                       !- Number of Surface Vertex Groups -- Number
of (X,Y,Z) groups in this surface
    9.5,                     !- Vertex 1 X-coordinate {m}
    18.67,                    !- Vertex 1 Y-coordinate {m}
    2.2,                     !- Vertex 1 Z-coordinate {m}
    9.5,                     !- Vertex 2 X-coordinate {m}
    18.67,                    !- Vertex 2 Y-coordinate {m}
    1.3,                    !- Vertex 2 Z-coordinate {m}
    0.5,                     !- Vertex 3 X-coordinate {m}
    18.67,                    !- Vertex 3 Y-coordinate {m}
    1.3,                    !- Vertex 3 Z-coordinate {m}
    0.5,                     !- Vertex 4 X-coordinate {m}
    18.67,                    !- Vertex 4 Y-coordinate {m}
    2.2;                     !- Vertex 4 Z-coordinate {m}

FenestrationSurface:Detailed,
    SouthWindow,             !- User Supplied Surface Name
    WINDOW,                  !- Surface Type
    WindowConst,             !- Construction Name of the Surface
    SouthWall1,              !- Base Surface Name
    ,                        !- OutsideFaceEnvironment Object
    0.5,                     !- View Factor to Ground
    ,                        !- Name of shading control
    ,                        !- WindowFrameAndDivider Name
    1,                       !- Multiplier
    4,                       !- Number of Surface Vertex Groups -- Number
of (X,Y,Z) groups in this surface
    0.5,                     !- Vertex 1 X-coordinate {m}
    0,                       !- Vertex 1 Y-coordinate {m}
    2.2,                     !- Vertex 1 Z-coordinate {m}
    0.5,                     !- Vertex 2 X-coordinate {m}
    0,                       !- Vertex 2 Y-coordinate {m}
    1.3,                    !- Vertex 2 Z-coordinate {m}
    9.5,                     !- Vertex 3 X-coordinate {m}
    0,                       !- Vertex 3 Y-coordinate {m}
    1.3,                    !- Vertex 3 Z-coordinate {m}
    9.5,                     !- Vertex 4 X-coordinate {m}
    0,                       !- Vertex 4 Y-coordinate {m}
    2.2;                     !- Vertex 4 Z-coordinate {m}


!-   ===========  ALL OBJECTS IN CLASS: SURFACE:SHADING:DETACHED:BUILDING
===========

Shading:Building:Detailed,
    SouthSurface,       !- User Supplied Surface Name
    OFF,                     !- TransSchedShadowSurf
    4,                       !- Number of Surface Vertex Groups -- Number
of (X,Y,Z) groups in this surface
    50,                      !- Vertex 1 X-coordinate {m}
    -8,                     !- Vertex 1 Y-coordinate {m}
    12,                      !- Vertex 1 Z-coordinate {m}
    50,                      !- Vertex 2 X-coordinate {m}
    -8,                     !- Vertex 2 Y-coordinate {m}
    0,                      !- Vertex 2 Z-coordinate {m}
    -40,                        !- Vertex 3 X-coordinate {m}
    -8,                     !- Vertex 3 Y-coordinate {m}
```

```
    0,                      !- Vertex 3 Z-coordinate {m}
    -40,                        !- Vertex 4 X-coordinate {m}
    -8,                     !- Vertex 4 Y-coordinate {m}
    12;                      !- Vertex 4 Z-coordinate {m}

Shading:Building:Detailed,
    NorthSurface,   !- User Supplied Surface Name
    OFF,                     !- TransSchedShadowSurf
    4,                       !- Number of Surface Vertex Groups -- Number
of (X,Y,Z) groups in this surface
    -40,                      !- Vertex 1 X-coordinate {m}
    26.67,                    !- Vertex 1 Y-coordinate {m}
    12,                     !- Vertex 1 Z-coordinate {m}
    -40,                      !- Vertex 2 X-coordinate {m}
    26.67,                    !- Vertex 2 Y-coordinate {m}
    0,                      !- Vertex 2 Z-coordinate {m}
    50,                     !- Vertex 3 X-coordinate {m}
    26.67,                    !- Vertex 3 Y-coordinate {m}
    0,                      !- Vertex 3 Z-coordinate {m}
    50,                     !- Vertex 4 X-coordinate {m}
    26.67,                    !- Vertex 4 Y-coordinate {m}
    12;                     !- Vertex 4 Z-coordinate {m}


!-   ===========  ALL OBJECTS IN CLASS: SHADING SURFACE REFLECTANCE
===========

ShadingProperty:Reflectance,
    SouthSurface,       !- Name of Surface:Shading Object
    0.2,                    !- Diffuse Solar Reflectance of Unglazed Part
of Shading Surface
    0.2,                    !- Diffuse Visible Reflectance of Unglazed
Part of Shading Surface
    0.3,                    !- Fraction of Shading Surface That Is Glazed
    WindowConst;            !- Name of Glazing Construction

ShadingProperty:Reflectance,
    NorthSurface,   !- Name of Surface:Shading Object
    0.2,                    !- Diffuse Solar Reflectance of Unglazed Part
of Shading Surface
    0.2,                    !- Diffuse Visible Reflectance of Unglazed
Part of Shading Surface
    0.1,                    !- Fraction of Shading Surface That Is Glazed
    WindowConst;            !- Name of Glazing Construction

!-   ===========  ALL OBJECTS IN CLASS: SCHEDULETYPE ===========

ScheduleTypeLimits,
    Any Number;             !- ScheduleType Name

ScheduleTypeLimits,
    Fraction,               !- ScheduleType Name
    0.0 : 1.0,              !- range
    CONTINUOUS;             !- Numeric Type


!-   ===========  ALL OBJECTS IN CLASS: SCHEDULE:COMPACT ===========

SCHEDULE:COMPACT,
    HeatSchedule,           !- Name
    Any Number,             !- ScheduleType
```

```
    Through: 12/31,          !- Complex Field #1
    For: AllDays,            !- Complex Field #2
    Until: 24:00,            !- Complex Field #3
    20;                      !- Complex Field #4

SCHEDULE:COMPACT,
    CoolSchedule,            !- Name
    Any Number,              !- ScheduleType
    Through: 12/31,          !- Complex Field #1
    For: AllDays,            !- Complex Field #2
    Until: 24:00,            !- Complex Field #3
    25;                      !- Complex Field #4

SCHEDULE:COMPACT,
    ON,                      !- Name
    Any Number,              !- ScheduleType
    Through: 12/31,          !- Complex Field #1
    For: AllDays,            !- Complex Field #2
    Until: 24:00,            !- Complex Field #3
    1;                       !- Complex Field #4

SCHEDULE:COMPACT,
    OFF,                     !- Name
    Any Number,              !- ScheduleType
    Through: 12/31,          !- Complex Field #1
    For: AllDays,            !- Complex Field #2
    Until: 24:00,            !- Complex Field #3
    0.0;                     !- Complex Field #4

SCHEDULE:COMPACT,
    N100,                    !- Name
    Any Number,              !- ScheduleType
    Through: 12/31,          !- Complex Field #1
    For: AllDays,            !- Complex Field #2
    Until: 24:00,            !- Complex Field #3
    100;                     !- Complex Field #4

SCHEDULE:COMPACT,
    Activity Sch,            !- Name
    Any Number,              !- ScheduleType
    Through: 12/31,          !- Complex Field #1
    For: AllDays,            !- Complex Field #2
    Until: 24:00,            !- Complex Field #3
    131.8;                   !- Complex Field #4

SCHEDULE:COMPACT,
    Office HVAC,             !- Name
    Any Number,              !- ScheduleType
    Through: 12/31,          !- Complex Field #1
    For: AllDays,            !- Complex Field #2
    Until: 24:00,            !- Complex Field #3
    1;                       !- Complex Field #4

SCHEDULE:COMPACT,
    Office Lighting,         !- Name
    Any Number,              !- ScheduleType
    Through: 12/31,          !- Complex Field #1
    For: AllDays,            !- Complex Field #2
    Until: 24:00,            !- Complex Field #3
    1;                       !- Complex Field #4
```

```
SCHEDULE:COMPACT,
    Office Occupancy,        !- Name
    Any Number,              !- ScheduleType
    Through: 12/31,          !- Complex Field #1
    For: AllDays,            !- Complex Field #2
    Until: 24:00,            !- Complex Field #3
    1;                       !- Complex Field #4


!-   ===========  ALL OBJECTS IN CLASS: PEOPLE ===========

PEOPLE,
    People1,                 !- Name
    Zone1,                   !- Zone Name
    Office Occupancy,        !- Number of People SCHEDULE Name
    area/person,                  !- Number of People calculation method
    ,                        !- Number of People
    ,                  !- People per Zone Area {person/m2}
    12.6344,                      !- Zone area per person {m2/person}
    0.5,                     !- Fraction Radiant
    ,                        !- user specified sensible fraction
    Activity Sch;            !- Activity level SCHEDULE Name


!-   ===========  ALL OBJECTS IN CLASS: LIGHTS ===========

LIGHTS,
    Lights1,                 !- Name
    Zone1,                   !- Zone Name
    Office Lighting,         !- SCHEDULE Name
    Watts/area,           !- Design Level calculation method
    ,                        !- Lighting Level {W}
    13.4553,                 !- Watts per Zone Area {W/m2}
    ,                        !- Watts per Person {W/person}
    0.0, !- Return Air Fraction
    0.35, !- Fraction Radiant
    0.25, !- Fraction Visible
    1.0, !- Fraction Replaceable -- activates dimming control by
DAYLIGHTING objects
    Ambient Lighting; !- End-Use Subcategory


!-   ===========  ALL OBJECTS IN CLASS: ELECTRIC EQUIPMENT ===========

ELECTRICEQUIPMENT,
    ElectricEquipment1,      !- Name
    zone1,                   !- Zone Name
    Office Lighting,         !- SCHEDULE Name
    Watts/area,          !- Design Level calculation method
    ,                        !- Design Level {W}
    16.1464,                 !- Watts per Zone Area {W/m2}
    ,                        !- Watts per Person {W/person}
    0,                       !- Fraction Latent
    0.3,                     !- Fraction Radiant
    0,                       !- Fraction Lost
    General;                 !- End-Use Subcategory


!-   ===========  ALL OBJECTS IN CLASS: INFILTRATION ===========

ZoneINFILTRATION:DesignFlowRate,
```

```
    Infiltration1,           !- Name
    zone1,                   !- Zone Name
    ON,                      !- SCHEDULE Name
    AirChanges/Hour,         !- Design Volume Flow Rate calculation method
    ,                        !- Design Volume Flow Rate {m3/s}
    ,                        !- Flow per Zone Area {m3/s-m2}
    ,                        !- Flow per Exterior Surface Area {m3/s-m2}
    1,                        !- Air Changes Per Hour
    1,                       !- Constant Term Coefficient
    ,                        !- Temperature Term Coefficient
    ,                        !- Velocity Term Coefficient
    ;                        !- Velocity Squared Term Coefficient
!
!-   ===========  ALL OBJECTS IN CLASS: DAYLIGHTING:CONTROLS ===========
!
Daylighting:Controls,
    zone1,                   !- Zone Name
    1,                       !- Total Daylighting Reference Points
    5,                       !- X-coordinate of first reference point {m}
    9.33,                     !- Y-coordinate of first reference point {m}
    0.7,                     !- Z-coordinate of first reference point {m}
    ,                        !- X-coordinate of second reference point {m}
    ,                        !- Y-coordinate of second reference point {m}
    ,                        !- Z-coordinate of second reference point {m}
    1,                       !- Fraction of zone controlled by first
reference point
    ,                        !- Fraction of zone controlled by second
reference point
    500,                     !- Illuminance setpoint at first reference
point {lux}
    ,                        !- Illuminance setpoint at second reference
point {lux}
    3,                       !- Lighting control type
    0,                       !- Azimuth angle of view direction clockwise
from zone y-axis (for glare calculation) {deg}
    22,                      !- Maximum allowable discomfort glare index
    0.0,                     !- Minimum input power fraction for continuous
dimming control
    0.0,                     !- Minimum light output fraction for
continuous dimming control
    1,                       !- Number of steps (excluding off) for stepped
control
    1;                       !- Probability lighting will be reset when
needed in manual stepped control
!
!-   ===========  ALL OBJECTS IN CLASS: COMPACT HVAC:THERMOSTAT ===========

HVACTemplate:THERMOSTAT,
     Setpoint,                !- Thermostat Name
     HeatSchedule,            !- Thermostat Heating Setpoint Schedule
     ,                        !- Thermostat Constant Heating Setpoint {C}
     CoolSchedule,            !- Thermostat Cooling Setpoint Schedule
     ;                        !- Thermostat Constant Cooling Setpoint {C}


!-   ===========  ALL OBJECTS IN CLASS: COMPACT HVAC:ZONE:PURCHASED AIR
===========


HVACTemplate:Zone:Unitary,
    zone1,                 !- Zone Name
```

```
    FurnaceDX,              !- Air Handling System Name
    Setpoint,               !- Thermostat Name
    autosize,               !- Zone Supply Air Max Flow Rate {m3/s}
    1.1,                    !- Zone Supply Air Sizing Factor
    Flow/Person,            !- Zone Outdoor air MethodFlow Type
    0.0025,                 !- Zone Outdoor air Flow Rate per Person {m3/s}
    0.0,                    !- Zone Outdoor air Flow per Zone Area {m3/s-m2}
    0.0,                    !- Zone Outdoor air Flow per Zone {m3/s}
    ,                       !- Zone Supply Plenum Name
    ,                       !- Zone Return Plenum Name
    None,                   !- Baseboard Heating Type
    ,                       !- Baseboard Heating Availability Schedule
    0.0;                    !- Baseboard Heating Capacity {W}

HVACTemplate:System:Unitary,
    FurnaceDX,                !- Air Handling System Name
    ON,                       !- System Availability Schedule
    zone1,                    !- Control Zone Name or Thermostat Location
    autosize,                 !- Supply Fan Max Flow Rate {m3/s}
    ON,                       !- Supply Fan Operating Mode Schedule
    .7,                       !- Supply Fan Total Efficiency
    600,                      !- Supply Fan Delta Pressure {Pa}
    .9,                       !- Supply Fan Motor Efficiency
    1,                        !- Supply Fan Motor in Air Stream Fraction
    SingleSpeedDX,            !- Cooling Coil Type
    ON,                       !- Cooling Coil Availability Schedule
    autosize,                 !- Cooling Coil Capacity {W}
    autosize,                 !- Cooling Coil Rated SHR
    2.5,                      !- Cooling Coil Rated COP
    Gas,                      !- Heating Coil Type
    ON,                       !- Heating Coil Availability Schedule
    autosize,                 !- Heating Coil Capacity {W}
    .8,                       !- Gas Heating Coil Efficiency
    0,                        !- Gas Heating Coil Parasitic Electric Load
{W}
    autosize,                 !- Maximum Outdoor air Flow Rate {m3/s}
    autosize,                 !- Minimum Outdoor air Flow Rate {m3/s}
    ,                         !- Minimum Outdoor air Schedule Name
    NoEconomizer,             !- Economizer Type
    NoLockout,                !- Economizer Lockout
    ,                         !- Economizer Upper Temperature Limit {C}
    ,                         !- Economizer Lower Temperature Limit {C}
    ,                         !- Economizer Upper Enthalpy Limit {J/kg}
    ,                         !- Supply Plenum Name
    ,                         !- Return Plenum Name
    BlowThrough,    !- Supply Fan Placement
    CycleOnAny,     !- Night Cycle Control
    ,               !- Night Cycle Control Zone Name
    None,           !- Heat Recovery Type
    ,               !- Sensible Heat Recovery Effectiveness
    ,               !- Latent Heat Recovery Effectiveness
    None,           !- Dehumidification Control Type
    ,               !- Dehumidification Control Zone Name
    60,             !- Dehumidification Setpoint {percent}
    None,           !- Humidifier Type
    ,               !- Humidifier Availability Schedule
    0.000001,       !- Humidifier Rated Capacity {m3/s}
    2690,           !- Humidifier Rated Electric Power {W}
    zone1,          !- Humidifier Control Zone Name
    50;             !- Humidifier Setpoint {percent}
```

```
!-   ===========  ALL OBJECTS IN CLASS: REPORT VARIABLE ===========

Output:Variable,*,Outdoor Dry Bulb,hourly;

Output:Variable,*,Outdoor Relative Humidity,hourly;

Output:Variable,*,Wind Speed,hourly;
Output:Variable,
    SouthWall1,               !- Key_Value
    Surface Outside Temperature,  !- Variable_Name
    hourly;                   !- Reporting_Frequency

Output:Variable,
    NorthWall1,               !- Key_Value
    Surface Outside Temperature,  !- Variable_Name
    hourly;                   !- Reporting_Frequency

Output:Variable,
    SouthWindow,              !- Key_Value
    Surface Outside Temperature,  !- Variable_Name
    hourly;                   !- Reporting_Frequency

Output:Variable,
    NorthWindow,              !- Key_Value
    Surface Outside Temperature,  !- Variable_Name
    hourly;                   !- Reporting_Frequency

Output:Variable,
    SouthWall1,               !- Key_Value
    Surface Ext Convection Coeff,  !- Variable_Name
    hourly;                   !- Reporting_Frequency

Output:Variable,
    NorthWall1,               !- Key_Value
    Surface Ext Convection Coeff,  !- Variable_Name
    hourly;                   !- Reporting_Frequency

Output:Variable,
    SouthWindow,              !- Key_Value
    Surface Ext Convection Coeff,  !- Variable_Name
    hourly;                   !- Reporting_Frequency

Output:Variable,
    NorthWindow,              !- Key_Value
    Surface Ext Convection Coeff,  !- Variable_Name
    hourly;                   !- Reporting_Frequency

Output:Variable,
    *,                        !- Key_Value
    DX Cooling Coil Electric Power,  !- Variable_Name
    hourly;                   !- Reporting_Frequency

Output:Variable,
    *,                        !- Key_Value
    DX Coil Total Cooling Rate,  !- Variable_Name
    hourly;                   !- Reporting_Frequency

Output:Variable,*,Lights Electric Power,hourly; !- Zone Average [W]
```

```
Output:Variable,*,Daylight Illum at Ref Point 1,hourly; !- Zone Average
[lux]


!-   ===========  ALL OBJECTS IN CLASS: REPORT ===========

  Output:VariableDictionary,
    IDF;                      !- Key Field

  Output:Surfaces:Drawing,
    dxf:wireframe;            !- Report Type

  Output:Constructions,
    Constructions;            !- Details Type 1


!-   ===========  ALL OBJECTS IN CLASS: REPORT:TABLE:PREDEFINED ===========

  OutputControl:Table:Style,
    ALL;                      !- Column Separator
```